



Universiteit  
Leiden  
The Netherlands

## Atacama Large Aperture Submillimeter Telescope (AtLAST) science: resolving the hot and ionized Universe through the Sunyaev-Zeldovich effect

Di Mascolo, L.; Perrott, Y.; Mroczkowski, T.; Raghunathan, S.; Andreon, S.; Ettori, S.; ... ; Wedemeyer, S.

### Citation

Di Mascolo, L., Perrott, Y., Mroczkowski, T., Raghunathan, S., Andreon, S., Ettori, S., ... Wedemeyer, S. (2025). Atacama Large Aperture Submillimeter Telescope (AtLAST) science: resolving the hot and ionized Universe through the Sunyaev-Zeldovich effect. *Open Research Europe*, 4. doi:10.12688/openreseurope.17449.2

Version: Publisher's Version

License: [Creative Commons CC BY 4.0 license](https://creativecommons.org/licenses/by/4.0/)

Downloaded from: <https://hdl.handle.net/1887/4290502>

**Note:** To cite this publication please use the final published version (if applicable).



CASE STUDY

REVISED

# Atacama Large Aperture Submillimeter Telescope

## (AtLAST) science: Resolving the hot and ionized Universe through the Sunyaev-Zeldovich effect

[version 2; peer review: 4 approved]

Luca Di Mascolo <sup>1,4</sup>, Yvette Perrott <sup>1,5</sup>, Tony Mroczkowski <sup>1,6</sup>, Srinivasan Raghunathan <sup>7</sup>, Stefano Andreon <sup>8</sup>, Stefano Ettori <sup>1,9,10</sup>, Aurora Simionescu <sup>11-13</sup>, Joshiwa van Marrewijk <sup>1,6</sup>, Claudia Cicone <sup>1,14</sup>, Minju Lee <sup>15,16</sup>, Dylan Nelson <sup>17</sup>, Laura Sommovigo <sup>18,19</sup>, Mark Booth <sup>1,20</sup>, Pamela Klaassen <sup>20</sup>, Paola Andreani <sup>1,6</sup>, Martin A. Cordiner <sup>21</sup>, Doug Johnstone <sup>1,22,23</sup>, Eelco van Kampen <sup>1,6</sup>, Daizhong Liu <sup>1,24,25</sup>, Thomas J. Maccarone <sup>26</sup>, Thomas W. Morris <sup>27,28</sup>, John Orlowski-Scherer <sup>29</sup>, Amélie Saintonge <sup>1,30,31</sup>, Matthew Smith <sup>1,32</sup>, Alexander E. Thelen <sup>33</sup>, Sven Wedemeyer <sup>1,14,34</sup>

<sup>1</sup>Laboratoire Lagrange, Observatoire de la Côte d'Azur, University of Côte d'Azur, Nice, Provence-Alpes-Côte d'Azur, 06304, France

<sup>2</sup>Astronomy Unit, Department of Physics, University of Trieste, Trieste, Friuli-Venezia Giulia, 34131, Italy

<sup>3</sup>INAF – Osservatorio Astronomico di Trieste, Trieste, 34014, Italy

<sup>4</sup>IFPU – Institute for Fundamental Physics of the Universe, Trieste, 34014, Italy

<sup>5</sup>Victoria University of Wellington, Wellington, New Zealand

<sup>6</sup>European Southern Observatory, Garching, 85748, Germany

<sup>7</sup>Center for AstroPhysical Surveys, National Center for Supercomputing Applications, Urbana, Illinois, 61801, USA

<sup>8</sup>INAF – Osservatorio Astronomico di Brera, Milano, 20121, Italy

<sup>9</sup>INAF – Osservatorio di Astrofisica e Scienza dello Spazio, Bologna, 40129, Italy

<sup>10</sup>INFN – Sezione di Bologna, Bologna, 40127, Italy

<sup>11</sup>SRON Netherlands Institute for Space Research, Niels Bohrweg 4, Leiden, 2333 CA, The Netherlands

<sup>12</sup>Leiden Observatory, Niels Bohrweg 2, Leiden University, Leiden, 2333 CA, The Netherlands

<sup>13</sup>Kavli Institute for the Physics and Mathematics of the Universe, University of Tokyo, Kashiwa, Chiba, 277-8583, Japan

<sup>14</sup>Institute of Theoretical Astrophysics, University of Oslo, Oslo, 0315, Norway

<sup>15</sup>Cosmic Dawn Center, Copenhagen, Denmark

<sup>16</sup>DTU-Space, Technical University of Denmark, Kongens Lyngby, 2800, Denmark

<sup>17</sup>Zentrum für Astronomie, Institut für Theoretische Astrophysik, Heidelberg University, Heidelberg, Baden-Württemberg, 69120, Germany

<sup>18</sup>Center for Computational Astrophysics, Flatiron Institute, New York, New York, 10010, USA

<sup>19</sup>Scuola Normale Superiore, Pisa, Tuscany, 56126, Italy

<sup>20</sup>UK Astronomy Technology Centre, Royal Observatory Edinburgh, Edinburgh, EH9 3HJ, UK

<sup>21</sup>Astrochemistry Laboratory, Code 691, NASA Goddard Space Flight Center, Greenbelt, Maryland, 20771, USA

<sup>22</sup>NRC Herzberg Astronomy and Astrophysics, Victoria, British Columbia, V9E 2E7, Canada

<sup>23</sup>Department of Physics and Astronomy, University of Victoria, Victoria, British Columbia, V8P 5C2, Canada

<sup>24</sup>Max-Planck-Institut für extraterrestrische Physik, Garching, Bayern, 85748, Germany

<sup>25</sup>Purple Mountain Observatory, Chinese Academy of Sciences, Nanjing, 210023, China

<sup>26</sup>Department of Physics & Astronomy, Texas Tech University, Lubbock, Texas, 79409-1051, USA

<sup>27</sup>Brookhaven National Laboratory, Upton, New York, 11973, USA

<sup>28</sup>Lawrence Berkeley National Laboratory, Berkeley, California, 94720, USA

<sup>29</sup>Department of Physics and Astronomy, University of Pennsylvania, 209 South 33rd Street, Philadelphia, PA, 19104, USA

<sup>30</sup>Department of Physics and Astronomy, University College London, London, England, WC1E 6BT, UK

<sup>31</sup>Max-Planck-Institut für Radioastronomie, Bonn, 53121, Germany

<sup>32</sup>School of Physics & Astronomy, Cardiff University, Cardiff, Wales, CF24 3AA, UK

<sup>33</sup>Division of Geological and Planetary Sciences, California Institute of Technology, Pasadena, California, 91125, USA

<sup>34</sup>Roseland Centre for Solar Physics, University of Oslo, Oslo, 0315, Norway

**v2** First published: 10 Jun 2024, 4:113

<https://doi.org/10.12688/openreseurope.17449.1>

Latest published: 05 Jun 2025, 4:113

<https://doi.org/10.12688/openreseurope.17449.2>

## Abstract

An omnipresent feature of the multi-phase “cosmic web” — the large-scale filamentary backbone of the Universe — is that warm/hot ( $\geq 10^5$  K) ionized gas pervades it. This gas constitutes a relevant contribution to the overall universal matter budget across multiple scales, from the several tens of Mpc-scale intergalactic filaments, to the Mpc intracluster medium (ICM), all the way down to the circumgalactic medium (CGM) surrounding individual galaxies from  $\approx 1$  kpc up to their respective virial radii ( $\approx 100$  kpc). The study of the hot baryonic component of cosmic matter density represents a powerful means for constraining the intertwined evolution of galactic populations and large-scale cosmological structures, for tracing the matter assembly in the Universe and its thermal history. To this end, the Sunyaev-Zeldovich (SZ) effect provides the ideal observational tool for measurements out to the beginnings of structure formation. The SZ effect is caused by the scattering of the photons from the cosmic microwave background off the hot electrons embedded within cosmic structures, and provides a redshift-independent perspective on the thermal and kinematic properties of the warm/hot gas. Still, current and next-generation (sub)millimeter facilities have been providing only a partial view of the SZ Universe due to any combination of: limited angular resolution, spectral coverage, field of view, spatial dynamic range, sensitivity, or all of the above. In this paper, we motivate the development of a wide-field, broad-band, multi-chroic continuum instrument for the Atacama Large Aperture Submillimeter Telescope (AtLAST) by identifying the scientific drivers that will deepen our understanding of the complex thermal evolution of cosmic structures. On a technical side, this will necessarily require efficient multi-wavelength mapping of the SZ signal with an unprecedented spatial dynamic range (from arcsecond to tens of arcminutes) and we employ detailed theoretical forecasts to determine the key instrumental constraints for achieving our goals.

## Keywords

galaxy clusters, intracluster medium, intergalactic medium, galaxy halos, cosmic background radiation, submillimeter facility

## Open Peer Review

### Approval Status

	1	2	3	4
<b>version 2</b>				
(revision)	✓	✓	✓	✓
05 Jun 2025	<a href="#">view</a>	<a href="#">view</a>	<a href="#">view</a>	<a href="#">view</a>
<b>version 1</b>				
10 Jun 2024	?	?	✓	?
	<a href="#">view</a>	<a href="#">view</a>	<a href="#">view</a>	<a href="#">view</a>

1. **François-Xavier Désert** , Univ. Grenoble Alpes, CNRS, IPAG, Grenoble, France

2. **Laura Salvati**, IAS, Université Paris-Saclay, CNRS, Orsay, France

3. **Elia Stefano Battistelli**, Sapienza University of Rome, Rome, Italy

4. **Mathieu Remazeilles** , Instituto de Física de Cantabria (CSIC - UC), Santander, Spain

Any reports and responses or comments on the article can be found at the end of the article.



This article is included in the European Research Council (ERC) gateway.



This article is included in the Horizon 2020 gateway.



This article is included in the Marie-Sklodowska-Curie Actions (MSCA) gateway.



This article is included in the Atacama Large Aperture Submillimeter Telescope Design Study collection.

**Corresponding author:** Luca Di Mascolo ([luca.di-mascolo@oca.eu](mailto:luca.di-mascolo@oca.eu))

**Author roles:** **Di Mascolo L:** Conceptualization, Formal Analysis, Investigation, Project Administration, Software, Supervision, Visualization, Writing – Original Draft Preparation, Writing – Review & Editing; **Perrott Y:** Formal Analysis, Visualization, Writing – Original Draft Preparation, Writing – Review & Editing; **Mroczkowski T:** Funding Acquisition, Supervision, Visualization, Writing – Original Draft Preparation, Writing – Review & Editing; **Raghunathan S:** Formal Analysis, Software, Visualization, Writing – Review & Editing; **Andreoni S:** Visualization, Writing – Original Draft Preparation, Writing – Review & Editing; **Ettori S:** Visualization, Writing – Original Draft Preparation, Writing – Review & Editing; **Simionescu A:** Writing – Original Draft Preparation, Writing – Review & Editing; **van Marrewijk J:** Formal Analysis, Software, Writing – Original Draft Preparation, Writing – Review & Editing; **Cicone C:** Funding Acquisition, Project Administration, Supervision, Writing – Review & Editing; **Lee M:** Project Administration, Supervision, Writing – Review & Editing; **Nelson D:** Investigation, Resources, Software, Visualization, Writing – Review & Editing; **Sommovigo L:** Software, Visualization; **Booth M:** Software, Supervision, Writing – Review & Editing; **Klaassen P:** Conceptualization, Funding Acquisition, Project Administration, Supervision, Writing – Review & Editing; **Andreani P:** Supervision; **Cordiner MA:** Writing – Review & Editing; **Johnstone D:** Writing – Review & Editing; **van Kampen E:** Project Administration, Writing – Review & Editing; **Liu D:** Writing – Review & Editing; **Maccarone TJ:** Writing – Review & Editing; **Morris TW:** Methodology, Software; **Orlowski-Scherer J:** Writing – Review & Editing; **Saintonge A:** Writing – Review & Editing; **Smith M:** Writing – Review & Editing; **Thelen AE:** Writing – Review & Editing; **Wedemeyer S:** Writing – Review & Editing

**Competing interests:** No competing interests were disclosed.

**Grant information:** This project has received funding from the European Union's Horizon 2020 research and innovation programme under grant agreement No [951815] (Towards an Atacama Large Aperture Submillimeter Telescope [AtLAST]). L.D.M. is supported by the European Research council under a Starting Grant, grant agreement No [716762] (Fundamental physics, Cosmology and Astrophysics: Galaxy Clusters at the Cross-roads [ClustersXCosmo]). L.D.M. further acknowledges financial contribution from the agreement ASI-INAF n.2017-14-H.0. This work has been supported by the French government, through the UCAJ.E.D.I. Investments in the Future project managed by the National Research Agency (ANR) with the reference number ANR-15-IDEX-01. Y.P. is supported by a Rutherford Discovery Fellowship ("Realising the potential of galaxy clusters as cosmological probes") and Marsden Fast Start grant ("Turbulence in the Intracluster Medium: toward the robust extraction of physical parameters"). S.A. acknowledges INAF grant "Characterizing the newly discovered clusters of low surface brightness" and PRIN-MIUR 20228B938N grant "Mass and selection biases of galaxy clusters: a multi-probe approach". S.E. acknowledges the financial contribution from the contracts Prin-MUR 2022 supported by Next Generation EU (n.20227RNLY3 The concordance cosmological model: stress-tests with galaxy clusters), ASI-INAF Athena 2019-27-HH.0, "Attività di Studio per la comunità scientifica di Astrofisica delle Alte Energie e Fisica Astroparticellare" (Accordo Attuativo ASI-INAF n. 2017-14-H.0), and from the European Union's Horizon 2020 programme under grant agreement No [871158] (Integrated Activities for the High Energy Astrophysics Domain [AHEAD2020]). M.L. acknowledges support from the European Union's Horizon Europe research and innovation programme under the Marie Skłodowska-Curie grant agreement No 101107795. D.N. acknowledges funding from the Deutsche Forschungsgemeinschaft (DFG) through an Emmy Noether Research Group (grant number NE 2441/1-1). T.Mo. acknowledges the support of L. Page. S.W. acknowledges support by the Research Council of Norway through the EMISSA project (project number 286853) and the Centres of Excellence scheme, project number 262622 ("Rosseland Centre for Solar Physics").

*The funders had no role in study design, data collection and analysis, decision to publish, or preparation of the manuscript.*

**Copyright:** © 2025 Di Mascolo L *et al.* This is an open access article distributed under the terms of the [Creative Commons Attribution License](#), which permits unrestricted use, distribution, and reproduction in any medium, provided the original work is properly cited.

**How to cite this article:** Di Mascolo L, Perrott Y, Mroczkowski T *et al.* **Atacama Large Aperture Submillimeter Telescope (AtLAST) science: Resolving the hot and ionized Universe through the Sunyaev-Zeldovich effect [version 2; peer review: 4 approved]** Open Research Europe 2025, 4:113 <https://doi.org/10.12688/openreseurope.17449.2>

**First published:** 10 Jun 2024, 4:113 <https://doi.org/10.12688/openreseurope.17449.1>

**REVISED Amendments from Version 1**

We have revised the manuscript to address all comments and suggestions provided by the referees. The new version of the paper offers a more detailed presentation of the proposed science cases. Among the key changes is a major extension of the introduction, which now provides a self-contained review of the relevant aspects of the SZ effect. We also included a more detailed discussion of the expectations for kSZ measurements, covering applications both in cosmological and astrophysical contexts. To facilitate comparison with other facilities, we added a new figure showing the different spectral coverages of the main current or upcoming telescopes that can be used to study the SZ effect.

A more precise description of all changes, along with detailed responses to the referees, is provided in the peer review reply documents.

**Any further responses from the reviewers can be found at the end of the article**

be the way it is. Ultimately, by understanding the nature of clusters and large scale structure, we will also be able to test the properties of the ubiquitous dark matter (Clowe *et al.*, 2006), and to peer into the dark universe itself.

## 1.2 AtLAST, in brief

With the ambitious goal of deeply improving our understanding of the formation and evolution of cosmic structures, we seek here to motivate deep, multi-band or multichroic high resolution and wide field observations with the Atacama Large Aperture Submillimeter Telescope (AtLAST; Klaassen *et al.*, 2020; Mroczkowski *et al.*, 2023; Mroczkowski *et al.*, 2025; Ramasawmy *et al.*, 2022). AtLAST is a proposed (sub)millimeter facility planned to be built on the Chajnantor Plateau. Taking advantage of the excellent atmospheric transmission high in the Atacama Desert, AtLAST will operate across the 30–950 GHz spectral range. The planned 50-meter class aperture will allow observers to map the (sub)millimeter sky at high angular resolution, reaching  $\approx 10$  arcsec at 150 GHz and  $\approx 1.5$  arcsec at 950 GHz. At the same time, AtLAST will feature an unparallel mapping speed, aiming at achieving an instantaneous field of view of 2 deg diameter thanks to its novel optical design which will be coupled to next-generation large-format receivers, each expected to comprise up to  $\sim 10^6$  detector elements. With the goal of building a multi-purpose facility that could support the heterogeneous science applications of the (sub)millimeter community, AtLAST is planned to simultaneously host six different instruments, allowing for swift and efficient switching across them (see the AtLAST Memos 3 and 4 for a summary). Such ambitious requirements are not met by any present facilities or any of their future upgrades, and have served as key technical drivers for the ongoing design effort (Klaassen *et al.*, 2020), starting with the preliminary optical design concept outlined in the AtLAST Memos 1 and 2 by R. Hills. We also note that the AtLAST aims to serve as a novel, sustainable facility, both from an energetic and social perspective (Kiselev *et al.*, 2024; Valenzuela-Venegas *et al.*, 2024; Viole *et al.*, 2023; Viole *et al.*, 2024). The full design concept has recently been presented in a series of dedicated papers (Gallardo *et al.*, 2024b; Kiselev *et al.*, 2024; Mroczkowski *et al.*, 2025; Puddu *et al.*, 2024; Reichert *et al.*, 2024), to which we refer the reader for more details.

The unprecedented combination of spectral coverage, angular resolution, and mapping speed will position AtLAST as a leading (sub)millimeter facility for addressing questions of cluster astrophysics as well as the contamination that could potentially plague cluster cosmology done at arcminute resolutions. At the same time, the observations discussed here are not simply to aid cosmological studies, but can probe interesting astrophysics and solve important questions about astrophysics in their own right — with the unique potential of providing a link between galaxy evolution, large-scale structure, and cosmological studies. Our primary tool here is the Sunyaev-Zeldovich effect, described below.

## 2 The multi-faceted Sunyaev-Zeldovich effect

The Sunyaev-Zeldovich (SZ) effects (Sunyaev & Zeldovich, 1970; Sunyaev & Zeldovich, 1972; Sunyaev & Zeldovich, 1980)

are caused by the up-scattering to higher energies of photons from the cosmic microwave background (CMB) by populations of free energetic electrons within cosmic structures. Depending on the specific velocity distribution of the scattering electrons, such an interaction imprints specific spatial and spectral variation in the surface brightness of the back-lighting CMB. As such, disentangling the relative contribution from each SZ component helps us exploit the different information they carry to study the physical properties of the ionized gas throughout the Universe. In this section we provide a brief introduction to the specific SZ contributions that we aim at probing with AtLAST that will be key for studying the varied astrophysical processes occurring in clusters and large-scale structures (we refer to [Figure 1](#) for a cartoon depiction, and to the subsections of [Section 3](#) for a detailed discussion in the AtLAST context). For more comprehensive reviews of the various aspects of the SZ effect, we further refer to, e.g., [Birkinshaw \(1999\)](#), [Carlstrom \*et al.\* \(2002\)](#), [Kitayama \(2014\)](#), and [Mroczkowski \*et al.\* \(2019\)](#).

## 2.1 Thermal component

The thermal SZ effect ([Sunyaev & Zeldovich, 1970](#); [Sunyaev & Zeldovich, 1972](#)) was proposed theoretically as an alternative to X-ray measurements to probe the thermodynamics of the hot gas in galaxy clusters. It is produced by the scattering of CMB photons by a reservoir of hot electrons in thermal equilibrium resulting in a spectral distortion of the CMB. For a

given direction  $\mathbf{n}$  on the sky, the classical (non-relativistic) thermal SZ effect induces a variation in the CMB temperature  $T_{\text{CMB}}$  with amplitude

$$\frac{\Delta T_{\text{CMB}}(\mathbf{n}; x)}{T_{\text{CMB}}} = g(x) y_{\text{TSZ}}(\mathbf{n}) = \left[ x \coth\left(\frac{x}{2}\right) - 4 \right] y_{\text{TSZ}}(\mathbf{n}), \quad (1)$$

for a given dimensionless frequency  $x = h\nu/k_B T_{\text{CMB}}$ , with  $h$  equal to the Planck constant,  $\nu$  the photon frequency, and  $k_B$  the Boltzmann constant. The second term in the equation denotes the thermal Compton-y parameter (hereafter,  $y_{\text{TSZ}}$ ), proportional to the integral along the line of sight  $l$  of the electron pressure distribution  $P_e(\mathbf{n}, l)$ ,

$$y_{\text{TSZ}}(\mathbf{n}) = \frac{\sigma_T}{m_e c^2} \int P_e(\mathbf{n}, l) dl. \quad (2)$$

Here,  $\sigma_T$ ,  $m_e$ , and  $c$  denote the Thomson cross section, electron mass, and speed of light, respectively. In other terms, the thermal SZ effect provides a direct proxy for the (thermal) pressure due to the free electrons in the ICM and, as such, the optimal tool for gaining a direct calorimetric view of the gas thermal properties.

## 2.2 Kinetic component

Shortly after the theoretical foundations of the thermal SZ effect, the kinetic SZ effect (see [Sunyaev & Zeldovich, 1980](#))

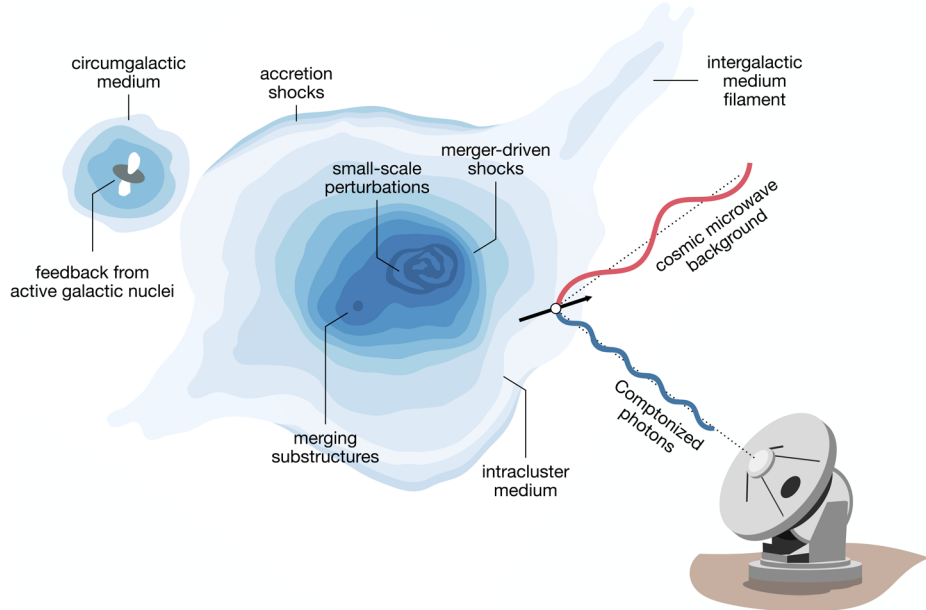


**Figure 1. Expanded diagram highlighting some of the aspects of galaxy clusters and large-scale structures that will be studied through the Sunyaev-Zeldovich (SZ) effect using AtLAST.** The SZ effect is caused by the interaction of photons from the cosmic microwave background (CMB) with reservoirs of energetic electrons within cosmic large-scale structures. Thanks to AtLAST's unparalleled capabilities, it will be possible to fully exploit multiple aspects of the SZ effect to characterize: the multi-scale properties of the intracluster medium (ICM; [Section 3.1](#), [Section 3.2](#), and [Section 3.3](#)) and the many dynamical processes like mergers and large-scale accretion events shaping the observational properties of galaxy clusters; the elusive low-mass and high-redshift end of cosmic haloes ([Section 3.4](#) and [Section 3.5](#)); how active galactic nuclei (AGN) impact the thermal properties of the circumgalactic medium (CGM) and of the ICM ([Section 3.6](#)); how the warm/hot component of cosmic baryons is distributed within cluster outskirts and the large-scale filaments of intergalactic medium (IGM; [Section 3.7](#)). The figure is an adaptation of the SZ schematic in [Mroczkowski \*et al.\* \(2019\)](#), which was based on that from L. van Speybroeck as adapted by J. E. Carlstrom.

was proposed as a way to measure gas momentum with respect to the CMB, our ultimate and most universal reference frame. Given a collection of electrons, characterized by a number density  $n_e(\mathbf{n}, l)$ , that are moving at a velocity with a component along the line of sight  $\beta_l(\mathbf{n}, l)$  (in units of speed of light), the CMB temperature variation is given by:

$$\frac{\Delta T_{\text{CMB}}(\mathbf{n}; x)}{T_{\text{CMB}}} = -\sigma_T \int n_e(\mathbf{n}, l) \beta_l(\mathbf{n}, l) dl = -y_{\text{ksz}}. \quad (3)$$

For the sake of consistency with literature (e.g., [Adam et al., 2017](#); [Biffi et al., 2022](#); [Monllor-Berbegal et al., 2024](#); [Ruan et al., 2013](#)) and of facilitating the comparison with the thermal SZ effect, we introduce here a pseudo-Compton-y parameter for the kinetic SZ effect  $y_{\text{ksz}} = \sigma_T \int n \beta dl$  in analogy to the thermal SZ  $y_{\text{tsz}}$ . We note that, while  $y_{\text{ksz}}$  is not effectively equivalent to a Compton-y parameter, it still provides a practical reference for the magnitude of the kinetic SZ signal when comparing it to any corresponding thermal SZ signal.

**2.3 Relativistic corrections and non-thermal component**  
The decade following the first prediction of the thermal and kinetic SZ effects saw developments in the theory regarding relativistic corrections to the thermal SZ and kinetic SZ effects as well as anticipating more exotic SZ effects from non-thermal and ultrarelativistic electron populations (e.g., [Chluba et al., 2012](#); [Chluba et al., 2013](#); [Colafrancesco et al., 2003](#); [Enßlin & Kaiser, 2000](#); [Itoh et al., 1998](#); [Nozawa et al., 1998](#)). In the single scattering approximation (see, e.g., [Chluba et al., 2014](#) and [Chluba & Dai, 2014](#) for an extension to case of multiple scatterings), a static and isotropic distribution of electrons with

optical depth  $\tau_e(\mathbf{n}) = \sigma_T \int n_e(\mathbf{n}, l) dl$  induces a distortion of the measured temperature of the underlying CMB with amplitude:

$$\frac{\Delta T_{\text{CMB}}(\mathbf{n}; x)}{T_{\text{CMB}}} = \frac{4 \sinh^2 x}{x^4} [j(x) - j_0(x)] \tau_e, \quad (4)$$

where  $j_0(x) = x^3(e^x - 1)^{-2}$  is the normalized blackbody spectrum at a given dimensionless frequency  $x$ . The quantity  $j(x)$  encompasses the full information regarding the momentum distribution of the scattering electrons and the relativistic treatment of the inverse Compton scattering process itself,

$$j(x) = \int_0^\infty j_0(x/t) \int_0^\infty f_e(p) P(t; p) dp dt. \quad (5)$$

Here, we introduced the redistribution function  $P(t; p)$  describing the probability for a mono-energetic electron distribution to upscatter a photon to  $t$  times its original frequency (see [Enßlin & Kaiser, 2000](#) for an analytical expression in the single scattering limit). The term  $f_e(p)$  instead denotes the electron momentum distribution, assuming an electron with speed  $v = \beta c$  and a dimensionless electron momentum  $p = \beta\gamma = \beta/\sqrt{1-\beta^2}$ . Different electron populations with a specific spectrum  $f_e(p)$  would thus result in characteristic spectral distortion. For instance, in the case of an electron reservoir in thermal equilibrium at a temperature  $T_e$ ,  $f_e(p)$  follows a relativistic Maxwell-Boltzmann distribution, i.e.,  $f_e(p; T_e) \propto \beta_e p^2 \exp(-\beta_e \sqrt{1+p^2})$  with  $\beta_e = m_e c^2 / k_B T_e$ . This implies that the spectral scaling  $j(x)$  becomes directly dependent on the specific temperature of the scattering electrons and deviates from the non-relativistic thermal SZ case introduced in [Section 2.1](#). As an example, we report in [Figure 2](#) the

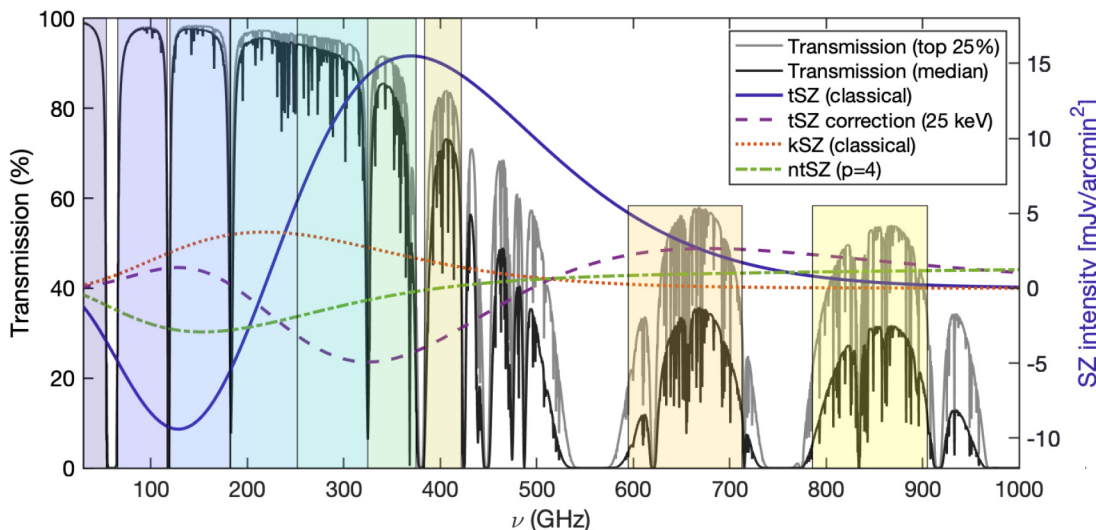


**Figure 2. Various SZ spectra versus transmission in the top quartile (lighter gray) and median (darker gray) atmospheric transmission conditions available at the Chajnantor Plateau ( $\approx 5000$  meters above sea level).** The left y-axis corresponds to transmission, and the right y-axis is appropriate for the thermal SZ (tSZ) intensity for a cluster with  $y_{\text{tsz}} = 10^{-4}$ . The kinetic SZ (kSZ) values assume a line of sight velocity component  $v_l = -10^3$  km/s (i.e. toward the observer, implying a net blueshift in the CMB toward the cluster) and an electron opacity  $\tau_e = 10^{-2}$ . The non-thermal SZ term (ntSZ) is computed assuming a population of mono-energetic relativistic electrons with normalized momentum  $p = 4$ . In all cases, we used SZpack to solve for the SZ spectral distortions ([Chluba et al., 2012](#)), and the am code for atmospheric transmission ([Paine, 2019](#)). The optimal continuum bands of the proposed AtLAST SZ observations, reported in [Table 1](#), are shown as background shaded regions.

relativistic correction to the thermal SZ spectrum in the specific case of  $T_e = 25$  keV. The net result is an overall reduction of the amplitude of the SZ decrement and increment peaks, along with a shift of the crossover point (i.e.,  $\Delta T_{\text{CMB}} = 0$ ) to higher frequencies. Lower and higher temperatures suppress and accentuate such effects, respectively, thus allowing one to use any deviation from the non-relativistic thermal SZ spectrum (Section 2.1) as a direct observational probe of the electron temperature  $T_e$ . In this regard, we note that, over the past few decades, several authors have worked on numerical integrations and asymptotic expansions of the scattering equations, with the specific aim of simplifying the estimation of the scattering integral (Equation 5) and, thus, of any temperature-dependent effect on the measured thermal SZ signal. This has resulted, for instance, in several effective formulations of the relativistic corrections to the thermal SZ effect in terms of electron temperature moments of varying order. We refer to Sazonov & Sunyaev (1998), Itoh *et al.* (1998), Challinor & Lasenby (1998), Chluba *et al.* (2012), Lee & Chluba (2024) for some relevant examples.

In addition to the above relativistic thermal corrections, non-thermal relativistic electrons — from, e.g., aged radio plasmas responsible of the cluster-scale radio haloes (van Weeren *et al.*, 2019) or AGN-driven relativistic outflows (Fabian, 2012; Werner *et al.*, 2019) — are expected to introduce non-trivial contributions to the overall SZ effect (e.g., Acharya *et al.*, 2021; Colafrancesco, 2008; Muralidhara & Basu, 2024; Pfrommer *et al.*, 2005; Prokhorov *et al.*, 2010). It is possible to gain a simple understanding of the expected SZ signature by considering a population of mono-energetic electrons  $f_e(p) = \delta(p - p_0)$ . This simplifies  $j(x)$  only to the integral over the blackbody component  $j_0(x)$ . An example derived under the assumption of  $p = 4$  is shown in Figure 2, showing how the non-thermal SZ effect exhibits a different spectral shape than the thermal SZ effect, making them ideally separable via a spectral analysis.

Finally, we note that the discussion above is only strictly valid under the assumption of an isotropic CMB and scattering fields, and negligible systemic velocities. The inclusion of anisotropies in any of these components would introduce additional contributions to the total SZ spectral distortion, whose amplitudes can however be more than two orders of magnitude smaller than dominant thermal, kinetic, and relativistic SZ signals. These effects will be explored in future works, and, for the moment, we refer the reader to, e.g., Mroczkowski *et al.* (2019), Lee & Chluba (2024), and references therein for more details.

## 2.4 Observational studies

Despite the great theoretical effort, observations of the SZ effects took longer to come to the fore, beginning with pioneering measurements such as Birkinshaw *et al.* (1984) and culminating more recently in several thousand measurements or detections from both low-resolution (1–10') SZ surveys (e.g., Bleem *et al.*, 2020; Bleem *et al.*, 2024; Hilton *et al.*, 2021; Huang *et al.*, 2020; Kornoelje *et al.*, 2025; Planck Collaboration, 2016b). In the past decades, dedicated observations at high angular (subarcminute) resolution have started come to the

fore, providing a detailed and direct perspective on the complex pressure structure of galaxy clusters (Mroczkowski *et al.*, 2019) — ranging from the study of resolved pressure profiles (Adam *et al.*, 2014; Di Mascolo *et al.*, 2019a; Halverson *et al.*, 2009; Kitayama *et al.*, 2020; Kitayama *et al.*, 2023; Romero *et al.*, 2020; Ruppin *et al.*, 2018), to the characterization of mergers (Adam *et al.*, 2017; Basu *et al.*, 2016; Di Mascolo *et al.*, 2019b; Di Mascolo *et al.*, 2021; Kitayama *et al.*, 2016; Mason *et al.*, 2010; Plagge *et al.*, 2013; Sayers *et al.*, 2013) and feedback-driven (Abdulla *et al.*, 2019; Orlowski-Scherer *et al.*, 2022) substructures, ICM turbulence (Adam *et al.*, 2025; Khatri & Gaspari, 2016; Romero *et al.*, 2023; Romero *et al.*, 2024) and of systems in the earliest phases of cluster evolution (e.g., Andreon *et al.*, 2023; Di Mascolo *et al.*, 2023; Gobat *et al.*, 2019; van Marrewijk *et al.*, 2024b).

The proposed millimeter/submillimeter facility, AtLAST, presents novel, unique capabilities that will revolutionize both deep targeted observations aiming for detailed astrophysical studies, as well as wide-field surveys aiming to push SZ observations to much lower mass limits and higher redshifts. Since the epoch of reionization, the majority of baryons have been making their way up to high enough temperatures ( $> 10^5$  K) that their emission is nearly completely undetectable at optical and near-infrared wavelengths, where the majority of telescopes operate. Such a hot phase is an omnipresent feature of the multi-phase cosmic web, representing a relevant contribution to the volume-filling baryonic matter budget on multiple scales — from Mpc-scale filaments of intergalactic medium (IGM), to the intracluster medium (ICM), and down to the circumgalactic medium (CGM) surrounding individual galaxies up to their virial radius (up to few 100s of kpc). Through the SZ effect, the millimeter/submillimeter wavelength regime offers a view of this important component of galaxies and their surrounding environments (clusters, groups, filaments) — components that are largely invisible to all but X-ray and SZ instruments.

## 3 Proposed science goals

Here we provide a summary of the main applications in the context of SZ studies enabled by AtLAST that will allow us to develop a more profound and complete understanding of the thermal history of the Universe, ultimately transforming our understanding of the numerous processes involved in structure formation, evolution, feedback, and the quenching of star formation in overdense environments. In this regard, we refer to Lee *et al.* (2024) and van Kampen *et al.* (2024) for companion AtLAST case studies focused on emission line probes of the cold circumgalactic medium (CGM) of galaxies and on providing a comprehensive survey of high- $z$  galaxies and protoclusters, respectively. Common to all the specific science cases discussed below is the need for a wide field, high angular resolution facility able to optimally probe the full SZ spectrum (Figure 2). More details about the optimal spectral setup, with a discussion on the optimal bands and corresponding noise performance are provided in Table 1. We further refer to Section 4 below for a more extended discussion of the technical requirements for the proposed science goals.

**Table 1. Frequencies, sensitivities and beam sizes for a large SZ survey carried out with AtLAST.** The sensitivity levels are computed assuming standard values for the weather conditions (2<sup>nd</sup> octile) and elevation ( $\alpha = 45$  deg). To account for the variation of the atmospheric transmittance and of the system temperature across a given band, the sensitivity is obtained by considering the in-band inverse root mean square average of the frequency-dependent system equivalent flux densities provided by the AtLAST sensitivity calculator (Klaassen, 2024; see also the online documentation for details on its implementation). The Compton  $y_{\text{tsz}}$  sensitivity estimates are instead computed by considering the in-band integral average of the surface brightness-to-Compton  $y_{\text{tsz}}$  weighted with respect to the atmospheric transmittance levels over the considered frequency range. Here we notice that the actual sensitivity of each individual band to the SZ effect can be significantly hampered by astrophysical background contamination, Galactic foregrounds, and correlated atmospheric noise. As such, the values reported should be taken as a rough estimate of AtLAST’s performance in the context of SZ studies. For a more accurate estimation of the expected thermal and kinetic SZ noise levels, we refer to the discussion in Section 4.3. The width of each band was computed as the frequency range that minimizes the output noise root-mean-square level in the corresponding band for a given integration time. (we refer to Section 4.2 for details). Finally, the noise levels reported in the last column are equivalent to the noise RMS that one would measure over a solid angle of 1 arcmin<sup>2</sup>, and is reported in order to facilitate the direct comparison with wide-field survey instruments.

band	ref. frequency	bandwidth	band edges	beam	sensitivity		survey noise
—	[GHz]	[GHz]	[GHz]	[arcsec]	[ $\mu\text{Jy beam}^{-1} \text{h}^{1/2}$ ]	[ $y_{\text{tsz}} \text{ h}^{1/2}$ ]	[ $\mu\text{K}_{\text{cmb}} - \text{arcmin h}^{1/2}$ ]
2	42.0	24	30–54	35.34	6.60	$7.43 \times 10^{-7}$	2.40
3	91.5	51	66–117	16.22	6.46	$1.05 \times 10^{-6}$	1.27
4	151.0	62	120–182	9.83	7.14	$2.82 \times 10^{-6}$	1.21
5	217.5	69	183–252	6.82	9.22	$2.32 \times 10^{-4}$	1.86
6	288.5	73	252–325	5.14	11.91	$1.37 \times 10^{-5}$	3.71
7	350.0	50	325–375	4.24	23.59	$2.76 \times 10^{-5}$	12.26
8	403.0	38	384–422	3.68	39.98	$6.31 \times 10^{-5}$	34.70
9	654.0	118	595–713	2.27	98.86	$2.16 \times 10^{-3}$	$1.67 \times 10^3$
10	845.5	119	786–905	1.76	162.51	$3.94 \times 10^{-2}$	$3.70 \times 10^4$

### 3.1 Thermodynamic properties of the ICM: radial profiles and small-scale perturbations

The morphological and thermodynamic properties of the ICM represent key records of the many physical processes shaping the evolution of galaxy clusters and groups. Non-gravitational processes — e.g., cooling, AGN feedback, different dynamical states and accretion modes (Battaglia *et al.*, 2012; Ghirardini *et al.*, 2019) — are expected to leave their imprint on the pressure distribution of the ICM in the form of deviations from the radial models derived under universal and self-similar assumptions for structure formation (see, e.g., Arnaud *et al.*, 2010; Nagai *et al.*, 2007; Sayers *et al.*, 2023). On cluster scales, shock fronts induced by cluster mergers as well as cosmological accretion deposit their kinetic energy into the ICM, contributing to its overall thermalization (Ha *et al.*, 2018; Markevitch & Vikhlinin, 2007). On smaller scales, turbulent motion (Khatri & Gaspari, 2016; Romero *et al.*, 2023; Schuecker *et al.*, 2004) can induce significant non-thermal contributions to the ICM pressure support, in turn hampering the validity of the hydrostatic equilibrium assumption. We thus need robust constraints on the level of turbulence affecting the energy budget of the ICM along with an independent census of the “hydrostatic mass bias” — the systematic discrepancy between

the true mass of a galaxy cluster and the value estimated from ICM-related proxies under the assumption of hydrostatic equilibrium (e.g., Biffi *et al.*, 2016) — via a combination of fluctuations and resolved hydrostatic mass information. This will be crucial for inferring corrections to the hydrostatic mass due to the non-thermalized gas (see, e.g., Angelinelli *et al.*, 2020; Ettori & Eckert, 2022) and therefore strengthening the role of thermodynamic quantities for cosmological purposes (Pratt *et al.*, 2019).

As discussed in Section 2.1, the thermal SZ effect provides an optimal probe of the pressure structure and thermal energy of the ICM. In fact, observational models for a statistically relevant sample of clusters are currently limited to the indirect determination of resolved pressure models for clusters up to  $z \lesssim 1$  (Arnaud *et al.*, 2010; McDonald *et al.*, 2014; Sayers *et al.*, 2023). Direct constraints of the properties of the ICM within protoclusters and clusters early in their formation have been obtained for only a handful of extreme systems ( $z > 1$ ; Andreon *et al.*, 2021; Andreon *et al.*, 2023; Brodwin *et al.*, 2016; Di Mascolo *et al.*, 2023; Gobat *et al.*, 2019; Tozzi *et al.*, 2015; van Marwijk *et al.*, 2024b) or limited samples (e.g., Ghirardini *et al.*, 2021b). Despite the significant time investment

with the Atacama Large Millimeter/Submillimeter Array (ALMA; Wootten & Thompson, 2009) or the 100-meter Green Bank Telescope (GBT; White *et al.*, 2022), these observations only allow one to perform a characterization of the physical and thermodynamic state of these early systems for a few select systems. Still, these have generally required the combination with ancillary X-ray observations, due to observational limitations including poor signal to noise or the data being limited to fewer than 5 bands.

In order to gain a radially resolved view of pressure profiles and of their small-scale perturbations for a large variety of clusters (in terms of dynamical state, mass, and redshift; see Figure 3), it is key to have simultaneous access to enhanced sensitivity, high angular resolution, and wide spectral coverage across the millimeter/submillimeter spectrum. These observations are important, as from hydrodynamical simulations the pressure distribution of high- $z$  galaxy clusters are predicted to diverge from the universal pressure models (Battaglia *et al.*, 2012; Gupta *et al.*, 2017), leading to a systematic offset between the mass-to-SZ observable scaling relation for high- $z$  haloes with respect to local ones (Yu *et al.*, 2015). Constraining such deviations is crucial as they carry fundamental information on the complex interplay between all those multi-scale processes — e.g., merger and accretion events, AGN and stellar feedback, turbulent motion — at epochs ( $z > 1$ ) when their impact from galactic to cluster scales are expected to be the strongest. In Figure 3, we provide a comparison between a set of fiducial thermal SZ models derived either from cluster

samples covering different mass and redshift ranges — and, thus, encompassing varied levels of bias due to the intrinsic scatter of the pressure profiles, deviations from self-similar evolution and hydrostatic equilibrium — or from heterogeneous simulations encoding different feedback prescriptions. Each model exhibits specific and characteristic radial behaviors, differing the others at levels that will be easily distinguishable by AtLAST. At the same time, tracing the pressure profiles out to the cluster outskirts will be key to pinpoint and characterize virial and accretion shocks (Anbajagane *et al.*, 2022; Anbajagane *et al.*, 2024; Hurier *et al.*, 2019), whose existence is a fundamental prediction of the current paradigm of large-scale structure formation (e.g., Ryu *et al.*, 2003; Zhang *et al.*, 2021). In particular, the location and properties of their SZ features can be exploited to study the mass assembly of galaxy clusters and to place direct constraints on their mass accretion rate (a quantity otherwise difficult to infer observationally; see, e.g., Baxter *et al.*, 2021; Baxter *et al.*, 2024; Lau *et al.*, 2015; Molnar *et al.*, 2009; Towler *et al.*, 2024). Further, pressure perturbations due to the turbulent motion within the ICM have been measured to result in fluctuations of the Compton  $y_{\text{SZ}}$  signal with fractional amplitude  $\lesssim 10^{-1}$  compared to the underlying bulk SZ signal (Khatri & Gaspari, 2016; Romero *et al.*, 2023). The enhanced sensitivity and calibration stability that will be achieved by AtLAST will allow it to easily probe this level of fluctuations, providing important albeit indirect information on the level of non-thermal pressure support in the ICM (we refer to Romero, 2024 for an extensive discussion). More in general, it is only with the unique technical prospects offered by

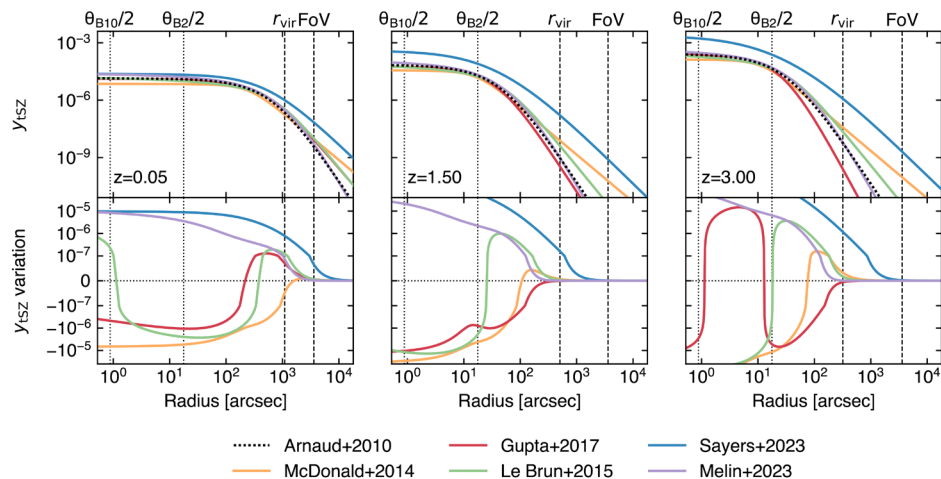


**Figure 3. Observed thermal Compton  $y_{\text{SZ}}$  profiles when considering different fiducial models for the ICM pressure distribution (top panels; Arnaud *et al.*, 2010; Gupta *et al.*, 2017; Le Brun *et al.*, 2015; McDonald *et al.*, 2014; Melin & Pratt, 2023; Sayers *et al.*, 2023) and respective variations (bottom panels) with respect to the universal pressure profile from Arnaud *et al.* (2010), commonly adopted as reference model for the inference of cluster masses.** In this plot, we consider a cluster with fixed mass ( $M_{500} = 10^{14} M_{\odot}$ ) for an arbitrary set of redshifts ( $z = \{0.05, 1.50, 3.00\}$ ). The different profiles are computed on heterogeneous samples in terms of mass and redshift ranges, and thus encode different biases associated to the intrinsic scatter of pressure profiles, deviations from self-similar evolution and hydrostatic equilibrium. Thanks to AtLAST's sensitivity to Compton  $y_{\text{SZ}}$  levels  $\lesssim 10^{-7}$ , it will be possible to characterize such effects, while providing a model for the evolution of ICM pressure across cosmic history. We note that the observed redshift evolution of the profiles is not only due to astrophysical effects or observational biases, but is also due to the assumption a fixed value for the cluster's  $M_{500}$ . Thus the redshift-dependent variation in amplitude and extent of the SZ profiles reflects the critical density and angular diameter distance for the redshift under consideration. As reference, we report as dashed vertical lines the virial radius of the model clusters and the instantaneous field of view expected for AtLAST (see Section 4). We further denote as dotted vertical lines the largest and smallest angular resolution  $\theta$ , achievable with AtLAST, respectively obtained in the proposed Band 2 and Band 10 (see Section 4.2 and Table 1 below).

AtLAST that we will be able to probe to thermal SZ signal down to the levels Compton  $y_{\text{tsz}} \approx 10^{-7}$  (Section 4.3) required to probe the full extent of the ICM pressure distribution (Figure 3), unparalleled by any of the current or forthcoming submillimeter facilities. To provide a simple visualization of AtLAST's expected capabilities, we show in left panel of Figure 4 the thermal SZ signal for a simulated massive cluster extracted from the TNG-Cluster suite Nelson *et al.* (2024). The Compton  $y$  sensitivity that will be targeted by AtLAST will provide the means not only to probe the virial region of galaxy clusters, but also to access in a systematic way the fainter structures populating cluster outskirts. It is also worth noting how the different dependence of the thermal SZ effect and X-ray emission on the electron density — linear and squared, respectively — causes the thermal SZ effect to exhibit a dynamic range between the core and outskirt signals that is significantly smaller than the corresponding X-ray emission. It is precisely this property that makes the SZ effect particularly effective in the study of low-surface brightness features.

### 3.2 Measuring the ICM temperature via relativistic SZ effect

As detailed in Section 2.3, accounting for the relativistic velocities of hot electrons introduces a temperature-dependent distortion of the SZ spectral model (Figure 2). The resulting relativistic SZ effect thus offers a valuable (yet largely unexplored) opportunity to directly measure the temperature of ICM electrons. This represents a key ingredient for enhancing our physical models of galaxy clusters and improving their utility as cosmological probes via more accurate tuning of mass calibrations and scaling relations (e.g., Lee *et al.*, 2020; Perrott, 2024; Remazeilles & Chluba, 2020). At the same time, having simultaneous access to the full ICM thermodynamics (via temperature  $T_e$ , as well as pressure  $P_e$  and density  $n_e$  measurements via the combination of the relativistic and purely

thermal SZ effects) for a large sample of clusters across a wide range of masses and redshift offers the key chance of building a temporal census of the ICM entropy distribution ( $\propto T_e n_e^{-2/3}$ , or  $\propto T_e^{5/3} P_e^{2/3}$  when considering thermodynamic quantities directly probed by the SZ effect; Voit, 2005). The many processes affecting cluster evolution — e.g., AGN and stellar feedback, injection of kinetic energy due to merger activity — are observed to modify the entropy profiles throughout the cluster volumes (e.g., Ghirardini *et al.*, 2017; Pratt *et al.*, 2010; Walker *et al.*, 2012), compared to a baseline model that includes only the non-radiative sedimentation of low-entropy gas driven by gravity (Tozzi & Norman, 2001; Voit *et al.*, 2005). As such, the spatially resolved study of the ICM entropy distribution provides a fundamental proxy of the thermal evolution of cosmic structures as well as the specific dynamical state of galaxy clusters.

Currently, estimates of the relativistic corrections to the thermal SZ effect are limited to a few pioneering studies targeting individual systems (Hansen *et al.*, 2002; Prokhorov & Colafrancesco, 2012) or focusing on stacking analyses (Erler *et al.*, 2018; Hurier, 2016; Remazeilles & Chluba, 2025). Still, even in the case of individual clusters with extremely rich observational spectral coverage (see, e.g., Butler *et al.*, 2022 and Zemcov *et al.*, 2012, focusing on the well-known cluster RX J1347.5-1154), SZ-based inferences of the ICM temperature have commonly resulted in constraints with limited significance. Higher angular resolutions, such as those offered by AtLAST, will be an asset for constraining SZ temperatures. First, the higher angular resolution allows spatially-distinct foregrounds such as radio sources, dusty galaxies and the Galactic dust foreground to be accurately modelled and removed. Second, the extraction of resolved pressure and temperature profiles provides the unique opportunity of performing the physical modeling of the ICM relying solely on the SZ effect.

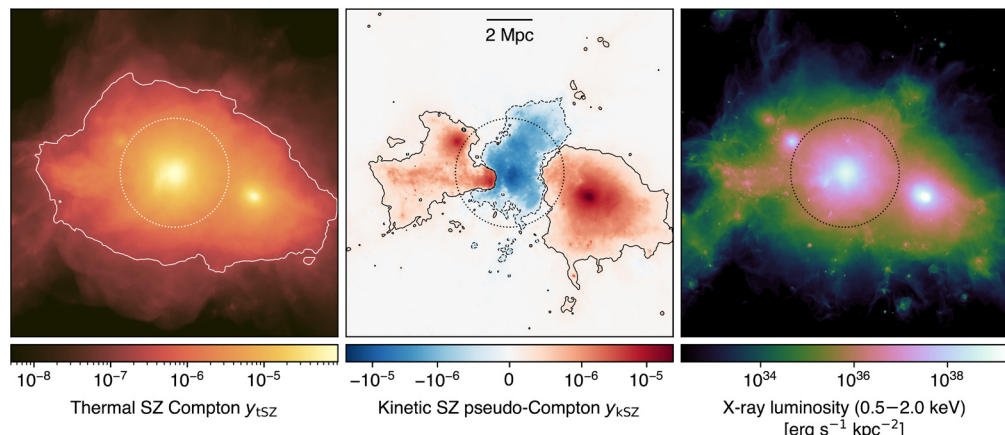


**Figure 4. Thermal (left) and kinetic (center) SZ effects, and X-ray luminosity (right) from a simulated massive cluster undergoing a major merger ( $M_{200} \approx 1.5 \times 10^{15} M_{\odot}$ ,  $z = 0$ ) extracted from the TNG-Cluster simulation (Nelson *et al.*, 2024). The contours in both panels trace levels of  $2 \times 10^{-7}$  both in  $y_{\text{tsz}}$  and  $y_{\text{ksz}}$ , roughly corresponding to the reference SZ depth for a deep AtLAST survey (Section 4.3; see also Section 1 for a definition of the thermal Compton  $y_{\text{tsz}}$  and kinetic pseudo-Compton  $y_{\text{ksz}}$  parameters). As a reference, we mark with a circle the virial radius of the galaxy cluster. This implies that AtLAST will be able to efficiently trace the SZ signal out to the low-density outskirts of clusters. At the same time, it will be possible to directly probe the velocity structure of individual galaxy clusters and their substructures.**

Though access to X-ray-independent temperature constraints will likely be achievable only for a subset of massive haloes (see Section 4.4 below for details), such an SZ-driven approach will still carry a key advantage: they are not biased in the same way as measurements relying on X-ray spectroscopy. In contrast, electron temperatures measured using X-ray data are weighted roughly by the X-ray emission, which scales as density-squared (see e.g., Mazzotta *et al.*, 2004) and is therefore subject to biases due to clumping and compression (e.g., Simionescu *et al.*, 2011). Further, observations can become prohibitive at large cluster radii, due to the low X-ray emissivity, and at high redshift, due to cosmological dimming. It is worth noting that Churazov *et al.* (2015) showed that the self-similar evolution of galaxy clusters would introduce a near independence of redshift of the X-ray luminosity at fixed cluster mass — when this is defined as the mass enclosed in the radius within which the average matter density equals some fiducial cosmic overdensity value (e.g.  $500 \times \rho_{\text{crit}}$ ). Nevertheless, we note that these considerations are valid only under the assumption that the local mass-observable scaling relations are applicable at high redshift. At the same time, both the resolved SZ signal and the respective cluster-integrated flux would still be  $(1 + z)^{3/2}$  larger than the X-ray emission from the same system at a given redshift  $z$ . On the other hand, since the SZ effect is characterized by a surface brightness that is inherently independent of redshift, ICM temperature constraints can in principle be derived without specific limits on the distance of the target systems.

Further, the temperatures inferred using data on the same clusters but taken using different X-ray observatories may suffer large systematic variations due to inherent calibration differences (Migkas *et al.*, 2024; Schellenberger *et al.*, 2015). In contrast, the SZ temperature estimate is pressure-weighted and is therefore predicted to be less biased by emission while being easier to constrain at large cluster radius due to the linear (instead of squared) dependence on density. And even in the case of low-mass (i.e., low-SZ surface brightness; see also Section 3.4) clusters for which it will not be possible to extract resolved SZ-based temperature information, the availability of deep, high angular resolution SZ observations for a large sample of systems will still allow for matching resolution with X-ray observations and to extract resolved full thermodynamic properties of the ICM (see Section 3.1 and Section 5.2.4). An exploratory study of AtLAST's expected capabilities to measure temperature via the relativistic SZ effect is presented in Section 4.4. We refer to this for more details on the impact of the specific spectral setup on the reconstruction of the relativistic SZ effect and on the technical requirements for extending such measurements over broad ranges of cluster masses and redshifts.

### 3.3 Kinematic perspective on large scale structures

The kinetic component of the SZ effect represents a valuable tool for revealing the peculiar motion of cosmic structures (Section 2.2). Nevertheless, its properties — namely its shape, the fact that the kinetic SZ signal is generally weaker than the thermal SZ effect (Figure 2), and that it traces the integrated

line of sight momentum — make the kinetic SZ effect somewhat elusive to measure and interpret. Further, the kinetic SZ spectral signature is consistent with a Doppler shift of the CMB photons, making it spectrally indistinguishable from small-scale primordial CMB anisotropies.

Past targeted kinetic SZ studies (e.g., Adam *et al.*, 2017; Mroczkowski *et al.*, 2012; Sayers *et al.*, 2013; Sayers *et al.*, 2019; Silich *et al.*, 2024a) have already reported direct measurements of the kinetic SZ signal due to the large-scale gas flows associated with merger events. All of these works focused on individual, relatively extreme clusters (either in terms of overall mass, dynamical state, or orientation of the merger direction with respect to the line-of-sight). The broad spectral coverage and the expected sensitivity of AtLAST, in combination with its capability of probing a high dynamic range of angular scales, will instead allow for systematically including the kinetic SZ information in the reconstruction of the thermodynamic characterization of large statistical samples of galaxy clusters and groups. A simple illustration of AtLAST's view of the kinetic SZ effect from a massive system is provided in Figure 4, showing how the expected sensitivity will enable constraints on the bulk motion of individual cluster substructures.

**3.3.1 Cosmological applications.** Statistical measurements of the kinetic SZ effect in disturbed and merging systems represent a crucial ingredient for cosmological studies via direct measurements of the amplitude and the growth rate of cosmological density perturbations (e.g., Bhattacharya & Kosowsky, 2007; Soergel *et al.*, 2018) and have come to the fore in recent years by achieving ever increasing detection significances (e.g., Amodeo *et al.*, 2021; Calafut *et al.*, 2021; Hadzhiyska *et al.*, 2024; Kusiak *et al.*, 2021; Schaan *et al.*, 2021; Vavagiakis *et al.*, 2021), often by introducing novel methodologies (e.g., McCarthy *et al.*, 2024; Patki *et al.*, 2024). Such statistical kSZ studies can also be used to distinguish  $\Lambda$ CDM from alternative cosmologies with modified gravitational forces (Bianchini & Silvestri, 2016; Kosowsky & Bhattacharya, 2009; Mueller *et al.*, 2015).

We note that, while the small scales corresponding to spherical multipoles  $\ell \approx 7000$  are expected to be dominated by the kinetic SZ effect (Smith & Ferraro, 2017), the contamination from the CIB will limit the potential of existing and forthcoming CMB experiments to probe beyond  $\ell \gtrsim 5000$  (Raghunathan & Omori, 2023). AtLAST, on the other hand, when outfitted with the low-noise multi-band direct detection instrumentation we advocate for here, will be able to probe much smaller scales than dedicated CMB experiments improving the sensitivity to the kinetic SZ effect on small-scales (see the discussion in Section 4.3.1 below). For example, AtLAST will be able to make a robust measurement of the kinetic SZ power spectrum with S/N of a few hundreds, a least 2–3× higher than what is expected from CMB-S4 (Raghunathan & Omori, 2023). Since the kinetic SZ signal contains contributions from the relativistic electrons within expanding ionizing bubbles during the epoch of reionization (EoR), the so-called “patchy

kinetic SZ” signal (e.g., Battaglia *et al.*, 2013; Knox *et al.*, 1998; McQuinn *et al.*, 2005; Reichardt, 2016), AtLAST’s improved sensitivity to the kinetic SZ power spectrum on small scales will be crucial to constrain EoR (Gorce *et al.*, 2020; Gorce *et al.*, 2022; Raghunathan & Omori, 2023; Reichardt *et al.*, 2021). In particular, AtLAST, using the full shape information of the kinetic SZ power spectrum, will be able to distinguish between different models of the patchy reionization process (Jain *et al.*, 2024).

One of the limitations of using the kinetic SZ power spectrum is the challenge in disentangling the two main contributions to the large-scale kinetic SZ signal: the high-redshift ( $z \gtrsim 6$ ) patchy reionization signal and the low-redshift ( $z \lesssim 3$ ) component due to bulk peculiar motion of ionized gas in the local Universe. These two signals are expected to have roughly similar shape (Battaglia *et al.*, 2013; Shaw *et al.*, 2012) and the current surveys do not have the sensitivity to distinguish between these two components, given the marginal detection significances of the kinetic SZ power spectrum from current surveys, which is further complicated by the foreground modeling (Gorce *et al.*, 2022; Reichardt *et al.*, 2021). AtLAST, with the high S/N detection of the kinetic SZ power spectrum and cross-correlation with galaxy surveys, will also be able to help in distinguishing between the two sources of the kinetic SZ signal.

Smith & Ferraro, 2017 proposed a new observable to mitigate the degeneracy between the two kinetic SZ sources for EoR studies. This method uses the trispectrum (4-point information) of the kinetic SZ signal which is expected to be dominated by the patchy reionization kinetic SZ effect (Ferraro & Smith, 2018; Smith & Ferraro, 2017). The technique was recently used by the South Pole Telescope (SPT) to set upper limits on the duration of EoR  $\Delta_{z_{re}} < 4.5$  (95 % confidence level) with a non-detection of the kinetic SZ trispectrum signal (Raghunathan *et al.*, 2024). The main challenge for kinetic SZ trispectrum analysis with SPT (Raghunathan *et al.*, 2024) was the foreground mitigation and the multi-band configuration from AtLAST will greatly aid in improving this avenue. The kinetic SZ power spectrum and trispectrum information from AtLAST when combined with other future probes like the large-scale reionization bump and the 21-cm observations, will further improve the EoR constraints significantly compared to what can be achieved by any of these probes individually.

**3.3.2 Resolved measurements.** The possibility of mapping the kinetic SZ effect at high angular resolution will open novel realms in the broader context of cluster studies. The resolved perspective will in fact be essential for correlating the kinetic information with the thermodynamic constraints based on the thermal SZ component and mitigate the spectral degeneracy of the kinetic SZ effect and the underlying primordial CMB anisotropies. On small scales, the velocity structure of the ICM will introduce local (potentially non-gaussian) deviations in the CMB radiation field observed in the direction of a galaxy cluster, allowing for their separation via advanced summary statistical estimators and statistical component separation (e.g., Auclair *et al.*, 2024; Régaldo-Saint Blancard & Eickenberg, 2024). Correlating the velocity structure with

information from facilities at other wavelengths on the baryonic and dark matter content of merging systems will represent a preferential probe of the collisional nature of dark matter (Silich *et al.*, 2024b). In the case of relatively relaxed systems (i.e., with velocity fields not manifesting complex morphologies), the joint analysis of the thermal and kinematic SZ effects would naturally complement the inference of the ICM pressure and temperature distributions with information on the bulk peculiar velocity of galaxy clusters and tighter constraints on the ICM density (Mroczkowski *et al.*, 2019).

The detailed spatial mapping of the kinetic SZ effect could also be used to characterize turbulent motions and to identify their driving dissipation scales which are relevant for feedback mechanisms. This can be done, in particular, by computing the velocity structure function (VSF), defined as the average absolute value of the line of sight velocity differences as a function of projected scale separation. The VSF is an effective way of characterizing turbulent motions and identifying their driving and dissipation scales (see, e.g., Ayromlou *et al.*, 2024; Ganguly *et al.*, 2023; Gatuzz *et al.*, 2023; Li *et al.*, 2020). Determining the driving scale of turbulence would constrain the relative importance of gas motions driven by AGN feedback on small scales and mergers on large scales, while the dissipation scale is sensitive to the microphysics of the ICM, such as its effective viscosity (Zhuravleva *et al.*, 2019). In general, constraints on the small-scale properties of the velocity field associated with turbulent motion (Nagai *et al.*, 2003; Sunyaev *et al.*, 2003), coherent rotation of gas within their host dark matter haloes (Altamura *et al.*, 2023; Baldi *et al.*, 2018; Bartalesi *et al.*, 2024; Baxter *et al.*, 2019; Cooray & Chen, 2002), or merger-induced perturbations (Biffi *et al.*, 2022) can complement the reconstruction of ICM thermodynamic fluctuations (Khatri & Gaspari, 2016; Romero *et al.*, 2023) and the potential mitigation of biases due to non-thermal pressure support (e.g., Angelinelli *et al.*, 2020; Ansarifard *et al.*, 2020; Ettori & Eckert, 2022; Shi *et al.*, 2016) discussed in Section 3.1. Perturbations in the kinetic SZ distribution will result in small-scale kinetic SZ fluctuations more than an order of magnitude smaller than the corresponding thermal SZ component (Biffi *et al.*, 2022; Mroczkowski *et al.*, 2019; Sunyaev *et al.*, 2003) even for massive systems. The clear requirement of extremely demanding observations (along with the difficulty in spectrally disentangling the kinetic SZ effect from the underlying CMB signal; Mroczkowski *et al.*, 2019) have so far limited the possibility of directly measuring any small-scale kinetic SZ feature. However, AtLAST will be able to efficiently measure percent-level deviations from the dominant thermal SZ effect (see, e.g., Section 4.4 below for a discussion in the context of relativistic SZ corrections) and to swiftly survey wide sky areas at  $\sim 1.5 - 35$  arcsec resolution, thus opening a novel observational window on ICM velocity substructures.

### 3.4 Overcoming cluster selection biases

It is becoming generally appreciated that X-ray selected clusters offer a biased view of the cluster population (Andreon *et al.*, 2017; Andreon *et al.*, 2019; Eckert *et al.*, 2011; Maughan *et al.*, 2012; Pacaud *et al.*, 2007; Planck Collaboration, 2011; Planck Collaboration, 2012; Stanek *et al.*, 2006). This is

because, in a given sample, bright clusters are over-represented (see, e.g., [Mantz et al., 2010](#) for discussion of Malmquist and Eddington biases), whereas those systems fainter-than-average for their mass are underrepresented, if not missing altogether. This bias is difficult to correct because the correction depends on assumptions about the unseen population ([Andreon et al., 2017](#); [Vikhlinin et al., 2009](#)). On the other hand, SZ-selected cluster samples are generally thought to offer a less biased view and indeed show a larger variety (e.g., in gas content) than X-ray selected samples (e.g., [Planck Collaboration, 2011](#); [Planck Collaboration, 2012](#)). Comparisons of the X-ray properties of SZ-selected systems (see, e.g., [CHEX-MATE Collaboration, 2021](#)) have highlighted the fact that ICM-based selection biases can depend on the specific morphology ([Campitiello et al., 2022](#)) or the presence of a dynamically relaxed cool core (the so-called “cool-core bias”; [Rossetti et al., 2017](#)).

However, the selection of clusters via their galaxies (i.e., based on the identification of cluster members) or via gravitational lensing (i.e., based on the effect of the cluster potential on the images of background sources) can provide an observational perspective that is potentially unbiased with respect to the thermodynamic state of the ICM. Although methods based on galaxies can still suffer from significant biases due to contamination and projection effects (e.g., [Donahue et al., 2002](#); [Willis et al., 2021](#)), the fact that they are not dependent on the ICM-specific biases have granted the possibility of unveiling the existence of a variety of clusters at a given mass larger than X-ray or current SZ-based approaches. In particular, the low-surface brightness end of the unveiled new population of clusters is changing our view of galaxy clusters. These are found to introduce significant scatter in many ICM-based mass-observable scaling relations ([Andreon et al., 2022](#)), at the very heart of our understanding of cluster physics and broadly used in the context of cluster cosmology. Characterizing such a population of low surface brightness clusters will necessarily require a major leap in the SZ sensitivity with respect to state-of-the-art facilities.

The possibility of performing deep, high angular resolution mapping over wide sky areas offered by AtLAST will allow observers to efficiently detect those clusters that are presently underrepresented in, or entirely missing from, catalogs due to an SZ or X-ray signal inherently fainter than expected from their mass. Indeed, clusters with low X-ray surface brightness tend to have low central values of Compton  $Y_{\text{SZ}}$  of the order of few  $10^{-6}$  (based on [Andreon et al., 2022](#)), at the very limit of long pointed observations with current single-dish telescopes, when not beyond their effective detection capabilities. In combination with X-ray, strong and weak-lensing data, this will allow for a thorough characterization of their physical and thermodynamic state, and for discriminating between any variation in the inherent properties of the intracluster gas and observational biases induced by any astrophysical processes more or less associated with the specific evolution and physics of the target clusters — e.g., energetic AGN feedback, recent merger events, low gas fraction, enhanced clustering of millimeter-bright galaxies.

### 3.5 Identification and thermodynamic characterization of high- $z$ clusters and protocluster

Next generation SZ facilities like Simons Observatory (SO; [Simons Observatory Collaboration, 2019](#)) and CMB-S4 ([Abazajian et al., 2016](#)) will extend our observational window into the high-  $z$  and low-mass realm (see, e.g., [Raghunathan et al., 2022](#) and [Figure 5](#)) of galaxy clusters and protoclusters. Tracing the earliest phases of their evolution will be crucial for constraining the physical origin of the thermal properties of the large-scale structures observed in the nearby Universe.

Nevertheless, current forecasts estimate that next-generation wide-field surveys ([Gardner et al., 2024](#)) will detect less than 20% of the most massive (proto)clusters ( $M_{200} \lesssim 10^{14} M_{\odot}$ ,  $z > 2$ ). This is mostly a consequence of the competing impact of inherently low SZ amplitudes (due to low mass, disturbed state, and severe deviations from full gas thermalization and virialization; [Bennett & Sijacki, 2022](#); [Li et al., 2023](#); [Sereno et al., 2021](#)), the low angular resolution of the facilities, and of the increasing contamination level due to, e.g., enhanced star formation and AGN activity, or possibly due to massive CGM gas and dust reservoirs at high redshift ([Lee et al., 2024](#)). And as already broadly discussed in [Section 3.1](#), extreme limitations are also faced in the case of high angular resolution measurements. Clearly, having access to deep, high angular resolution and multi-band SZ observations will allow observers to simultaneously tackle all such issues, making AtLAST the optimal telescope that will definitively shape our perspective on high-  $z$  (proto)clusters. To provide a direct comparison of AtLAST’s expected capabilities in probing the low-mass and high- $z$  realm with state-of-the-art and planned facilities, we show in [Figure 5a](#) forecast of the mass-redshift detection threshold for different survey strategies proposed for AtLAST. AtLAST will be capable of improving upon current SZ cluster surveys ([Bleem et al., 2020](#); [Bleem et al., 2024](#); [Hilton et al., 2021](#); [Planck Collaboration, 2016b](#)) almost by an order of magnitude in the lowest detectable mass, practically independently of the redshift. Also in the case of the reference next-generation CMB surveys — CMB-S4 ([Abazajian et al., 2019](#); [Raghunathan et al., 2022](#)), CMB-HD ([Sehgal et al., 2019](#); [The CMB-HD Collaboration, 2022](#)) —, the large collecting area and dense focal-plane arrays will allow AtLAST to achieve a 2–4× improvement in the mass detection limit. This has two key advantages: at low redshift, the possibility of probing the low-mass end of the galaxy cluster and group population would make the SZ effect entirely competitive with respect to X-ray observations (see, for instance, the comparison in [Figure 5](#) between the eROSITA sample and the AtLAST mass-redshift limits at  $z \lesssim 0.5$ ); at high redshift ( $z \gtrsim 1.5$ ), this would turn into the possibility of probing all those low-mass haloes that are currently not accessible due to a combination of limited sensitivity and the steep decline of the cosmic halo mass function at high redshift ([Asgari et al., 2023](#); [Cooray & Sheth, 2002](#)).

The correlation of the constraints on the physical and thermodynamic properties of (proto)cluster complexes with the properties of the galactic populations observed within them will further allow for directly linking the evolution of the forming intracluster gas to the multi-phase protocluster environment and

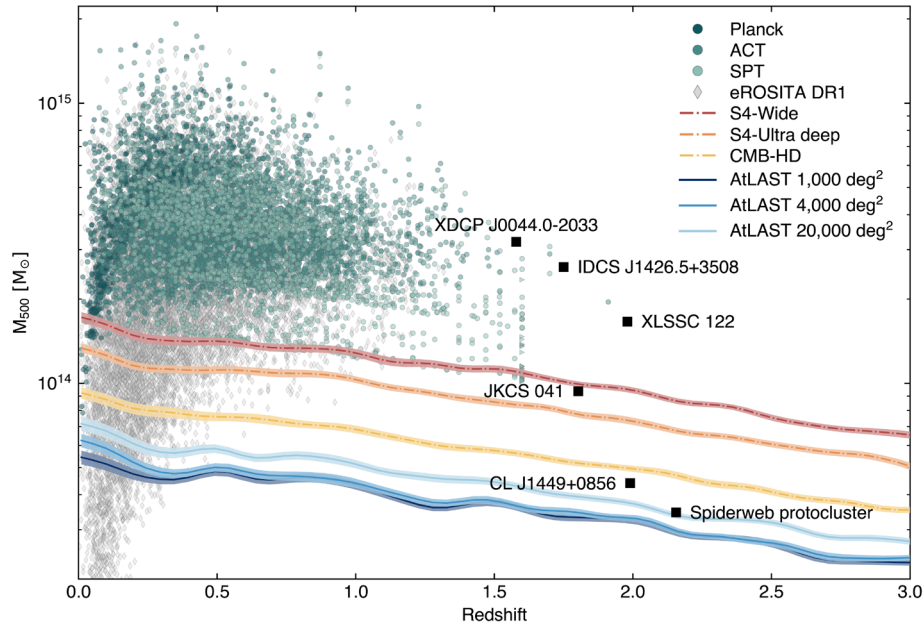


**Figure 5. Mass vs. redshift detection forecast for AtLAST assuming different survey strategies (covering 1000 deg<sup>2</sup>, 4000 deg<sup>2</sup>, and 20000 deg<sup>2</sup>, respectively, for a fixed survey time of 5 years) in comparison with next-generation wide-field millimeter surveys (Abazajian et al., 2016; Sehgal et al., 2019) and the eROSITA all-sky (X-ray) survey (Bulbul et al., 2024).** Poisson realizations of the thermal SZ confusion were simulated in the AtLAST survey case, while the other resolution surveys used Gaussian realizations appropriate in the case where the lower resolution and sensitivity limit the ability to surpass the thermal SZ confusion limit. We refer to Raghunathan (2022) for a more general discussion of the different treatments of the SZ confusion noise. For comparison, we report as green points the clusters from the available SZ survey samples (Bleem et al., 2020; Bleem et al., 2024; Hilton et al., 2021; Kornoelje et al., 2025; Planck Collaboration, 2016b), as well as relevant high- $z$  clusters from the literature: XDCP J0044-2033 (Tozzi et al., 2015), IDCS J1426.5+3508 (Brodwin et al., 2016), JKCS 041 (Andreon et al., 2023), XLSSC 122 (Mantz et al., 2018; van Marrewijk et al., 2024b), CL J1449+0856 (Gobat et al., 2019), and the Spiderweb protocluster (Di Mascolo et al., 2023). This figure is adapted from Raghunathan et al. (2022). AtLAST will provide an order of magnitude improvement with respect to state-of-the-art SZ facilities, as well as X-ray telescopes in the high-redshift domain. Thanks to the improved mapping speed, AtLAST will also outperform next-generation CMB experiments, allowing a systematic exploration of the low-mass and high-redshift population of cosmic haloes.

its only partially understood impact on galaxy formation and evolution (Figure 6). Current multi-wavelength observations have highlighted that the environmental effects might act on Mpc scales and well beyond the more or less virialized regions within these protocluster galaxy overdensities (Alberts & Noble, 2022). These studies however rely on the characterization of environmental processing solely from the perspective of protocluster galaxies (Overzier, 2016). On the other hand, the wide field, the extreme sensitivity and the capability of AtLAST to trace low density regions thanks to the SZ effect will allow for an efficient imaging of the complex galaxy-environment puzzle with a comprehensive glance of the multi-scale and multi-phase nature of high- $z$  (proto)cluster systems.

### 3.6 Impact of AGN feedback and halo heating

Acting in practice as a calorimeter of astrophysical electron populations, the thermal SZ effect can shed light on the interplay of feedback processes and heating of large-scale halos from galactic to cluster scales. This is particularly relevant in the context of AGN studies, in relation to the specific impact of feedback and AGN-driven outflows in contributing to the heating of cosmic haloes (Fabian, 2012). In fact, despite the

importance of supermassive black holes (SMBH) in driving the evolution of cosmic structures, we still have a limited understanding of the complex connection between multi-scale physical properties of SMBH and their host galaxies (Gaspari et al., 2020). Current multi-wavelength observations support a rough duality in the feedback framework (Padovani et al., 2017), with the level of radiative efficiency depending on the specific scenario regulating SMBH accretion (Hlavacek-Larrondo et al., 2022; Husemann & Harrison, 2018). From the perspective of the observational properties of the hot ICM/CGM phase, different feedback models would naturally result in different levels of energy injection and, thus, in deviations from the halo thermal budget expected from virial considerations. At the same time, the strong interaction of winds and jets with the surrounding medium introduces a significant amount of non-thermal support to the overall pressure content — in the form, e.g., of turbulent motion, buoyantly rising bubbles of extremely hot plasma ( $\gtrsim 100$  keV) and associated shock-heated gas cocoons (Abdulla et al., 2019; Ehlert et al., 2019; Marchegiani, 2022; Orlowski-Scherer et al., 2022; Pfrommer et al., 2005). All this implies, however, that gaining a detailed view of the thermodynamic properties of the circumgalactic

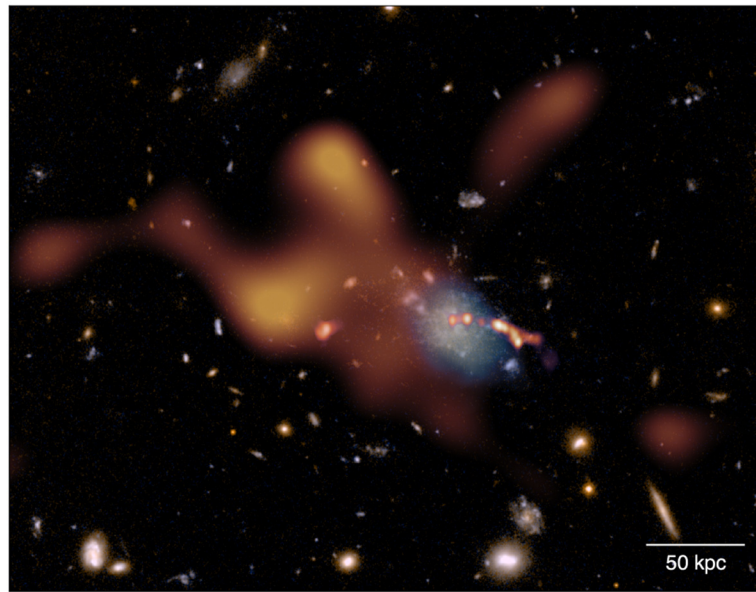


**Figure 6. Composite Hubble Space Telescope (HST) image based on ACS/WFC F475W and F814W data of the Spiderweb protocluster field.** Overlaid (orange) is the thermal SZ signal from the ICM assembling within the protocluster complex as observed by ALMA over a total of more than 12 h of on-source integration time. In a similar amount of time and with the same spectral tuning, AtLAST will achieve a depth comparable to ALMA, however providing a dramatic improvement of  $\sim 10^3$  in field of view and, thus, in overall mapping speed. At the same time, AtLAST will provide a novel perspective on the reservoirs of cold gas (light blue overlay; [Ements et al., 2016](#)) coexisting with the warm/hot phase within protocluster cores (see the CGM science case study by [Lee et al. \(2024\)](#) for a discussion). For comparison, we also include the bright jet of radio emission output from the central galaxy as observed by VLA (the linear east-west feature, shown in red; [Carilli et al., 2022](#)). The present figure is adapted from [Di Mascolo et al. \(2023\)](#) and the corresponding ESO Press Release [eso2304](#).

haloes would allow us to obtain better insights into the AGN energetics and improve our feedback models.

Recently, multiple studies (e.g., [Chakraborty et al., 2023](#); [Grayson et al., 2023](#); [Moser et al., 2022](#)) showed that obtaining high angular resolution observations of the thermal SZ effect (in combination with X-ray observations) would allow for constraining the distinct contribution from different feedback models. In fact, measurements of the integrated thermal SZ signal have already been broadly demonstrated to provide an efficient means for probing the evolution of the imprint of feedback on the thermal energy of cosmic structures ([Crichton et al., 2016](#); [Hall et al., 2019](#); [Yang et al., 2022](#)). Concurrently, the first observational studies based on the cross-correlation of the thermal and kinetic SZ signals (e.g., [Amodeo et al., 2021](#); [Das et al., 2023](#); [Schaan et al., 2021](#); [Vavagiakis et al., 2021](#)) have already shown independent and competitive constraints. Recently, [Coulton et al. \(2024\)](#) demonstrated that the so-called “patchy screening” can provide an alternative and highly complementary perspective on feedback mechanisms. These are however limited mostly to stacking measurements of arcminute-resolution SZ data, and are thus hampered by systematics deriving from the low angular resolution of the wide-field survey data employed (e.g., the impossibility of cleanly separating first and higher-order halo terms; [Hill et al., 2018](#); [Moser et al., 2021](#); [Moser et al., 2023](#); [Popik et al., 2025](#)). On the other hand, targeted observations at higher angular resolution currently comprise an extremely small set of

high- $z$  quasars ([Brownson et al., 2019](#); [Jones et al., 2023](#); [Lacy et al., 2019](#)). The overall limited sensitivity as well as interferometric effects such as poor *uv*-coverage and the filtering of large scales, however, resulted only in what appear to be low significance detections of the SZ signal in the direction of these systems. While these works have been pioneering for high resolution studies, they so far provide little constraining power on the AGN energetics and feedback scenarios.

In fact, as demonstrated using numerical predictions for different feedback models ([Yang et al., 2022](#)), extending our observational constraints to include a broad range of masses and redshifts, as well as distinguishing between different feedback models, will be highly impractical with current high angular (subarcminute) resolution facilities. Further, beyond the large-scale imprints of feedback on cosmic haloes, it is worth noting that strongly asymmetric outflows from quasars, as well as gas inflows, would result in small-scale distortions of the overall SZ signal due to the localized thermal, kinetic and relativistic SZ contributions (see, e.g., [Bennett et al., 2024](#)). Similarly, the inflation of cavities by large-scale jets and the consequent generation of shock fronts and turbulent motion would imprint observable deviations in the global SZ signal in the direction of AGN hosts ([Ehlert et al., 2019](#)). Having access to sensitive, multi-frequency observations as provided by AtLAST would thus be crucial, on the one hand, for reducing any biases associated with the missing decomposition of the different SZ components as well

as any contamination (due to, e.g., millimeter/submillimeter bright emission from the AGN within the studied haloes). On the other hand, it will allow for cleanly dissecting the spectral and morphological features characteristic of the different feedback scenarios.

The SZ signal from AGN-inflated bubbles has instead been robustly detected in one, extreme case (MS 0735.6+7421; [Abdulla et al., 2019](#); [Orlowski-Scherer et al., 2022](#)). Still, the observations required 10s hours with the current-generation MUSTANG-2 instrument ([Dicker et al., 2014](#)), and 100s of hours with the previous-generation CARMA interferometer ([Woody et al., 2004](#)), and were limited to single frequency observations. Since the SZ signal scales as the amount of energy displaced, future observations with current instruments to observe additional, less energetic AGN outbursts could require much more time on the source. As such, this singular example serves largely as a proof-of-principle for further, future resolved studies. We note that some progress will be made in this decade with, e.g., TolTEC ([Bryan et al., 2018](#)), though the Large Millimeter Telescope Alfonso Serran (LMT; [Hughes et al., 2010](#)) was designed to achieve a surface accuracy of  $\sim 50 \mu\text{m}$  (2.5x worse than AtLAST), and regardless will be limited by the atmospheric transmission to  $\nu \lesssim 350 \text{ GHz}$  in all but the most exceptional weather (see, e.g., the site comparison in [Klaassen et al., 2020](#)). Other single dish facilities delivering similarly high resolution will be limited to similar, if not lower frequencies — e.g., the 45-meter Nobeyama Radio Observatory (NRO), the 100-m GBT, the 64-m Sardinia Radio Telescope (SRT; [Prandoni et al., 2017](#)), and the Institute for Millimetric Radio Astronomy (IRAM) 30-meter telescope —, while ALMA has difficulty recovering scales larger than 1' in all but its lowest bands (see [Section 4](#)).

The reconstruction of the thermal properties of the CGM will have an impact beyond the context of the evolution of the physical processes driving the heating of cosmic haloes. In fact, it will be possible to swiftly build a multi-phase picture of the CGM by concurrently tracing its cold phase along with direct constraints on the otherwise elusive warm/hot constituent — comprising  $\approx 80\%$  of the total baryonic material in the CGM overall (e.g., [Schimek et al., 2024](#)). This is an unparalleled feature of (sub)millimeter measurements, that necessarily require a combination of high spectral and angular resolution, along with the capability of mapping large-scale diffuse signals. Clearly, AtLAST will be the optimal facility for such a task. For a broader discussion of the importance of multi-phase CGM studies in the context of galaxy formation and evolution, we refer to the companion AtLAST CGM science case study by [Lee et al. \(2024\)](#).

### 3.7 Galaxy cluster outskirts and intercluster structures

A significant portion of the baryonic content of the Universe at  $z \lesssim 3$  is expected to lie well beyond the virial boundaries of cosmic structures ([Cen & Ostriker, 1999](#)). This diffuse “warm-hot intergalactic medium” (WHIM) is expected to have temperatures  $T_e \approx 10^5 - 10^7 \text{ K}$ , largely invisible at optical wavelengths and generally too low in temperature for all

but the deepest X-ray observations, often being limited to line-of-sight absorption studies ([Nicastro et al., 2018](#)). Obtaining a detailed view of the large-scale WHIM is however crucial. Accurately constraining the actual amount of matter constituting the WHIM will provide fundamental information on the “missing baryons” budget associated to this specific phase of the filamentary IGM (e.g., [Shull et al., 2012](#)). This will be connected to the specific mechanisms driving the heating of large-scale structure on cosmological scales: on the one hand, matter inflows and mergers along large-scale filaments driving strong accretion and virialization shocks ([Anbajagane et al., 2022](#); [Anbajagane et al., 2024](#); [Baxter et al., 2021](#) see also [Section 3.1](#)); on the other hand, the impact of feedback processes and of the environmental preprocessing of galaxies (e.g., [Alberts & Noble, 2022](#); [Fujita, 2004](#)).

To date, the identification and characterization of the physical properties of the filamentary WHIM has been performed mostly through stacked SZ and/or X-ray measurements (e.g., [de Graaff et al., 2019](#); [Singari et al., 2020](#); [Tanimura et al., 2019](#); [Tanimura et al., 2020](#); [Tanimura et al., 2022](#)), and is often dominated by the hottest extremes of the range of temperatures expected for the WHIM (see [Lokken et al., 2023](#) for discussion). Recently, direct SZ imaging of a nearby intercluster bridge was presented in [Hincks et al. \(2022\)](#), which used the combination of ACT+ *Planck* data to reveal details at a much higher spatial dynamic range than the previous results using *Planck* alone. The results are shown in [Figure 7](#). Among the key aspects of this work is the fact that it has served as an invaluable pathfinder for the imaging of IGM substructures via the SZ effect. This is a direct consequence of the key advantage provided by observations of the thermal and kinetic SZ effects — which scale linearly with the electron density (see [Section 2](#)) — over X-ray surface brightness measurements — which scale as the density squared — in the broader context of the study of low-density environments like large-scale filaments and cluster outskirts.

Still, observations like the one by [Hincks et al. \(2022\)](#) clearly highlight how the possibility of proving IGM filaments at modestly high ( $\sim 6\times$ ) resolution is still limited to nearby ( $z \approx 0.05$ ) massive clusters. Deep maps with AtLAST will instead allow for improved spatial dynamic range and higher fidelity, enabling such studies for many more clusters going to both higher redshifts and lower mass regimes.

Thanks to its sensitivity and to the possibility of recovering large scales over extremely wide fields, AtLAST will provide the ideal tool for searching for the presence of the SZ effect in accreting and unbound intergalactic gas surrounding the virialized volume of clusters and groups (we refer to [Figure 4](#) for a simulated perspective on AtLAST’s capability of probing cluster outskirts). In particular, this will allow for routinely exploring intercluster structures in a large number of cluster pairs without the need for time demanding observations. For instance, it will be possible to achieve the same Compton  $y_{\text{SZ}}$  (or surface brightness) sensitivity as in the observation of the A399–A401 observations by [Hincks et al. \(2022\)](#), see also

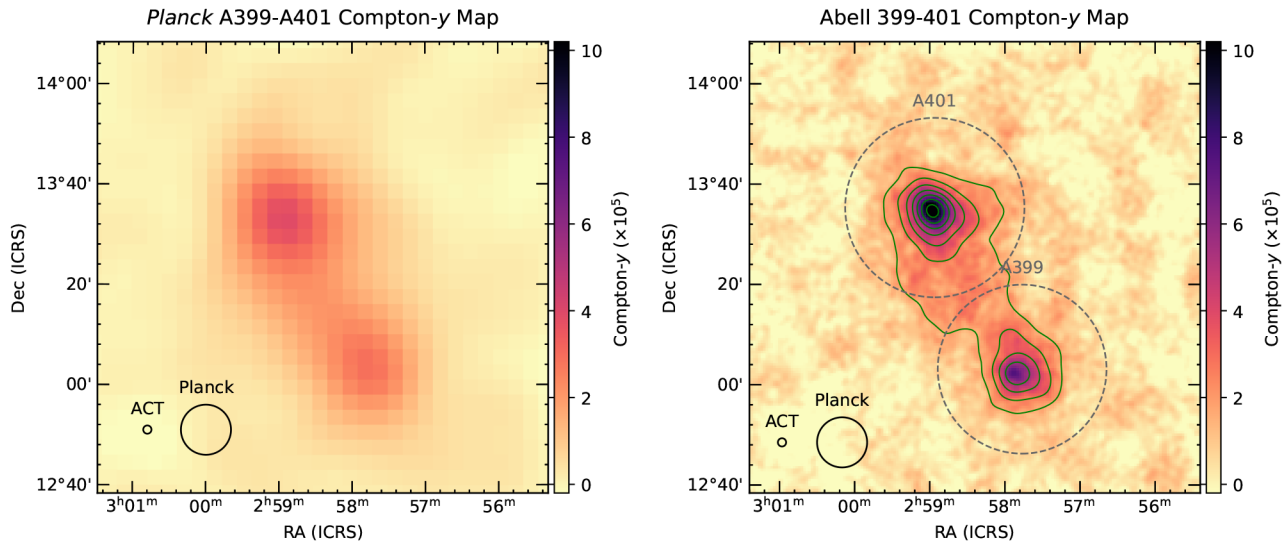


**Figure 7. Comparison of the thermal Compton- $\gamma_{tsz}$  maps produced with *Planck* alone (left, 10' resolution) and by combining *Planck* and *ACT* (right, 1.7' resolution; we refer to [Madhavacheril et al. 2020](#) for details on the data combination procedure).** When considering the same observing frequency, AtLAST will deliver an  $\sim 8.3 \times$  improvement in resolution (e.g., by achieving beam full-width-half-maximum of 9.83" in the proposed 151 GHz Band 4, compared to the  $1.40' \times 1.34'$  ACT beam at 148 GHz), and  $69.4 \times$  the instantaneous sensitivity per beam, with respect to that of ACT (and other 6-m CMB experiments) for the same observing frequencies, allowing one to image substructures in intercluster bridges and directly identify and remove source contamination. The figure has been reproduced and adapted with permission from [Hincks et al. \(2022\)](#).

Figure 7) in less than  $\sim 10$  h of integration, but with better spectral coverage and an order of magnitude improvement in the angular resolution. Clearly, such a comparison is only based on sensitivity considerations and only holds in the case of filaments extending over scales comparable to AtLAST's instantaneous field of view (as in the reported case of A399-A401). Large-scale filtering resulting from either sub-optimal scanning strategies or the limited capability of disentangling any large-scale signals from atmospheric common-mode noise fluctuations can severely impact the possibility of detecting intergalactic filaments extending beyond degree scales (see, however, the discussion in Section 4.1 below). On the other hand, we can consider as a rough lower limit of the expected amplitude for large-scale filaments the results from previous stacking experiments on intergalactic gas. For instance, [de Graaff et al. \(2019\)](#) provide estimates of the average SZ signal to have amplitudes in Compton  $y_{tsz}$  unit of  $\lesssim 10^{-8}$ , corresponding to a maximum amplitude of the thermal SZ signal of  $\gtrsim -64$  nJy beam $^{-1}$  for the decrement, and  $\lesssim 9.5$  nJy beam $^{-1}$  for the increment. Although impractical for performing any direct imaging of WHIM between and around individual galaxies, the extreme observing speed of AtLAST will allow for extending the stacking constraints to higher redshift and smaller physical scales, providing a resolved evolutionary perspective on the hot phase of the cosmic web and the processes driving their thermal properties. Similarly, the combination of the broad spectral coverage with the arcsecond-level angular resolution will allow for reducing contamination from inter-filamentary structures, either in the form of a Poisson

SZ noise from small-mass haloes within the filaments themselves or of bright (sub)millimeter emission from individual galaxies. At the same time, this will provide the broad spectral coverage will allow for reducing contamination from inter-filamentary structures, while providing the means for directly inferring robust temperature constraints (currently representing the main limitation for using the SZ effect for determining the overall contribution of WHIM to the missing baryon budget). In this regard, we refer the reader to the discussion about temperature reconstruction using measurements of the relativistic corrections to thermal SZ effect (Section 2.3 and Section 3.2).

### 3.8 Beyond SZ intensity measurements

In the discussion above, we have focused solely on the novel observational opportunities that will be opened by AtLAST's capabilities in observing the SZ effects and, in general, (sub)millimeter sky in total intensity. As summarized in the AtLAST Science Overview by [Booth et al. \(2024a\)](#), other science case studies have clearly highlighted how the integration of polarimetric capabilities will allow for opening up to major observational advances — for instance, for the study of the magnetic field in flaring regions of our Sun ([Wedemeyer et al., 2024](#)) or embedded in the interstellar medium of the Milky Way ([Klaassen et al., 2024](#)) and nearby galaxies ([Liu et al., 2024](#)).

In the context of the SZ effect, the high polarization sensitivity that will be offered by AtLAST could provide the means for

gaining an unprecedented perspective on the polarized counterparts to the dominant SZ terms introduced in [Section 2](#) and [Section 3](#). Any anisotropy in the radiation field — e.g., the quadrupole term of CMB radiation ([Sazonov & Sunyaev, 1999](#)), analogous the generation of primordial CMB polarization ([Hu & White, 1997](#); [Kamionkowski \*et al.\*, 1997](#)) — or in the scattering medium — e.g., in the case of clusters in transverse motion on the plane of the sky ([Sazonov & Sunyaev, 1999](#); [Sunyaev & Zeldovich, 1980](#)) or in the presence of local pressure anisotropies ([Khabibullin \*et al.\*, 2018](#)) — induce characteristic polarization features that carry key information on the collisional nature of ICM, the velocity structure of haloes and large-scale structures, or on the primordial CMB anisotropies (see [Khabibullin \*et al.\*, 2018](#) and [Lee & Chluba, 2024](#) for detailed discussions; we further refer to [Mroczkowski \*et al.\*, 2019](#) for a general review). In fact, as summarised in [Khabibullin \*et al.\* \(2018\)](#), the degree of polarization expected for any polarized SZ component falls below the  $\sim 10\text{--}8$  level, corresponding to a surface brightness  $\lesssim 10$  nK. In turn, directly constraining any polarized contributions to the SZ effect will represent a key challenge in terms of overall polarization sensitivity, decontamination from foreground and background sources, as well as overall polarization accuracy and control of any cross-polarization leakages ([Mroczkowski \*et al.\*, 2025](#); [Puddu \*et al.\*, 2024](#)). Properly forecasting the possibility of measuring the faint polarized SZ effect will thus require a dedicated effort that could include, along with the associated astrophysical effects, any bias associated with specific choices in instrument and optical design for AtLAST, and we leave this for future work.

#### 4 Technical justification

The challenging nature of the proposed exploration of the thermal properties of the multi-scale realm of cosmic structure discussed above — from intergalactic filaments, to the ICM in forming systems and the CGM surrounding individual galaxies — will necessarily require a major leap in our observational capabilities. Here, we provide a brief list of the technical requirements that will be key for pursuing the aforementioned science drivers.

- **Broad spectral coverage.** The different components of the SZ effect exhibit different, well-defined spectral signatures ([Section 2](#)). It is therefore to disentangle the different SZ contributions from each other, as well as from any contaminating signal, given sufficiently broad spectral coverage. Crucial for achieving an optimal spectral separation of the SZ effects is an extensive, multi-band coverage of the entire relevant frequency range accessible by AtLAST.
- **Few arcsecond-level angular resolution.** This will be essential to constrain the thermodynamic properties of the ICM and CGM down to their cores, along with any small-scale structures associated to the tumultuous evolution of galaxy clusters ([Section 3.1](#)) and galaxies ([Section 3.6](#)). At the same time, it will mitigate the contamination due to the emission at (sub)millimeter wavelengths from compact sources associated with

the massive cluster haloes or populating foreground and background fields, allowing for a more effective extraction of the SZ signals.

- **Wide-field capabilities**, aiming at achieving an instantaneous degree-square field of view. This will provide the means for probing the diffuse SZ signal from the warm/hot gas within cluster outskirts, (several) Mpc-intergalactic filaments, and protocluster complexes ([Section 3.5](#) and [Section 3.7](#)), while allowing for efficiently surveying the (sub)millimeter sky in search of the faint end of the cluster population ([Section 3.4](#)).
- **Sensitivity.** Probing inherently faint and diffuse signals — as in the case of IGM filaments ([Section 3.7](#)) or the relativistic and kinetic SZ terms ([Section 3.2](#) and [Section 3.3](#)) — will require an improvement in the noise performance well beyond the reach of state-of-the-art and any forthcoming (sub)millimeter facilities. As discussed in the previous section, we specifically aim at achieving noise levels in units of Compton  $y \lesssim 5 \times 10^{-7}$ .

In this section, we will expand upon such requirements and identify the critical aspects for pursuing the proposed SZ studies with AtLAST.

#### 4.1 Overview of the instrumental requirements

The field of view of a (sub)millimeter telescope represents a key parameter in the context of SZ science. Current large single-dish telescopes lose signals on scales larger ( $\approx 2\text{--}6'$ ; see, e.g., [Adam \*et al.\*, 2015](#); [Andreon \*et al.\*, 2023](#); [Muñoz-Echeverría \*et al.\*, 2023](#); [Okabe \*et al.\*, 2021](#); [Ricci \*et al.\*, 2020](#); [Romero \*et al.\*, 2020](#); [Ruppin \*et al.\*, 2018](#)) than the instantaneous fields of view of their respective high-resolution instruments — e.g., MUSTANG-2 ([Dicker \*et al.\*, 2014](#)), NIKA2 ([Adam \*et al.\*, 2018](#)), TolTEC ([Bryan \*et al.\*, 2018](#)), MISTRAL ([Battistelli \*et al.\*, 2024](#); [Paiella \*et al.\*, 2024](#)) — where much of the most interesting, faint target SZ signals exist. We note that continuum observations using the 12-meter antennas in the ALMA Total Power Array (TPA; [Iguchi \*et al.\*, 2009](#)) suffer even more egregiously from being unable to remove atmospheric contamination due to their limited fields of view. They also suffer from the poor mapping speeds associated with single beam observations, and from relatively small collecting areas. The issue associated with large-scale filtering is arguably more restrictive in the case of interferometric observations, which generally feature maximum recoverable scales that fall within the sub-arcminute regime (e.g., ALMA Bands 4–10; we refer to the [ALMA Technical Handbook](#) for further details). So far, instruments with much larger instantaneous fields of view, which are therefore better able to recover larger scales, have been employed in the context of CMB/SZ survey experiments like the Atacama Cosmology Telescope (ACT; [Swetz \*et al.\*, 2011](#)), the South Pole Telescope (SPT; [Carlstrom \*et al.\*, 2011](#)), SO ([Simons Observatory Collaboration, 2019](#)), CMB-S4 ([Abazajian \*et al.\*, 2016](#)), CCAT (Fred Young Submillimeter Telescope or FYST; [CCAT-Prime Collaboration, 2023](#)). Still, such survey telescopes universally feature small

apertures ( $\leq 10\text{-m}$ ) with correspondingly limited collecting areas, resulting in arcminute-level angular resolution and poor source sensitivity, which leaves these telescopes largely unsuitable for exploring the small-scale morphologies of galaxy clusters and protoclusters (apart from a few systems in the nearby Universe). With its unparalleled combination of high angular resolution and field-of-view, AtLAST will thus be ideally positioned to fill the gap between current and future wide-field survey facilities and high-resolution single-dish and interferometric telescopes, finally opening a (sub)millimeter perspective on the cosmic structures and their multi-scale properties.

In general, larger scales are difficult to recover due to the large, and largely common mode, atmospheric signal which dominates. A field of view of reduced size requires a tailored observational strategy and data reduction pipeline to mitigate signal loss at large scales. Nevertheless, even in such a case, the recovery of astrophysical information beyond the maximum recoverable scales of such facilities would still be severely hampered. This would critically affect many of the proposed science goals, particularly those requiring both wide field of views and extended recoverable scales. Intergalactic filaments are in fact expected to extend over tens of Mpc (e.g., [Galárraga-Espinosa et al., 2020](#)) and, thus, extending over degresscales in the case of nearby superclusters ([Ghirardini et al., 2021a](#)). Similar physical extents are observed also in the case of high-  $z$  protocluster complexes ( $\lesssim 20$  arcmin; see, e.g., [Cantalupo et al., 2019](#); [Hill et al., 2020](#); [Jin et al., 2021](#); [Matsuda et al., 2005](#)). And as shown in [Figure 3](#) and [Figure 4](#), effectively probing the distribution of the ICM thermodynamic properties out to the cluster outskirts requires mapping the SZ signal beyond  $\sim 1$  deg in cluster-centric distance. Therefore, the capability of gaining instantaneous observations of structures extending from few arcminutes up to degree scales will represent a crucial benefit of AtLAST compared to state-of-the-art and future telescopes covering the same observational windows. We note that the expected large-scale performance of AtLAST is currently based on the extrapolation of the results from past and current small-aperture survey telescopes and high-resolution facilities. In fact, as mentioned above, the main single-dish (sub)millimeter facilities currently used for pursuing resolved SZ science have been directly proven to be capable of probing signal on spatial scales comparable to their field of view. This is the case, for instance, of the NIKA ([Adam et al., 2015](#)) and NIKA2 ([Kéruzoré et al., 2020](#); [Muñoz-Echeverría et al., 2023](#); [Ruppin et al., 2018](#)) instruments, whose effective spatial transfer functions are characterized by large-scale half-power widths even  $\sim 2\times$  larger than their fields of view (1.9' and 6.5', respectively). As mentioned above, similar results are obtained also in the case of small-aperture survey telescopes — with, e.g., ACT reporting 1% signal losses for  $\ell \simeq 400$  ([Naess et al., 2025](#)), roughly matching its 22'  $\times$  26' field of view ([Swetz et al., 2011](#)). And at the same time, [Romero et al. \(2020\)](#) demonstrated how proper modelling of atmospheric noise contributions on field-of-view scales could lead to significant enhancements in the effective sensitivity to, and our ability to recover, large-scale spatial modes.

It is crucial to note that present-day pathfinders for AtLAST, such as the 100-m GBT or IRAM 30-m, operate in less optimal sites, under atmospheric conditions that are significantly worse than those available on the Llano de Chajnantor in the Atacama (e.g. [Klaassen et al., 2020](#)). Therefore, while they have exceeded expectations in recovering scales comparable to or larger than their instantaneous fields of view, we expect AtLAST to provide even better performance in terms of atmospheric noise mitigation, large-scale signal recovery, and overall mapping efficiency. The detailed characterization of the expected spatial transfer function of AtLAST and the impact on this of different atmospheric conditions, mapping strategies, spectral bands, and detector array configurations will be explored in a future work. Preliminary tests on a reduced configuration are however already reported by [van Marrewijk et al. \(2024a\)](#), showing results that are consistent with those reported for existing (sub)millimeter facilities.

Multi-band observations are also critical to suppress/mitigate non-SZ signals below the detection threshold, making wide spectral coverage essential for many of the science goals detailed above. Current high resolution facilities on large telescopes have at most three bands, and are limited to relatively low-frequency observations — e.g.  $\leq 350$  GHz for the LMT ([Hughes et al., 2010](#)),  $\leq 270$  GHz for the IRAM 30-meter telescope, and  $\leq 115$  GHz for the 100-meter GBT ([White et al., 2022](#)), the 64-meter SRT ([Prandoni et al., 2017](#)), or any potential single dish component of the ngVLA ([Selina et al., 2018](#)). This implies that any current or next-generation facilities will provide limited constraining power for the relativistic and kinetic SZ, as well as contamination from the cosmic infrared background or diffuse dust contamination.

Most foregrounds should be spatially distinguishable from the SZ signal. However there may be a spatially coincident large-scale dust component originating from within clusters themselves (e.g., [Erler et al., 2018](#)) which makes at least two bands in the range 400–900 GHz indispensable to trace the Rayleigh-Jeans tail of the dust spectral energy distribution and to mitigate biases in the SZ spectral modeling. An additional band at  $\approx 1200$  GHz would be even more helpful to resolve degeneracies between dust and SZ signals, but this is precluded by the severe reduction in atmospheric transmission.

To meet the observational requirements for pursuing the proposed scientific goals ([Section 3](#)), we perceive the most salient instrumentation requirements to be the ability to achieve high continuum mapping speeds over large areas and in multiple bands. This would convert into the key demand of densely filling the telescope focal plane with a large count of multi-frequency detectors. In this regard, the different detectors (e.g., transition edge sensor bolometers or kinetic inductance detectors) already in use in current state-of-the-art continuum cameras — such as MUSTANG-2 ([Dicker et al., 2014](#)), NIKA2 ([Adam et al., 2018](#)), TolTEC ([Bryan et al., 2018](#)) or MISTRAL ([Paiella et al., 2024](#)) — have already demonstrated a high technical readiness level, providing background-limited performance in the (sub)submillimeter the possibility of being read out in large numbers (tens-to-hundreds

of thousands, as noted in [Klaassen et al., 2020](#)) through frequency multiplexing, allowing the construction of large imaging arrays. We further refer to the [AtLAST Memo 4](#) for details on the expected instrumental specifications for AtLAST.

To illustrate the observational capabilities of the proposed AtLAST continuum setup, we generate mock observations using the `maria` simulation library ([van Marrewijk et al., 2024a](#)) and consider a simulated galaxy cluster extracted from the Dianoga hydrodynamical cosmological simulations ([Bassini et al., 2020](#); [Rasia et al., 2015](#)) as input. The results are shown in [Figure 8](#). For comparison, we include simulated observations performed with MUSTANG-2 and jointly with ALMA and the 7-m Atacama Compact Array (ACA; [Iguchi et al., 2009](#)). The clear result is the superior capability of AtLAST in recovering spatial features over a broad range of scales at high significance, while MUSTANG-2 and ACA+ALMA suffer from limited sensitivity and significant large-scale filtering, respectively. We note that, in this test, we are considering only single-band observations at the same frequency to facilitate the comparison. Although ALMA Band 1 offers an improved sensitivity, spatial dynamic range, and field of view compared to Band 3, it still provides a limited sampling of large-scale SZ structures (with a maximum recoverable scale MRS  $\lesssim 1.20'$  when ALMA is in its most compact configuration).

#### 4.2 Optimizing the spectral setup

As mentioned broadly in [Section 3](#) and discussed in the introduction to this section, among the critical aspects for performing a robust reconstruction of the SZ effect is the requirement of cleanly separating the multiple spectral components of the SZ signal from contaminating sources. From a technical point of view, this converts to maximizing the spectral coverage while requesting maximum sensitivity (i.e., lowest noise root-mean-square) for each of the bands. Given the deteriorating atmospheric transmission when moving to higher frequencies, this is not obtained by trivially expanding the effective bandwidth arbitrarily. At the same time, we would like to consider a minimum setup in order not to result in an oversampling of the target spectral range. If a finer spectral sampling would allow for improved capabilities of AtLAST in terms of component separation, each band would entail additional demands in terms of instrument complexity and overall costs.

A summary of the selected bands, specifically optimized to minimize the output noise root-mean-square level per given integration time, is provided in [Table 1](#). [Figure 10](#) provides a direct comparison of the spectral coverage proposed for AtLAST and of other (sub)millimeter facilities, clearly highlighting how AtLAST will be capable of surpassing other telescopes by accessing a uniquely wide frequency range. Our low-frequency

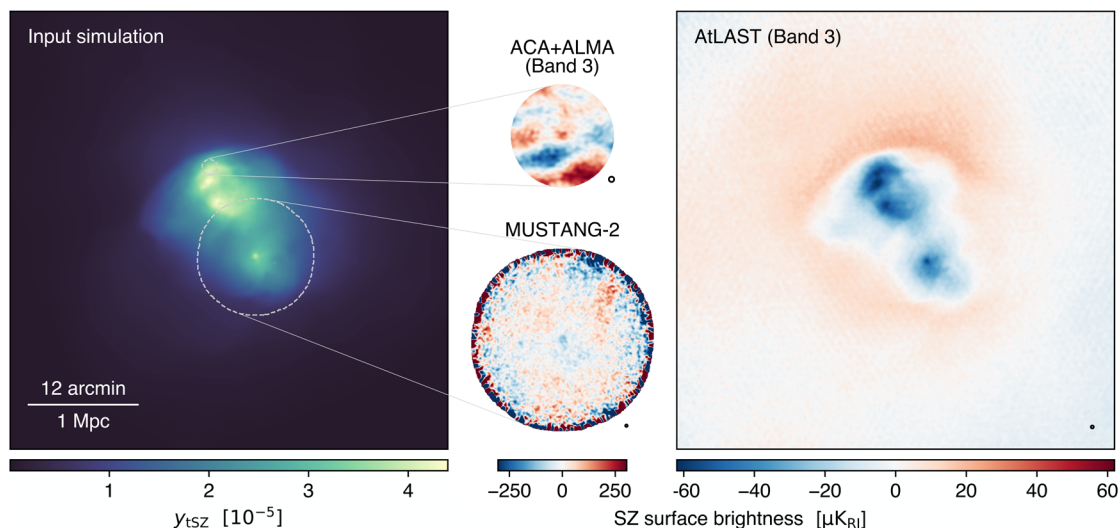


**Figure 8. Compton  $y_{\text{tsz}}$  (thermal SZ signal) distribution for a simulated nearby galaxy clusters ( $M_{500} = 1.28 \times 10^{15} M_{\odot}$ ,  $z = 0.0688$ ; left) as observed by ALMA+ACA in Band 3 (top center), MUSTANG-2 (bottom center), and by AtLAST in Band 3 (right).** The ALMA+ACA and MUSTANG-2 observations were both generated at 90 GHz, the nominal bandpass center of the MUSTANG-2 receiver ([Dicker et al., 2014](#)). The respective beams are shown in the bottom right corner of each panel. The input simulation is extracted from the Dianoga cosmological simulation suite ([Bassini et al., 2020](#); [Rasia et al., 2015](#)). Overlaid as dashed white circles are the ACA+ALMA and MUSTANG-2 footprints. We note that the respective panels on the central column are scaled up arbitrarily with the goal of highlighting any observed features, and do not reflect the relative angular sizes of the fields. For all cases, we consider an on-source time of 8 hours. The mock AtLAST and MUSTANG-2 observations are generated using the `maria` simulation tool (see [van Marrewijk et al., 2024a](#) for details), assuming an AtLAST setup with the minimal detector counts of 50,000 ([Section 4.3](#)). For ACA+ALMA, we employ the `simobserve` task part of the Common Astronomy Software Applications (CASA; [CASA Team, 2022](#)). All the simulated outputs are in  $\mu\text{K}_{\text{RJ}}$  brightness temperature units, with the ALMA and MUSTANG-2 maps shown using the same color scale. Despite the fact the different images are generated adopting a minimal simulation setup (e.g., do not include any foreground and background contamination terms beyond the atmospheric noise), this figure clearly demonstrates the key advantage provided by AtLAST's extended spatial dynamic range and sensitivity for probing the SZ effect from galaxy clusters.

set ( $\lesssim 300$  GHz) extend upon the multi-band set-up proposed for CMB-S4 (Abazajian *et al.*, 2016), shown in forecasts to provide an optimal suppression of the contribution from astrophysical foregrounds and backgrounds (Abazajian *et al.*, 2019). Nevertheless, motivated by the expected coverage of the  $\lesssim 30$  GHz range by future radio facilities (e.g. SKA, ngVLA), we decided not to include the synchrotron-specific 20 GHz band. Still, the spectral setup proposed over the millimeter wavelength range will be useful well beyond the SZ science. Having access to sensitive and high resolution continuum measurements will offer, for instance, the opportunity of probing the high-frequency regime of the free-free and synchrotron emission from individual galaxies to get dust-unbiased perspective on star formation (Condon, 1992; Murphy *et al.*, 2011; Murphy *et al.*, 2012; we further refer to the AtLAST science case by Liu *et al.*, 2024), accessing key information on the coronal origin of the millimeter-wave signature of radio quiet AGN (Behar *et al.*, 2018; del Palacio *et al.*, 2025; Panessa *et al.*, 2019), or shedding light on the elusive Anomalous Microwave Emission (AME) and its potential association with spinning and magnetized interstellar dust (Dickinson *et al.*, 2018).

On the other hand, given the centrality of the high-frequency ( $\gtrsim 500$  GHz) for maximizing AtLAST's capability of separating different SZ components and the signal from contaminating sources (see Section 4.4), we extend the overall spectral coverage beyond 300 GHz to include four additional bands up to 900 GHz. Compared to FYST's choice of survey

bands (CCAT-Prime Collaboration, 2023), our choice will allow one to better sample the high-frequency end of AtLAST's spectral range and, in turn, to gain a better handle on the relativistic SZ effect and on the dust emission from any extended intracluster reservoirs or within individual galaxies (either associated with the clusters, or in background and foreground fields). In this regard, we show in Figure 9 the redshift-dependent spectral model for dusty star-forming galaxies (based on the results by Sommovigo *et al.*, 2022). By probing the full Rayleigh-Jeans tail of the dust spectral energy distribution, it will be possible, on the one hand, to gain thorough insight into the dust content of galaxies (and, thus, star-formation processes; Casey *et al.*, 2014; Schneider & Maiolino, 2024) across a wide range of redshift. On the other, it will provide the means for mitigating the dust contamination of the high-frequency end of the SZ spectrum. We further refer to van Kampen *et al.*, 2024 for a direct comparison of the large-scale distribution of submillimeter bright sources observed by the arcminute-resolution ACT and AtLAST.

It is worth highlighting that the high angular resolution provided by AtLAST will be a key aspect in complementing and significantly enhancing the possibility of cleanly subtracting the emission from compact foreground/background sources, allowing for their clean separation from the SZ effect by means of a full multi-frequency and multi-scale approach. We here note, though, that an accurate spectral modelling of the multi-faceted contributions to the SZ effect (and of their contaminants) can not forego the inclusion of beam chromaticity effects in

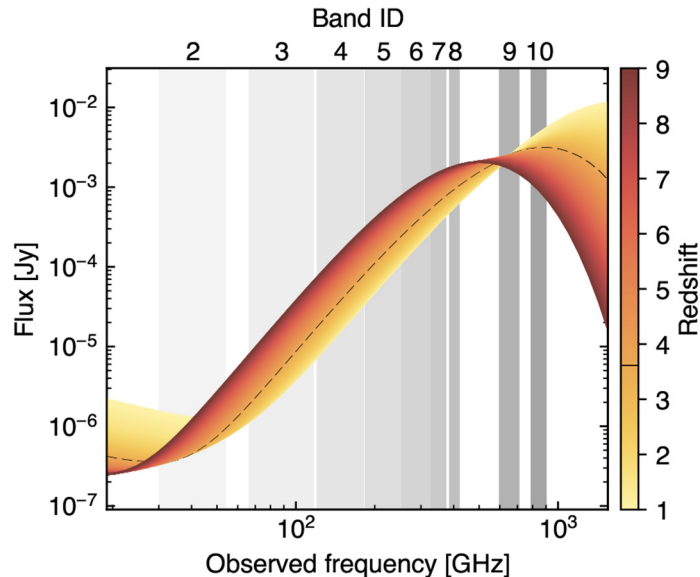


**Figure 9. The high-frequency bands (Band 8-10) will be crucial for optimally sampling the peak of the dust continuum emission from individual high- $z$  background galaxies.** Along with inferring the physical properties of their dust content, this will be crucial for minimizing the contamination of the SZ signal due to cospatial dusty components (see also Section 4.4). As a reference, we show here model emission for star-forming galaxies at varying redshift. Here, the dust contribution is based on the  $z$ -dependent dust temperature model from Sommovigo *et al.* (2022) for a dust mass  $M_d = 10^8 M_\odot$  (consistent with the galaxy REBELS sample; Bouwens *et al.*, 2022). The low-frequency radio component reproduces the radio model from Delvecchio *et al.* (2021), assuming an infrared-to-radio luminosity ratio of  $q_{IR} = 2.646$ . The dashed line denotes the lowest redshift at which the dust emission peak falls within the AtLAST spectral range ( $z \approx 3.60$ ), thus allowing for an accurate modelling of the corresponding spectrum.

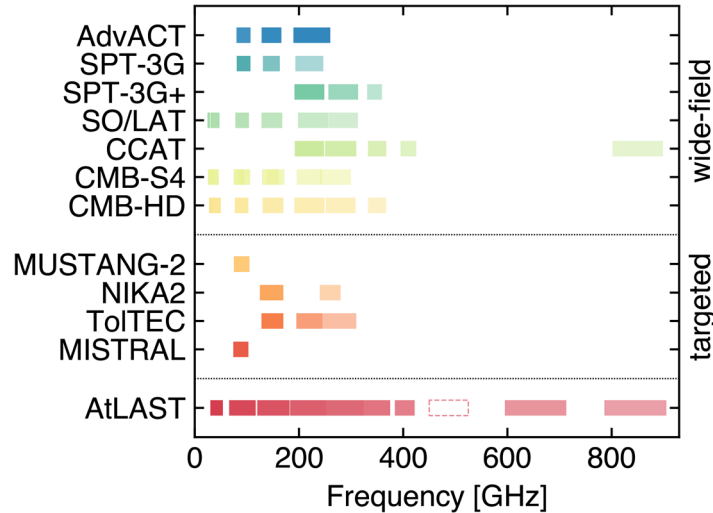


**Figure 10. Comparison of the expected AtLAST bands (see Table 1 and Figure 2) with the spectral coverage for the main previous, existing, or planned (sub)millimeter facilities suitable for dedicated SZ studies.** The listed wide-field survey instruments are: Advanced ACT receivers (Thornton *et al.*, 2016); SPT-3G (Sobrin *et al.*, 2018; Sobrin *et al.*, 2022) and the corresponding SPT-3G+ extensions (Anderson *et al.*, 2022); SO Large Aperture Telescope (LAT) receivers (Bhandarkar *et al.*, 2025; Zhu *et al.*, 2021); CCAT Prime-Cam (Vavagiakis *et al.*, 2018; Vavagiakis *et al.*, 2022); CMB-S4 LAT cameras (Gallardo *et al.*, 2022; Gallardo *et al.*, 2024a); CMB-HD receivers (Sehgal *et al.*, 2019). The reported high-angular resolution instruments employed for targeted SZ observations are, instead: GBT/MUSTANG-2 (Dicker *et al.*, 2014), IRAM/NIKA2 (Adam *et al.*, 2018), LST/ToTEC (Bryan *et al.*, 2018), and SRT/MISTRAL (Paiella *et al.*, 2024). The AtLAST band shown using dashed contours corresponds to the ~500 GHz spectral window, excluded in our forecasts due to the limited sensitivity resulting from the low atmospheric transmission and narrow effective bandwidth. Even when excluding such a band, AtLAST will provide a uniquely wide spectral coverage.

the analysis. The frequency-dependent variation of the angular resolution both for different bands and across the broad passband of a given spectral window can in fact introduce spurious biases in the measured spectral properties of any target continuum emission. A recent forecast analysis by Giardiello *et al.* (2025) has however highlighted how a simple forward modelling treatment of beam chromaticity can significantly mitigate its impact on CMB power spectrum studies. Although we envision adopting a similar approach also in the case of AtLAST SZ measurements, we postpone to future dedicated works the exploration of practical solutions for allowing for a spatio-spectral modelling of high dynamic range observations.

Finally, we note that we are currently investigating the possibility of integrating an additional band covering the  $\sim 500$  GHz atmospheric window, but the low transmission and limited fractional bandwidth are expected to limit the effectiveness of such an addition in terms of an increase of the overall SZ sensitivity. However, we emphasize that AtLAST coverage of the ALMA Band 8 frequencies up to  $v = 492$  GHz would be fundamental for other application in the context of AtLAST science. We refer the interested readers to the companion AtLAST case studies by Lee *et al.* (2024) and Liu *et al.* (2024).

#### 4.3 Sensitivity estimates and detector requirements

As broadly discussed in the previous sections, performing a clean and robust separation of the multiple spectral components

comprising the millimeter/submillimeter astronomical sky will present the biggest observational challenge to achieving our proposed SZ science goals. Any contributions from instrumental noise, Galactic foregrounds, and extragalactic backgrounds that are not properly accounted for in the component separation or spectral analyses can result in residual noise or systematic biases. As such, this represents a limiting factor in the detectability of any SZ signal and could be interpreted as the final SZ depth of the proposed observations.

**4.3.1 Resolved measurements.** To obtain a straightforward estimate of the instrumental performance expected when adopting the proposed spectral setup (Table 1), we extend the analysis performed by Raghunathan (2022) and Raghunathan & Omori (2023) to simulate an AtLAST-like facility. We refer to these works for a more extended description of the technical details on the simulation products.

In brief, we generate multi-frequency mock sky maps, including contributions from the CMB, radio galaxies, and dusty star-forming galaxies, along with either the kinetic and thermal SZ fields depending on whether we are estimating the thermal or kinetic SZ residuals, respectively. The CMB signal is generated as a random realization with its spectrum given by the lensed CMB power spectrum for our reference cosmology as extracted from CAMB (Lewis *et al.*, 2000). The radio and infrared galaxies are modelled assuming a Gaussian

approximation to their Poisson distribution, where we adopt the measurements by the South Pole Telescope (George *et al.*, 2015) as reference power spectra. The thermal SZ distribution is obtained by generating a Poisson distribution of haloes according to the Tinker *et al.* (2008) halo mass function, and then pasting a thermal SZ signal on each halo. The thermal SZ signal is modeled using a generalized Navarro-Frenk-White (Nagai *et al.*, 2007) which has been calibrated using X-ray observations (Arnaud *et al.*, 2010). The dimensionless pressure profile is integrated along the line-of-sight to obtain the Compton  $y_{\text{SZ}}$  which is further integrated within the angular extent of the cluster  $r_{500}$  to get the integrated cluster Compton  $Y_{\text{SZ}}$ . We use the generalization of the Planck  $Y_{\text{SZ}}$ -to-mass scaling relation (Planck Collaboration, 2016a) proposed by Louis & Alonso (2017) and Madhavacheril *et al.* (2017) to introduce a mass and redshift evolution of the signal. For the kinetic SZ term, we consider a flat power spectrum with amplitude  $3 \mu\text{K}^2$ , consistent with Raghunathan & Omori (2023) and based on the SPT results reported by Reichardt *et al.* (2021). Finally, the noise spectrum is assumed to be described as a combination of a white noise component ( $\Delta_r$ ) and an atmospheric component as  $N_\ell = \Delta_r^2 [1 + (\ell / \ell_{\text{knee}})^{\alpha_{\text{knee}}}]$ . The white noise levels are given in Table 1 and the large-scale atmospheric component is modeled using the  $\ell_{\text{knee}}$  and  $\alpha_{\text{knee}}$  with values coming from Raghunathan *et al.* (2022) and Raghunathan (2022) assuming a Chilean survey. For simplicity, we neglect any relativistic and non-thermal SZ component or any Galactic contributions, but note that these could induce major uncertainties in the reconstruction of the thermal and kinetic SZ effects

on large scales (Raghunathan *et al.*, 2022). Similarly, we are here considering the thermal SZ effect from the individual haloes not to be correlated with the signal from radio and dusty star-forming galaxies. However, for clusters close to the SZ confusion noise or in the presence of significant star formation and radio activity (e.g., in the case of protocluster complexes; Section 3.5), the spatially correlated contamination from (sub)millimeter bright sources could degrade the overall sensitivity to the thermal SZ signal. Still, Raghunathan (2022) showed that, in the case of wide-field CMB surveys like CMB-S4, the inclusion of a correlated component in the contamination from compact sources would bias the thermal SZ estimates low by  $\lesssim 0.2\sigma$ . In the case of AtLAST, we expect that the possibility of exploiting its high angular resolution (and, thus, the lower confusion noise) for enhancing the ability of performing a spatial component separation will allow for minimizing the bias from any spatially correlated contamination. We aim a properly testing this in a future work, and, for the moment, we limit ourselves to referring to the analysis in the aforementioned work by Raghunathan (2022). We further refer to this for a detailed discussion of the effect of thermal SZ confusion noise in the context of wide-field SZ surveys, along with a strategy for mitigating its impact on the detection of low-mass haloes.

In Figure 11 we present the result of an optimal internal linear combination of the simulated multi-frequency AtLAST maps when adopting a wide-field survey strategy over a period of 5 years and when covering different sky fractions. AtLAST will be able to probe both the thermal and kinetic

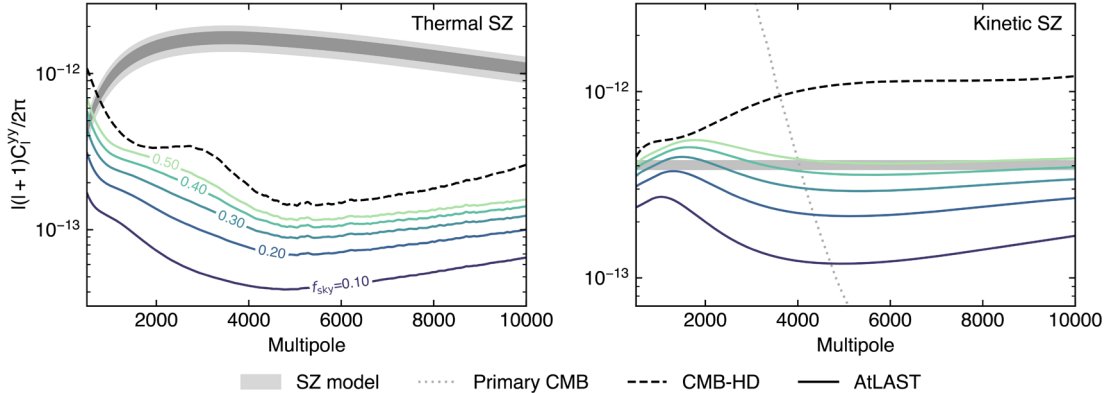


**Figure 11.** Noise power spectra for the thermal SZ Compton  $y_{\text{SZ}}$  (left panel) and kinetic SZ Compton  $y_{\text{kSZ}}$  (right panel) residuals as a function of the sky coverage ( $f_{\text{sky}}$ ) in the case of a wide-field AtLAST survey (adapted from Raghunathan *et al.*, 2022 and Raghunathan & Omori, 2023, which we refer to for details). In both panels, we include as a reference the residual noise curve expected in the case of the CMB-HD survey (dashed black line; Sehgal *et al.*, 2019). The dotted gray line in the right panel shows the temperature power spectrum for the primary CMB converted to Compton  $y_{\text{SZ}}$  units following Equation 3. The shaded band in the left panel denotes the power spectrum for our fiducial thermal SZ sky based on Battaglia *et al.* (2010) with the signal level and the  $1\sigma$  and  $2\sigma$  credible intervals scaled to match the measurements from Atacama Cosmology Telescope (ACT; Choi *et al.*, 2020) and South Pole Telescope (SPT; Reichardt *et al.*, 2021). As a reference kinetic SZ signal (gray band in the right panel), we consider the same power spectrum level  $\ell(\ell+1)C_\ell^{TT} / 2\pi = \ell(\ell+1)C_\ell^{yy} / 2\pi T_{\text{CMB}}^2 = 3 \mu\text{K}^2$  adopted by Raghunathan & Omori (2023) based on the results from SPT (Reichardt *et al.*, 2021). We note that extending the model to multipoles  $\ell \gtrsim 10,000$  would necessarily require a major extrapolation of the thermal and kinetic SZ spectral models over angular scales falling below the resolution of state-of-the-art CMB survey experiments and for which we currently have no constraints. AtLAST will be uniquely positioned to probe at high significance the thermal and kinetic SZ power spectra over this unexplored range of angular scales.

SZ signals down to Compton  $y_{\text{ISZ}}$  and  $y_{\text{KSZ}}$  levels  $\lesssim 5 \times 10^{-7}$  over an extreme dynamic range of spatial scales when considering a deep blind survey approach ( $< 4000 \text{ deg}^2$ ). As shown previously in [Figure 5](#), this implies that the proposed spectral configuration will allow AtLAST to reach, at better angular resolution, a mass limit almost 2× lower than CMB-HD ([Sehgal et al., 2019](#)), a reference concept for a next-generation 30-meter CMB experiment.

**4.3.2 Targeted observations.** When considering narrow-field targeted observations, we estimate that AtLAST will be able to reach a beam-level Compton  $y$  depth of  $\sim 2 \times 10^{-6}$  per hour of integration time. Previous studies (e.g., [Dolag et al., 2016](#); [Raghunathan, 2022](#)) have predicted that the confusion noise floor due to the thermal SZ signal from low-mass haloes — either in the proximity of more massive systems due to physical association or projection effects, or falling below a given detection threshold — amounts to  $y_{\text{ISZ}} \simeq 2 - 5 \times 10^{-7}$  in the case of  $< 10^{13} M_\odot$  galaxy clusters (corresponding to the predicted detection threshold for AtLAST). As such, the estimated sensitivity implies that AtLAST will obtain SZ-confusion-limited observations in  $\sim 100$  h of on source integration time in deep, targeted maps. Nevertheless, this sensitivity estimate corresponds to the residual Compton  $y$  root-mean-square noise obtained when applying a constrained internal linear combination procedure to a simple set of mock targeted observations. We would like to stress that the generation of these simulated AtLAST maps and the consequent sensitivity estimation differs from the analysis presented above for a wide-field survey case. In particular, we generate flat-sky sky realizations at the AtLAST bands including, differently than [Raghunathan \(2022\)](#), both Galactic foregrounds and extragalactic background components. This is intended to propagate any uncertainties associated with the de-projection of large-scale contamination and with the Poisson distribution of extragalactic sources. In particular, the foreground model is based on the `pysm3` models ([Thorne et al., 2017](#)), but we ported and adapted the code to extend the stochastic components down to arcsecond scales. The output mock realization comprises the dust (`d11` model), AME (`default`), free-free (`default`) and synchrotron (`s6`) from the Milky Way. Further, we consider a background signal comprising a random CMB realization, as well as infrared and radio backgrounds from unresolved sources as extracted from the SIDES ([Béthermin et al., 2017](#)) and RadioWeb-Sky simulations ([Li et al., 2022](#)), respectively. To reproduce a clean subtraction of any dominant contaminating compact sources, we excluded all the radio and infrared components with fluxes in at least two bands larger than 3× the corresponding noise root-mean-square. As such, it should be considered as a rough ground reference for the actual depth achievable with future AtLAST measurements. Further, we currently lack accurate models for any of the aforementioned model components down to arcsecond scales, and the adopted extrapolation could introduce unconstrained biases in the noise estimates. Future forecasting studies will particularly investigate how different observation strategies, source subtraction, and modeling techniques will

affect the contamination mitigation and the effective SZ sensitivity.

**4.3.3 Optimal detector count.** Achieving the frontier capabilities discussed in the previous sections will necessarily demand a considerable mapping speed and, thus, a crucial effort in the optimization of the detector array. To estimate a minimal detector count for filling the focal plane, we consider the sensitivity estimates reported in [Table 1](#) as target depths for surveys with varying observing period and sky coverage (see [Figure 5](#)). The results are reported in [Figure 12](#). A detector count  $n_{\text{det}} \simeq 5 \times 10^4$  is sufficient for achieving the sensitivity goal in the case of a narrow survey configuration ( $1000 \text{ deg}^2$ ) both in Band 2 and Band 3, key for tracing the decrement regime of the thermal SZ signal. For the same bands, the same  $n_{\text{det}}$  constraints would allow to achieve a similar survey sensitivity also in the intermediate  $4000 \text{ deg}^2$  case over  $\sim 4 - 5$  years. Nevertheless, extending these considerations to other bands or a wide-field scenario would require a significant increase in  $n_{\text{det}}$ . For instance, in the case of Band 5—crucial for constraining the departures from the thermal SZ effect due to kinetic and relativistic contributions — such a boost would range over almost an order of magnitude.

As broadly highlighted in [Section 3](#), constraining the small-scale fluctuations in the thermal and kinetic SZ effects, while tracing the temperature-dependent relativistic SZ corrections would imply measuring deviations from the global SZ distribution order of magnitudes smaller than the bulk, non-relativistic thermal SZ signal. This would in turn require a significant reduction of any systematic effects hampering the overall calibration accuracy. In this regard, an interesting technical aspect of AtLAST is the plan for integrating a continuous control system feedback loop relying on monitoring sensors to track in real time any deformations in the primary mirror alignment in order to provide rapid response compensation or corrections. Such a “closed-loop” control system will move beyond more common “open-loop” solutions based on the estimation of deformation corrections from external information (e.g., pre-computed look-up tables, or dedicated calibration observations for astro-holography), and will allow for actively tracking the alignment of the primary mirror panels (we refer to [Mroczkowski et al., 2025](#) and [Reichert et al., 2024](#) for details). Ongoing developments — such as the laser system for the SRT ([Attoli et al., 2023](#)) or the wavefront sensing system on the NRO 45-m telescope ([Nakano et al., 2022](#); [Tamura et al., 2020](#)) — are now showing that active closed-loop metrology systems can keep the errors in the beam down to sub-percent levels, meaning the beam will be diffraction limited and stable throughout observations. This in turn will improve the calibration accuracy and reduce systematics (see, e.g., [Naess et al., 2020](#) for discussion of the diurnal effects on the ACT beams) that have been shown to impact CMB and SZ results at the several percent level in the case of passive optics (3 – 5%; [Hasselfield et al., 2013](#); [Lungu et al., 2022](#)), with the result that the daytime data have generally been excluded from cosmological analyses. Future dedicated forecasts will analyze

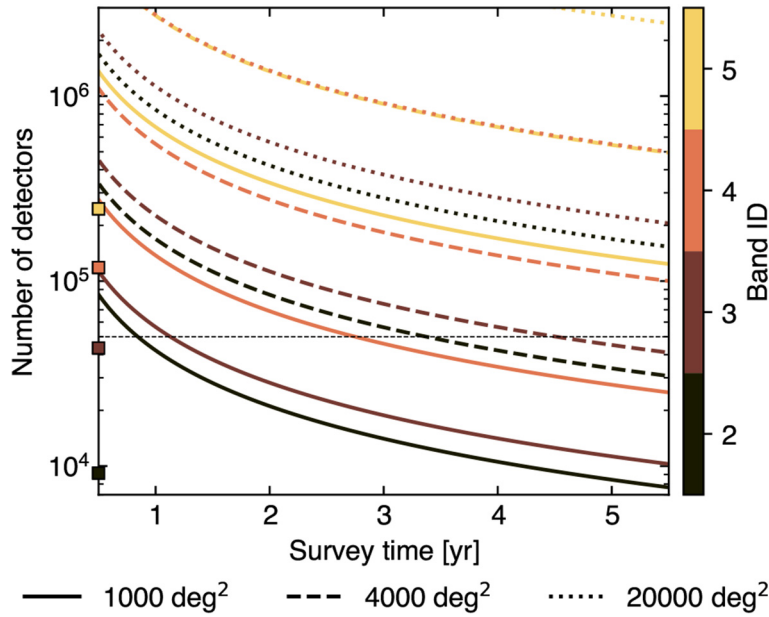


**Figure 12. Required number of detectors to reach the target sensitivity estimates listed in Table 1 for different bands and considering different survey strategies.** For comparison, the squares on the ordinate marks the detector counts required in each band for fully covering a 1 deg<sup>2</sup> field of view. The horizontal line traces the minimal number of detectors (50,000) identified for reaching the target depth in Band 2 and 3 in the case of 1000 deg<sup>2</sup> and 4000 deg<sup>2</sup> surveys. We note that this is consistent with the estimated specifications reported in the AtLAST Memo 4 for the 1<sup>st</sup> generation instruments.

the benefits of metrology for secondary CMB measurements using AtLAST, including improvements to the calibration, reduction of systematics, and the ability to recover larger angular scales on sky. However, the salient takeaway message is that uncertainties in the beam should no longer be a leading source of systematic error.

#### 4.4 Mock reconstruction of the relativistic SZ effect

The relative amplitude of the relativistic component compared to the thermal and kinetic SZ effects makes this modeling task highly challenging. To test the prospects of using AtLAST measurements for performing a spectral separation and analysis of the SZ effect, we thus perform a mock reconstruction of the intracluster temperature using the relativistic SZ effect.

**4.4.1 SZ-only reconstruction.** As a test case, we consider a galaxy cluster with temperature  $T_e = 10$  keV and Compton  $y_{\text{ISZ}} = 10^{-4}$ . We note that, despite representing relatively extreme (but realistic) values, the setup  $(T_e, y_{\text{ISZ}}) = (10 \text{ keV}, 10^{-4})$  is chosen to facilitate this first study of the AtLAST capabilities of providing spectral constraints on temperature-dependent distortions of the thermal SZ effect. A broader exploration of the parameter space will be presented in Section 4.4.3. The amplitude of the SZ signal at each of the selected bands in the minimal spectral set is obtained by integrating the relativistically-corrected thermal SZ (rtSZ) spectrum across each band assuming flat bandpasses. We then obtained estimates for the corresponding uncertainties based on the sensitivity

estimates from the AtLAST sensitivity calculator (Klaassen, 2024). First, we compute the integration time required to achieve a signal-to-noise (S/N) of 50 in Band 8, arbitrarily chosen among the two spectral windows closest to the peak in the rtSZ effect (Figure 2 & Figure 13). The resulting noise root-mean-square is defined as the corresponding uncertainty. The uncertainties  $\delta I$  for each of the remaining bands are thus computed assuming the same integration time as for the Band 8 estimation above, but taking into account both the differing point-source sensitivities and beam sizes across frequency bands,

$$\frac{\delta I(n)}{\delta I(8)} = \frac{\sigma(n)}{\sigma(8)} \times \frac{\Omega(8)}{\Omega(n)}. \quad (6)$$

Here,  $n$  denotes the band index ( $n = \{2, \dots, 10\}$ ), while  $\sigma$  and  $\Omega(v)$  are the flux density RMS and the beam size at a given frequency  $v$ , respectively. The resulting simulated measurements are shown in Figure 13.

The derived SZ measurements can then be used to perform a simple joint inference of the Compton  $y_{\text{ISZ}}$  and electron temperature for the target case. If only lower-frequency data points ( $\lesssim 200$  GHz) are measured, then there is a complete degeneracy between  $T_e$  and the Compton  $y_{\text{ISZ}}$  parameter. In this spectral range, in fact, an increase in the electron temperature reduces the signal in a similar manner as decreasing the overall Compton  $y_{\text{ISZ}}$  amplitude. When higher-frequency points are included, the degeneracy can be minimized as shown in Figure 14. By dropping one band at a time from the fit, we

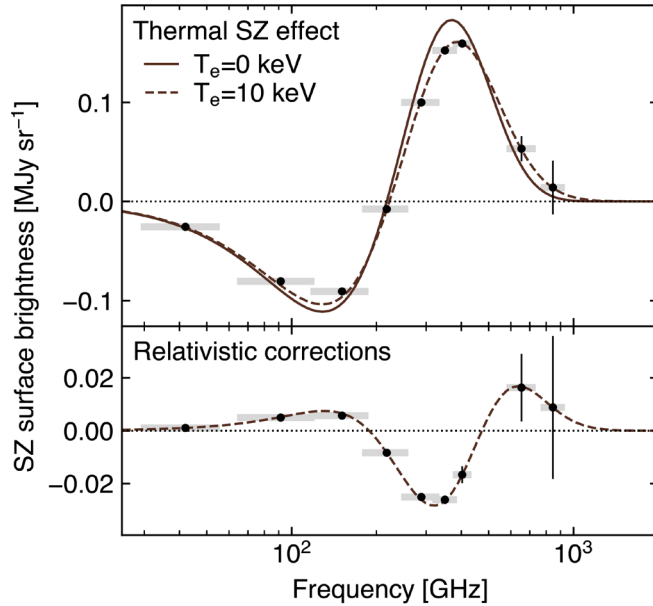


**Figure 13.** Predicted rtSZ measurements for a cluster with a temperature of 10 keV and Compton  $y_{\text{tsz}}$  of  $10^{-4}$ , assuming flat bandpasses in the Bands 2-10 (denoted as gray bands; see also Table 1). For a comparison, we include the spectral signature for the classical formulation of the the thermal SZ effect, i.e., derived under the non-relativistic assumption for the ICM electrons ( $T_e = 0 \text{ keV}$ ; see Section 2.1 and Section 2.3 for a discussion). We assume the same exposure time in each band and account for flux sensitivity and beam size differences, tuned to achieve a SNR = 50 in Band 8. For comparison, the non-relativistic approximation is also shown. The bottom axis shows the difference between the relativistic and non-relativistic spectra.

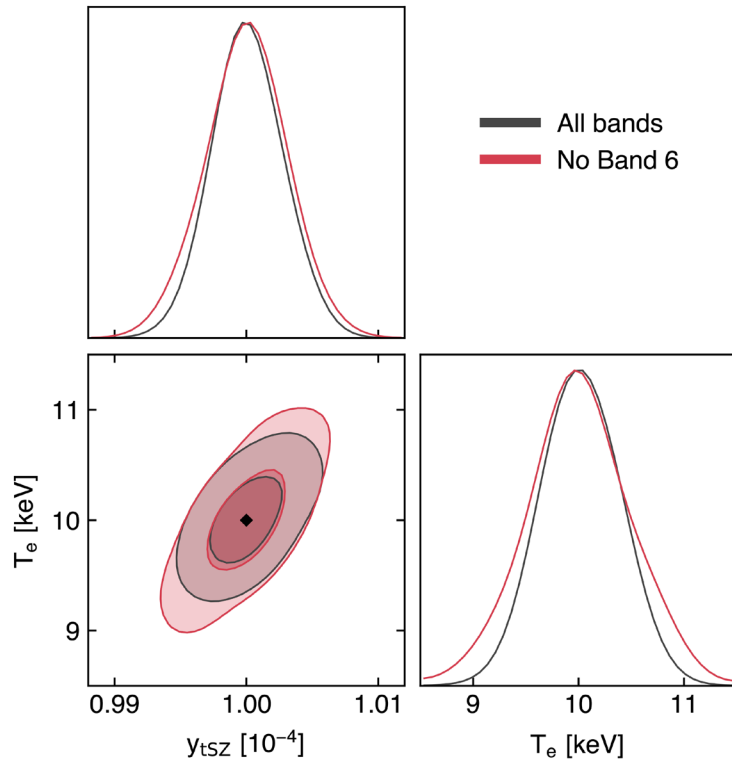


**Figure 14.** Fits to the simulated measurements shown in Figure 13, using all bands (grey) and all except Band 6 (red). The black diamond denotes the input parameters. Despite these are recovered accurately, excluding Band 6 increases the  $y_{\text{tsz}} - T_e$  degeneracy substantially.

find that Band 6 ( $\approx 240$  GHz) has the greatest influence in breaking the degeneracy since the signal-to-noise on the difference between nearly-degenerate models is greatest in this band.

**4.4.2 SZ+dust reconstruction.** So far, we have assumed that the only signal present is the SZ signal. However, in reality there will of course be other astrophysical foregrounds and backgrounds present along the line of sight, resulting in non-negligible contamination of the overall SZ signal observed in the direction of a galaxy cluster. In this test, we however assume that signals that are not spatially correlated to the SZ effect can be removed by means of component separation methods (see Section 4.2) or targeted forward modeling procedures in the case of unresolved compact sources (e.g., Andreon *et al.*, 2021; Di Mascolo *et al.*, 2019a; Kéruzoré *et al.*, 2020; Kitayama *et al.*, 2020; Paliwal *et al.*, 2024; Ruppin *et al.*, 2017). However, previous studies (e.g. Erler *et al.*, 2018) showed that there is a spatially correlated signal within clusters associated with the diffuse dust emission. To understand the impact on the capability of AtLAST in constraining any rtSZ deviation, we repeat the above test by adding an additional dust-like spectral component (Figure 14). In particular, we assume a modified black body signal given by (Erler *et al.*, 2018)

$$I_{dust}(\nu) = A_{dust}^{857} \left( \frac{\nu}{\nu_0} \right)^{\beta_{dust} + 3} \frac{\exp[h\nu_0 / (k_B T_{dust})] - 1}{\exp[h\nu / (k_B T_{dust})] - 1}, \quad (7)$$

where  $\nu_0 = 857$  GHz is chosen as the reference frequency, and  $A_{dust}^{857}$  is the amplitude at this frequency. To generate a dust signal, we use the parameter fits for  $A_{dust}^{857}$ ,  $\beta_{dust}$  and  $T_{dust}$  as provided by Erler *et al.* (2018), and add them as free parameters to our fit with uniform priors on all parameters. The uncertainties on the measurements in each band are the same as in the SZ-only case (Section 4.4.1).

In this case, more bands become necessary to correctly constrain the rtSZ temperature and disentangle the rtSZ and

dust spectral components. The best minimal combination comprises Bands 2, 4, 6, 8 and 10, that provide almost identical constraints to the full set of bands on the rtSZ parameters, while achieving a lower precision on the dust parameters (as shown in Figure 16). Most importantly, it is important to note that the broad spectral coverage offered by the proposed setup allows a clean separation of the rtSZ and dust signals with only a marginal impact on the rtSZ constraints compared to the SZ-only case (Section 4.3.1).

**4.4.3 Required sensitivity and time forecasts.** The reference SNR of 50 employed above was mainly intended to achieve a general perspective on the spectral constraining power of the proposed setup without being limited by the inherent significance of the test SZ signal. Thus, we now investigate what SNR is required to achieve good temperature constraints from rtSZ measurements. In particular, we run similar fits for different values of the reference SNR and different temperatures.

The impact of the varying S/N on the temperature reconstruction is summarized in Figure 17. If we require, for example, an unbiased reconstruction of the electron temperature with a precision of 1 keV, a reference S/N  $\approx 30$  is sufficient for all the temperatures tested. When dust is included, S/N should increase to levels  $\approx 40$  to be able to constrain the temperature for all except the hottest clusters at the reference precision. Such an effect is caused by the increased impact of relativistic corrections on the high frequency end of the SZ spectrum for the hotter clusters, in turn introducing a more prominent degeneracy with the dust spectral component.

Although AtLAST will be able to observe clusters spanning a broad range in mass and redshift (and, hence, temperature), the example analysis presented in the previous section is aimed only at forecasting AtLAST capabilities of measuring relativistic deviations from the standard thermal SZ and not at testing the expected detection threshold as a function of cluster

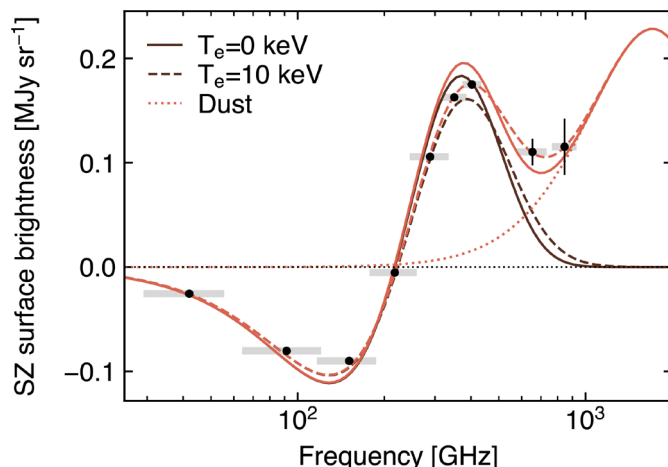


**Figure 15.** Same as Figure 13, but with the addition of a modified black body dust component based on the model from Erler *et al.* (2018). The red dotted line shows the dust signal. The red solid and dashed lines show the total signal from the dust and non-relativistic and relativistic signals respectively.

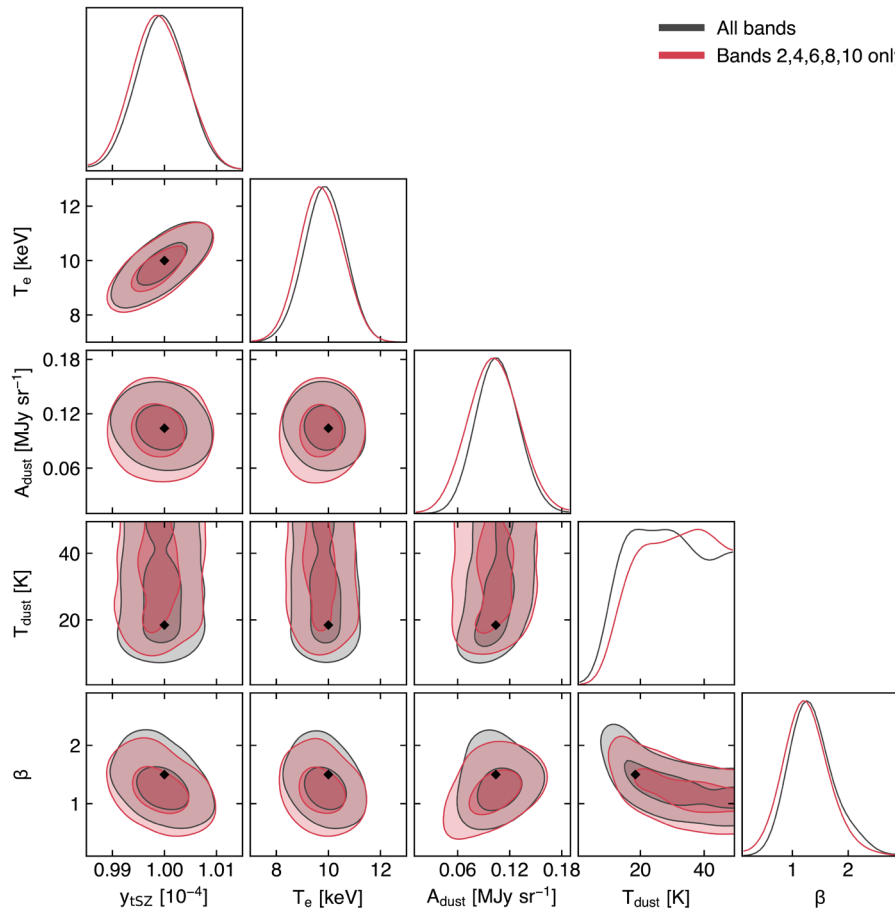


**Figure 16.** Fits to the simulated measurements shown in Figure 15, using all bands (grey) and Bands 2, 4, 6, 8 and 10 only (blue). With this optimal set of five bands, the constraints on the rtSZ parameters are almost equivalent to the constraints with all bands, but we obtain a slightly reduced constraining power on the dust parameters. The dotted diamonds denote the input parameters.

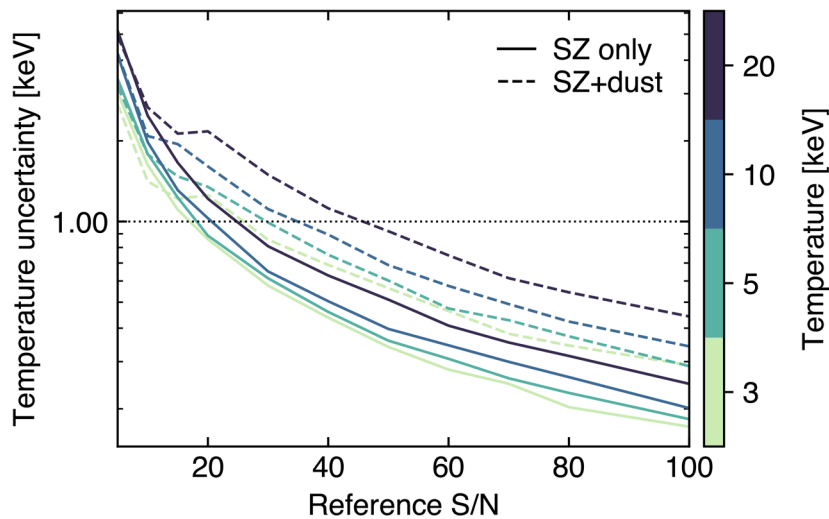


**Figure 17.** Precision achieved on the temperature reconstruction as a function of the signal-to-noise (S/N) in the reference band (384–422 GHz; Band 8) and for a range of ICM temperatures. The horizontal line denotes the target temperature accuracy  $T_e = 1$  keV discussed in the text. A level of  $S/N \geq 40$  will be sufficient for constraining the temperature in any of the tested cases, also in the presence of dust contamination.

properties. To take into account the evolution of the rtSZ effect with the mass and redshift of a galaxy cluster, we aim here at estimating the required observing time to reach a target SNR in Band 8, our reference spectral window (Section 4.4.1).

To do so, we construct cluster signal maps for a range of masses and redshifts, using the physical model given in [Olamiae et al. \(2012\)](#) and [Javid et al. \(2019\)](#). Assuming hydrostatic equilibrium, this model gives us physically consistent pressure and temperature profiles which we use with the SZPACK ([Chluba et al., 2012](#); [Chluba et al., 2013](#)) temperature-moment method to predict relativistic SZ effect signal maps, taking into account the spatial variation of the temperature. The resulting observing time predictions for a reference S/N of 30 are shown in [Figure 18](#). For reasonable observing times (< 16 hours on source) we can get average temperature constraints for most clusters at redshifts up to  $z \approx 0.1$ , and high-mass clusters ( $M_{200} \gtrsim 4 \times 10^{14} M_{\odot}$ ) up to arbitrarily high redshift. It is important to note that the enhanced angular resolution of AtLAST could easily allow one to obtain spatially resolved information on the temperature distribution, once the SNR requirements are satisfied for each spatial element considered for the analysis — e.g., radial bins or spectrally homogeneous regions as generally considered in high-resolution X-ray studies (e.g., [Sanders, 2006](#)).

## 5 AtLAST SZ studies in a multi-probe context

AtLAST will provide an unprecedented speed and spectral grasp across the (sub)millimeter spectrum. This will make AtLAST inherently relevant beyond just SZ science, and will open up possibilities for fundamental synergies in the multi-wavelength and multi-probe exploration of the Universe.

### 5.1 AtLAST scientific cross-synergies

Thanks to the novel multi-instrument design ([Mroczkowski et al., 2025](#)), AtLAST will be aimed at representing a high-impact (sub)millimeter facility with a broad and varied scientific reach ([Booth et al., 2024a](#); [Booth et al., 2024b](#)). As such, this will set the ground for a natural cross-synergy across the different scientific applications identified as part of the AtLAST Science Development effort.

In the case of a wide-field continuum survey discussed [Section 4.3](#), the multi-band coverage and the extended temporal span will make the SZ-driven observations extremely valuable for temporally-dependent studies as for transient surveys ([Orlowski-Scherer et al., 2025](#)). Similarly, the multiple bands and likely polarization sensitivity will be useful in the study of Galactic dust, molecular clouds, and circumstellar discs ([Klaassen et al., 2024](#)), building on the lower resolution results with, for example, the Simons Observatory ([Hensley et al., 2022](#)).

Related to the science goals proposed in this work, the availability of a wide-field spectroscopic survey of the distant Universe ([van Kampen et al., 2024](#)) will immediately enhance the validity of the SZ identification and study of high- $z$  clusters and protoclusters by providing accurate redshift information. The broad spectral coverage achieved thanks to the proposed multi-band setup will actually play a crucial role in maximizing the redshift domain. At the same time, as already mentioned in previous sections, having access simultaneously to constraints on the physical properties of large-scale environments via the SZ effect ([Section 3.5](#)) and on the associated galaxy populations (via the spectral characterization of their cold molecular

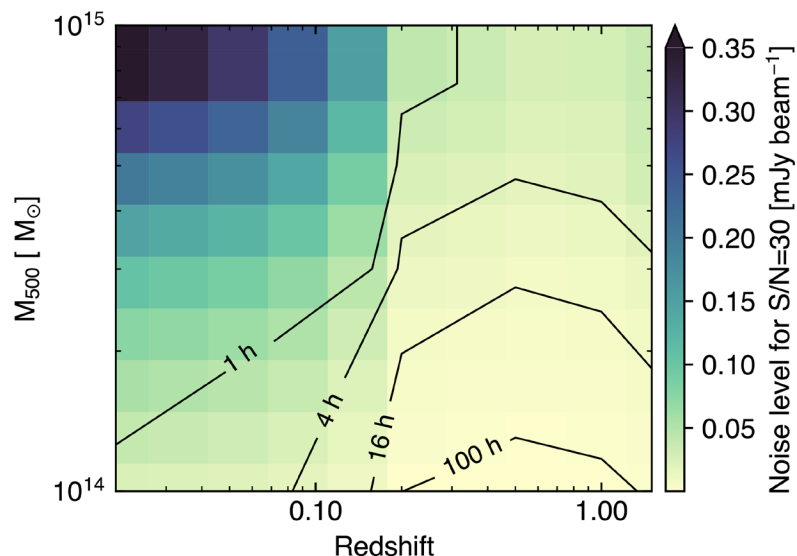


**Figure 18.** Beam-level noise root-mean-square and observing times as a function of cluster redshift and mass  $M_{200}$  required to reach an SNR of 30 in the reference spectral band (384–422 GHz; Band 8), allowing average SZ temperatures to be well constrained. AtLAST will enable inexpensive measurements of the ICM temperature for the most massive systems in the local universe ( $z \lesssim 0.2$ ), but the expected integration time remains relatively limited also for the less massive and distant systems.

gas and the inference of their dust content; see Figure 9) will represent an unprecedented opportunity in the context of galaxy-environment co-evolution studies.

Similarly, the information on the warm/hot component of galactic haloes will be essential for building a comprehensive picture of the diffuse and multi-phase CGM (Lee *et al.*, 2024). A combination of the novel perspective offered by AtLAST on the cold contribution with the tight measurements of the thermal and kinetic properties of such elusive haloes (Section 3.6) will represent the only way for shedding light on the many potential evolutionary routes of the elusive large-scale CGM.

## 5.2 Synergies with other state-of-the-art and forthcoming facilities

In the context of large scale structures, AtLAST's constraints on the multi-faceted SZ effect will be highly complementary to multi-wavelength information on the galaxy motions and distribution, the gravitational potentials of the systems, the X-ray emission, magnetic field structure, and the highly non-thermal and relativistic emission traced by radio emission. Below, we highlight some of the key facilities and experiments that provide the most synergy with AtLAST.

**5.2.1 Radio.** The radio waveband offers information that can complement and enhance many of the science cases outlined above, and next-generation instruments such as the Square Kilometer Array (SKA; Huynh & Lazio, 2013) and the next-generation Very Large Array (ngVLA; Selina *et al.*, 2018) will have the angular resolution and sensitivity required to provide it. On the one hand, getting a clear view of the resolved SZ effect and searching for intrinsic scatter and surface brightness fluctuations requires sensitive detection and removal of contaminating radio sources (e.g., Dicker *et al.*, 2021; Dicker *et al.*, 2024). While this will already be possible with AtLAST's data itself thanks to its spectral coverage and  $\approx 5''\lambda$  mm $^{-1}$  resolution (i.e. 10'' at 2 mm), interferometric observations at lower frequency (SKA-MID) will aid in pinpointing the location and morphology of the radio sources, while also being more sensitive to fainter sources as most will be brighter at lower frequency.

On the other hand, radio information provides a powerful complementary probe of the astrophysics in the cluster, being sensitive to magnetic fields and populations of non-thermal electrons. The reference surveys proposed for the SKA (Prandoni & Seymour, 2015) predict the detection of  $\sim 1\ 000$ s of radio halos with SKA1-LOW, out to redshifts of at least 0.6 and masses  $M_{500} > 10^{14} M_{\odot}$  (Cassano *et al.*, 2015; Ferrari *et al.*, 2015; see also, e.g., Knowles *et al.*, 2021, Knowles *et al.*, 2022, Duchesne *et al.*, 2024 for preliminary results from SKA precursors), along with potential first detections of the polarization of radio halos (Govoni *et al.*, 2015). This offers the opportunity not only to compare the detailed astrophysics of the thermal and non-thermal components of clusters, shedding light on the turbulent properties currently limiting the accuracy of mass estimation (see Section 3.1), but also to potentially discover new populations of clusters via their radio signals. When also observed by AtLAST, these populations will offer insight

into the variation in cluster properties when selecting by different methods (see also Section 3.4). Faraday Rotation Measure observations of polarized sources behind galaxy clusters as well as studies of tailed radio galaxies *in* clusters will enable the study of cluster magnetic fields in unprecedented detail (Bonafede *et al.*, 2015; Johnston-Hollitt *et al.*, 2015a; Johnston-Hollitt *et al.*, 2015b), contributing to our astrophysical understanding and ability to make the realistic simulations crucial for interpreting observations.

Ultimately, the direct correlation of the SZ information with the spatial, spectral, and polarimetric properties of the multitude of radio structures observed in the direction of galaxy clusters will be essential for constraining the detailed mechanisms governing particle (re)acceleration within the ICM (van Weeren *et al.*, 2019). Specifically, there is mounting evidence that the non-thermal plasma observed in the form of (multi-scale) radio halos (e.g., Cuciti *et al.*, 2022; Gitti *et al.*, 2015) as well as intercluster bridges (e.g., Bonafede *et al.*, 2022; Botteon *et al.*, 2020b; Radiconi *et al.*, 2022) originates due to turbulent (re)acceleration (Brunetti & Jones, 2014; Brunetti & Lazarian, 2007; Cassano *et al.*, 2023; Eckert *et al.*, 2017). On the other hand, radio relics are connected to (re)acceleration at shock fronts (Akamatsu & Kawahara, 2013; Botteon *et al.*, 2020a; van Weeren *et al.*, 2017). While it is clear that cluster mergers are driving both processes (turbulence and shocks), our understanding of the physics of (re)acceleration in clusters is limited by two factors: (i) information about the distribution of gas motions in the ICM is currently sparse and usually inferred via indirect methods (for a review, see Simionescu *et al.*, 2019), and (ii) characterizing shocks in the low-density cluster outskirts, where radio relics are usually found, is very challenging. Detailed mapping of the thermal (sensitive to shocks) and kinetic (sensitive to gas motions) SZ signals throughout the volume of a large sample of galaxy clusters (potentially extending out into the cosmic web), and how these signals relate to features observed in the radio band, will be invaluable towards painting a clear picture of the connection between large-scale structure assembly, magnetic field amplification, and cosmic ray acceleration.

Understanding the impact of AGN feedback, on the other hand, (Section 3.6) requires complementary observations of the AGN themselves. Gitti *et al.* (2015) finds that even with early SKA1 (50% sensitivity), all AGN with luminosity  $> 10^{23} \text{ W Hz}^{-1}$  can be detected up to  $z \leq 1$  with subarcsecond resolution, and the radio lobes thought to be responsible for carving out the X-ray cavities should be detectable in any medium – large mass cluster at any redshift in the SKA1-MID deep tier surveys. Moreover, SKA1-MID is predicted to detect intercluster filaments at around 2.5 – 6 $\sigma$  (Giovannini *et al.*, 2015), providing information on their magnetic fields as a complement to the SZ information on their thermodynamic properties (Section 3.7).

At the top of the SKA frequency range, it will be possible to directly access thermal SZ information. Future extensions to the SKA-MID Phase 1 setup (with the integration of the

high-frequency Band 6; we refer to the [SKA Memo 20-01](#) for details) and the ones envisioned for [SKA Phase 2](#) (2030+) will allow SKA to probe the low-frequency ( $\lesssim 24$  GHz) domain of the SZ spectrum, less affected by kinetic and relativistic deviations than the range probed by AtLAST. In fact, [Grainge et al. \(2015\)](#) find that 1 hour of integration is sufficient for obtaining a  $14\sigma$  detection of the SZ effect from a  $M_{200} = 4 \times 10^{14} M_{\odot}$  cluster at  $z > 1$ . On the other hand, the clean perspective offered by AtLAST on the multiple SZ components will provide the means, e.g., for cleanly disentangling the SZ footprint of galaxy clusters from the faint, diffuse signal from mini- to cluster-scale radio haloes, large-scale relics, and back-/foreground and intracluster radio galaxies, enhancing their joint study.

**5.2.2 Millimeter/submillimeter.** Millimetric/submillimetric survey experiments like SO ([Simons Observatory Collaboration, 2019](#)) and its upgrades, CCAT-prime/FYST ([CCAT-Prime Collaboration, 2023](#)), upgrades to the South Pole Telescope ([Anderson et al., 2022](#)), and ultimately CMB-S4 ([Abazajian et al., 2016](#)) will cover roughly half the sky over the next few years to a decade, predominantly in the Southern sky. Along with past and current facilities, these however have  $\sim$  arcmin resolution, well-matched to the typical angular size of clusters in order to optimize their detection but not optimal for peering inside clusters to explore astrophysical effects (aside from few nearby exceptional clusters). Nevertheless, while limited to resolutions approximately  $\sim 8\times$  lower than AtLAST at the same frequencies, their data will provide robust constraints at large scales, lending itself naturally to joint map-making and data combination, as well as valuable source finders for deep AtLAST follow-up. On the other hand, AtLAST will be able to resolve any structures probed by these wide-field surveys, defining a natural and intrinsic synergy.

At still higher resolutions, ALMA will undergo a number of upgrades improving its bandwidth and sensitivity over the next decade. These upgrades are called the Wideband Sensitivity Upgrade (WSU; [Carpenter et al., 2023](#)), which in the context of SZ science could deliver  $2 - 4\times$  ALMA's current bandwidth. Wide field mapping capabilities are however not part of the key goals for the WSU, and it is unlikely ALMA will ever map more than a few tens of square arcminutes. Nevertheless, the improved sensitivity and bandwidth could allow for exploiting ALMA to complement AtLAST observations with a high spatial resolution view of astrophysics through detailed follow-up studies. At the same time, such observations will require AtLAST to recover more extended scales (see [Section 4](#)). The necessity of such a combination will however allow us to fully leverage the synergistic strengths of single-dish and interferometric facilities for gaining an unprecedented view of the hot baryonic content of the Universe, along with its multi-phase counterparts.

**5.2.3 Optical/infrared.** The [Euclid](#) mission ([Euclid Collaboration et al., 2022; Laureijs et al., 2011](#)) has recently started surveying the optical/infrared sky, and is expected to result in the identification of  $\gtrsim 10^5$  galaxy clusters and

protoclusters across the entire cluster era ( $0 \lesssim z \lesssim 2$ ; [Euclid Collaboration, 2019](#)). Complemented with data from the Legacy Survey of Space and Time (LSST) survey by the forthcoming Vera C. Rubin Observatory ([Ivezic et al., 2019](#)), these will represent a wealth of complementary constraints on the cluster and protocluster populations that will be essential for enhancing the scientific throughput of AtLAST in the context of SZ studies. The characterization of the weak lensing footprint of galaxy clusters and groups jointly with resolved information on the thermodynamics of their ICM will enable a thorough exploration of the many processes biasing our cluster mass estimates ([Section 3.1](#)). At the same time, the detailed characterization of the SZ signal from the vast number of weak-lensing selected systems (and, thus, with different selection effects than surveys relying on ICM properties) will allow for studying in detail the origin of the under-luminous clusters ([Section 3.4](#)). Similarly, AtLAST will provide an unprecedented view on the ICM forming within the wealth of high- $z$  galaxy overdensities that will be identified by [Euclid/LSST](#), in turn providing an unbiased means for constraining the physical processes driving the thermalization of protoclusters complexes into the massive clusters we observe at  $z \lesssim 2$ .

More in general, the access to a rich set of imaging and spectroscopic measurements by wide-field surveys — [Euclid](#), Rubin Observatory, and the next generation [Nancy Grace Roman Space Telescope](#) ([Spergel et al., 2015](#)), SPHEREx ([Doré et al., 2014](#)) — along with deep, targeted observation from high-resolution facilities — e.g., JWST ([Gardner et al., 2006](#)), or the upcoming [Extremely Large Telescope](#) — will be greatly complemented by the resolved, wide perspective of AtLAST on the SZ Universe. Tracing the faint warm/hot backbone of large-scale structure ([Section 3.7](#)), as well as tightly correlating resolved thermodynamic constraints for the large-scale cluster environment with the physical properties of the galaxies embedded within them ([Alberts & Noble, 2022; Boselli et al., 2022](#)) and the distribution of the more elusive intracluster light ([Contini et al., 2014](#)), will be essential to shed light on their complex and dynamical co-evolution.

In addition, to facilitate precision cosmology studies with [Euclid/LSST](#), it is imperative to gain a better understanding of the impact of galactic processes on the redistribution of baryons over large scales. Different prescriptions of feedback employed in various cosmological simulations alter the predicted amplitude and scale dependence of the matter power spectra at separations under 10 Mpc on a level that is considerably larger than the statistical uncertainty expected from upcoming cosmology experiments ([Chisari et al., 2019; van Daalen et al., 2020](#)). Mapping the gaseous contents in the low-density outskirts of galaxy groups and WHIM filaments through sensitive AtLAST measurements will thus provide invaluable observational priors necessary to model baryonic feedback for survey cosmology.

**5.2.4 X-ray.** On the X-ray side, [Chandra](#) and [XMM-Newton](#), launched in 1999 with CCDs capable of  $0.5 - 5''$  spatial resolution, are still providing a reasonable thermodynamic

mapping of the brightest regions of the collapsed structures up to redshift  $\sim 1.2$ . The *e***ROSITA** telescope (launched in 2019) has recently delivered the first release of its X-ray all-sky surveys (Merloni *et al.*, 2024) and new catalogs of cluster candidates up to redshift  $z \simeq 1.3$  (Bulbul *et al.*, 2024). Still, the large point spread function ( $\sim 15''$ ) and the limited sensitivity does not allow for resolving the temperature structure of the ICM and any derived quantities (e.g., pressure, entropy, mass) with the exception of nearby and bright galaxy clusters (e.g., Iljenkarevic *et al.*, 2022; Liu *et al.*, 2023; Sanders *et al.*, 2022; Whelan *et al.*, 2022).

The 5 eV spectral resolution of the *Resolve* microcalorimeter onboard **XRISM**, launched in September 2023, has just started a systematic investigation of the gas kinematics in hot, X-ray bright galaxy clusters (XRISM Collaboration, 2025a; XRISM Collaboration, 2025b; XRISM Collaboration, 2025c). However, these studies will be limited by the low ( $\sim 1.3'$ ) angular resolution, small field of view and effective area, especially at soft X-ray energies. This particularly hinders the study of less massive haloes (galaxy groups and CGM) and the mapping of extended cluster outskirts and WHIM filaments. Forthcoming space missions are expected to improve all these performances through the development of next-generation instruments with higher both spectral and spatial resolutions over a wider field of view and with a larger collecting area: *NewAthena* (expected to be adopted as a L-mission by ESA in 2027 for a launch in 2037) will outperform the current satellites thanks to the larger effective area by an order of magnitude with a spatial resolution better than 10 arcsecs (Cruise *et al.*, 2025); *LEM* (a proposed US Probe mission; Patnaude *et al.*, 2023) is designed to effectively map the thermodynamics and kinematics of the low-density CGM and WHIM using spectral imaging of soft X-ray line emission; *AXIS* (another US Probe proposal) will extend and enhance the science of sensitive, high angular resolution X-ray imaging; HUBS, a Chinese mission with a X-ray microcalorimeter operating in the 0.1-2 keV band over a large field of view (1x1 degree<sup>2</sup>) with  $<1$  arcmin resolution (expected launch: 2031) that will focus on the science of CGM, WHIM and filaments around galaxy clusters (see, e.g., Zhao *et al.*, 2025).

The complementarity of SZ and X-ray measurements of the warm/hot content of cosmic large-scale structures has long represented a valuable asset for a cross-enhancement of the respective astrophysical information. The different dependence of these tracers on the physical properties of the ionized gas has been broadly exploited — from, e.g. obtaining tighter constraints on the thermodynamics of the hot gas in distant clusters and cluster outskirts (e.g., Andreon *et al.*, 2021; Castagna & Andreon, 2020; Ghirardini *et al.*, 2019; Ghirardini *et al.*, 2021b; Lepore *et al.*, 2024; Ruppin *et al.*, 2021) and large-scale filaments (e.g., Akamatsu *et al.*, 2017; Hineks *et al.*, 2022; Planck Collaboration, 2013), to studying local deviations from particle and thermal equilibrium (e.g., Basu *et al.*, 2016; Di Mascolo *et al.*, 2019b; Sayers *et al.*, 2021), deriving detailed morphological models of the three-dimensional distribution of ionized gas (e.g., De Filippis *et al.*, 2005; Kim *et al.*, 2023; Limousin *et al.*, 2013; Sereno *et al.*, 2018;

Umetsu *et al.*, 2015), or obtaining measurements of the Hubble–Lemaître parameter independently of more standard probes (e.g., Bonamente *et al.*, 2006; Kozmányan *et al.*, 2019; Wan *et al.*, 2021).

The enhanced sensitivity, spatial resolution, and mapping speed of AtLAST for various flavors of the SZ effect, combined with the capabilities of next-generation X-ray facilities, will undoubtedly take these already existing synergies one leap further. On the other hand, the novel high spectral resolution imaging capabilities in the soft X-ray band (expected to become available in the next decade with, e.g., *LEM* and *Athena*) will give rise to new opportunities for complementary measurements with the SZ band. Namely, X-ray observations are primarily expected to map the line emission or absorption signals from *metals* in the diffuse, warm-hot gas permeating large-scale structure WHIM filaments or the low-mass haloes of individual L\* galaxies (i.e., with a luminosity equal to the characteristic luminosity of the Schechter function; Schechter, 1976). The X-ray continuum emission from these targets will be swamped by the foreground continuum from our own Milky Way, and extremely difficult to probe (see, for instance, Kraft *et al.*, 2022). The ideal path to obtaining a full picture of the physical properties of this diffuse gas component of the cosmic web, therefore, is to combine diagnostics about the metal content (from X-ray line intensities), metal dynamics (from X-ray line widths and shifts), temperature (from X-ray line ratios and relativistic SZ terms) with the gas pressure cleanly measured through the thermal SZ signal. We can then solve for the gas density (knowing the pressure and temperature), and the gas metallicity (knowing the metal content and gas density). Taking this one step even further, by detecting the kinetic SZ signal from the same gas, it will be possible to compare the velocities of metal-poor (primordial) gas from the kinetic SZ measurements which may be different than the velocities of metals probed from the X-ray lines. This will provide truly groundbreaking information about the circulation of gas and metals in and out of galaxies, by offering the opportunity to map, for instance, metal-rich outflows driven by feedback, and metal-poor inflows driven by accretion from the cosmic web, leading to a revolution in our understanding of galaxy evolution.

## 6 Summary and conclusions

AtLAST will provide a transformational perspective on the SZ effect from the warm/hot gas in the Universe. The high angular resolution enabled by the 50-meter aperture, the extensive spectral coverage, and the extreme sensitivity swiftly achievable over wide areas of the (sub)millimeter sky will provide the unprecedented opportunity to measure the SZ signal over an instantaneous high dynamic range of spatial scales (from few arcsecond to degree scales) and with an enhanced sensitivity ( $\lesssim 5 \times 10^{-7}$  Compton  $y_{\text{SZ}}$ ).

Such a combination of technical advances will allow us to constrain simultaneously the thermal, kinematic, and relativistic contribution to the SZ effect for a vast number of individual systems, ultimately opening a novel perspective on the evolution

and thermodynamics of cosmic structures. Such an unmatched capability will provide the means for exploring key astrophysical issues in the context of cluster and galaxy evolution.

- By resolving the multi-faceted SZ footprint of galaxy clusters, low-mass groups, and protoclusters, it will be possible to trace the temporal evolution of their thermodynamic properties across (and beyond) the entire cluster era ( $z \lesssim 2$ ), over an unprecedented range in mass. The complementary information on the full spectrum of small-scale ICM perturbations that will be accessed thanks to AtLAST's superior resolution and sensitivity will thus allow us to build a complete picture of the many intertwined processes that make galaxy clusters deviate from the otherwise hydrostatic equilibrium and self-similar evolution. At the same time, we will be able to get a complete census of the cluster population, circumventing the inherent biases associated with current cluster selection strategies. Overall, such studies will allow AtLAST to be pivotal in firming the role of galaxy clusters as key cosmological probes.
- The possibility offered by AtLAST of accessing the low-surface brightness regime will open an SZ window on the low-density warm/hot gas within the cosmic large-scale structure — ranging from the characterization of the mostly unexplored properties of the assembling ICM seeds within protocluster overdensities to the barely bound outskirts of galaxy clusters. These represent the environments where the same process of virialization begins. As such, they are ideal for studying how deviations from thermalization, gas accretion, and strong dynamical processes impact the thermal history of galaxy clusters.
- By tracing the imprint on the thermodynamics properties of circumgalactic medium surrounding galaxies and of the cluster cores, AtLAST will allow us to constraint the energetics and physical details of AGN feedback. This will provide the means for moving a fundamental step forward in our understanding of the crucial impact of AGN on the evolution of the warm/hot component of cosmic structures over a wide range of spatial scales and across cosmic history.

To achieve these ambitious goals, it will be essential to satisfy the following technical requirements:

- **Degree-scale field of view.** The superior angular resolution achievable thanks to the 50-meter aperture planned for AtLAST will need to be complemented by the capability of effectively recovering degree-level large scales. Such a requirement is motivated by the aim of mapping the SZ signal from astrophysical sources at low or intermediate redshift that are inherently extended on large scales (e.g., intercluster filaments) and with diffuse signals (e.g., protocluster overdensities).

At the same time, we aim at performing a deep ( $\sim 10^{-7}$  Compton  $y$ ) and wide-field ( $> 1000$  deg $^2$ ) SZ survey, key for effectively probing a varied sample of SZ sources. In turn, our requirement consists of an instantaneous field of view covering  $> 1$  deg $^2$ . Clearly, combining wide-field capabilities with enhanced sensitivity will be highly demanding in terms of minimal detector counts. To reach the target sensitivities reported in Table 1, we forecast that the focal plane array should be filled by  $\gtrsim 50,000$  detectors per spectral band.

- **Wide frequency coverage.** To perform a spectral inference of the multiple SZ components, along with their clean separation from foreground and background astrophysical contamination, it will be crucial to probe the spectral regime from 30 GHz up to 905 GHz with multi-band continuum observations. We specifically identify an overall set of nine spectral bands (centered at 42.0, 91.5, 151.0, 217.5, 288.5, 350.0, 403.0, 654.0, and 845.5 GHz), specifically selected to maximize the in-band sensitivity at fixed integration time. By testing this spectral configuration in the context of a mock spectral component separation, we demonstrated that such a choice allows for achieving a clean separation of multiple SZ components, as well as of the signal from dominant contamination sources.
- **Sub-percent beam accuracy.** An accurate calibration will be essential for reducing potential systematics in the small-amplitude fluctuations of the SZ signal associated with local pressure and velocity perturbations, or to relativistic distortions. As such, we require a sub-percent level control of the beam stability.

## Ethics and consent

Ethical approval and consent were not required.

---

## Data availability

No data are associated with this article.

## Software availability

The calculations used to derive integration times for this paper were done using the AtLAST sensitivity calculator (Klaassen, 2024), a deliverable of Horizon 2020 research project “Towards AtLAST”, and available from [this link](#).

## Acknowledgements

We thank William Coulton for useful insights on the CMB systematics and recovery of larger scales, and Matthieu Béthermin for the support with the analysis and processing of the SIDES simulations, Rémi Adam and Charles Romero for the details about the transfer function processing for NIKA/NIKA2 and MUSTANG/MUSTANG2, and Neelima Sehgal for the details on the planned CMB-HD spectral setup. We further thank Adam D. Hincks and the ACT collaboration for sharing the *Planck* and ACT SZ data for Abell 399–401.

## References

Abazajian K, Addison G, Adshead P, et al.: **CMB-S4 science case, reference design, and project plan.** *arXiv e-prints.* arXiv:1907.04473, 2019.  
[Publisher Full Text](#)

Abazajian KN, Adshead P, Ahmed Z, et al.: **CMB-S4 science book, first edition.** *arXiv e-prints.* arXiv:1610.02743, 2016.  
[Publisher Full Text](#)

Abdulla Z, Carlstrom JE, Mantz AB, et al.: **Constraints on the thermal contents of the X-ray cavities of cluster MS 0735.6+7421 with Sunyaev-Zel'dovich effect observations.** *Astrophys J.* 2019; **871**(2): 195.  
[Publisher Full Text](#)

Acharya SK, Majumdar S, Nath BB: **Non-thermal Sunyaev-Zeldovich signal from radio galaxy lobes.** *Mon Not R Astron Soc.* 2021; **503**(4): 5473–5484.  
[Publisher Full Text](#)

Adam R, Adane A, Ade PAR, et al.: **The NIKA2 large-field-of-view millimetre continuum camera for the 30 m IRAM telescope.** *Astron Astrophys.* 2018; **609**: A115.  
[Publisher Full Text](#)

Adam R, Bartalucci I, Pratt GW, et al.: **Mapping the kinetic Sunyaev-Zel'dovich effect toward MACS J0717.5+3745 with NIKA.** *Astron Astrophys.* 2017; **598**: A115.  
[Publisher Full Text](#)

Adam R, Comis B, Macías-Pérez JF, et al.: **Pressure distribution of the high-redshift cluster of galaxies CL J1226.9+3332 with NIKA.** *Astron Astrophys.* 2015; **576**: A12.  
[Publisher Full Text](#)

Adam R, Comis B, Macías-Pérez JF, et al.: **First observation of the thermal Sunyaev-Zel'dovich effect with Kinetic Inductance Detectors.** *Astron Astrophys.* 2014; **569**: A66.  
[Publisher Full Text](#)

Adam R, Eynard-Machet T, Bartalucci I, et al.: **PITSZI: Probing intra-cluster medium turbulence with Sunyaev-Zel'dovich imaging: Application to the triple merging cluster MACS J0717.5+3745.** *Astron Astrophys.* 2025; **694**: A182.  
[Publisher Full Text](#)

Akamatsu H, Fujita Y, Akahori T, et al.: **Properties of the cosmological filament between two clusters: a possible detection of a large-scale accretion shock by Suzaku.** *Astron Astrophys.* 2017; **606**: A1.  
[Publisher Full Text](#)

Akamatsu H, Kawahara H: **Systematic X-ray analysis of radio relic clusters with Suzaku.** *Publ Astron Soc Jpn.* 2013; **65**(1): 16.  
[Publisher Full Text](#)

Alberts S, Noble A: **From clusters to proto-clusters: the infrared perspective on environmental galaxy evolution.** *Universe.* 2022; **8**(11): 554.  
[Publisher Full Text](#)

Altamura E, Kay ST, Chluba J, et al.: **Galaxy cluster rotation revealed in the MACSIS simulations with the kinetic Sunyaev-Zeldovich effect.** *Mon Not R Astron Soc.* 2023; **524**(2): 2262–2289.  
[Publisher Full Text](#)

Amodeo S, Battaglia N, Schaan E, et al.: **Atacama cosmology telescope: modeling the gas thermodynamics in BOSS CMASS galaxies from kinematic and thermal Sunyaev-Zel'dovich measurements.** *Phys Rev D.* 2021; **103**(6): 063514.  
[Publisher Full Text](#)

Anbagajane D, Chang C, Baxter EJ, et al.: **Cosmological shocks around galaxy clusters: a coherent investigation with DES, SPT, and ACT.** *Mon Not R Astron Soc.* 2024; **527**(3): 9378–9404.  
[Publisher Full Text](#)

Anbagajane D, Chang C, Jain B, et al.: **Shocks in the stacked Sunyaev-Zel'dovich profiles of clusters II: measurements from SPT-SZ + Planck Compton- $\gamma$  map.** *Mon Not R Astron Soc.* 2022; **514**(2): 1645–1663.  
[Publisher Full Text](#)

Anderson AJ, Barry P, Bender AN, et al.: **SPT-3G+: mapping the high-frequency cosmic microwave background using Kinetic Inductance Detectors.** In: *Millimeter, Submillimeter, and Far-Infrared Detectors and Instrumentation for Astronomy XI.* 2022; **12190**: 1219003.  
[Publisher Full Text](#)

Andreon S, Moretti A, Trinchieri G, et al.: **Why are some galaxy clusters underluminous? The very low concentration of the CL2015 mass profile.** *Astron Astrophys.* 2019; **630**: A78.  
[Publisher Full Text](#)

Andreon S, Romero C, Aussel H, et al.: **Witnessing the Intracluster medium assembly at the cosmic noon in JKCS 041.** *Mon Not R Astron Soc.* 2023; **522**(3): 4301–4309.  
[Publisher Full Text](#)

Andreon S, Romero C, Castagna F, et al.: **Thermodynamic evolution of the  $z = 1.75$  galaxy cluster IDCS J1426.5+3508.** *Mon Not R Astron Soc.* 2021; **505**(4): 5896–5909.  
[Publisher Full Text](#)

Andreon S, Trinchieri G, Moretti A: **Low X-ray surface brightness clusters: implications on the scatter of the M-T and L-T relations.** *Mon Not R Astron Soc.* 2022; **511**(4): 4991–4998.  
[Publisher Full Text](#)

Andreon S, Wang J, Trinchieri G, et al.: **Variegated galaxy cluster gas content: mean fraction, scatter, selection effects, and covariance with X-ray luminosity.** *Astron Astrophys.* 2017; **606**: A24.  
[Publisher Full Text](#)

Angelinelli M, Vazza F, Giocoli C, et al.: **Turbulent pressure support and hydrostatic mass bias in the Intracluster Medium.** *Mon Not R Astron Soc.* 2020; **495**(1): 864–885.  
[Publisher Full Text](#)

Ansarifard S, Rasia E, Biffi V, et al.: **The Three Hundred Project: correcting for the hydrostatic-equilibrium mass bias in X-ray and SZ surveys.** *Astron Astrophys.* 2020; **634**: A113.  
[Publisher Full Text](#)

Arnaud M, Pratt GW, Piffaretti R, et al.: **The universal galaxy cluster pressure profile from a representative sample of nearby systems (REXCESS) and the  $Y_{\text{SZ}} - M_{\text{500}}$  relation.** *Astron Astrophys.* 2010; **517**: A92.  
[Publisher Full Text](#)

Asgari M, Mead AJ, Heymans C: **The halo model for cosmology: a pedagogical review.** *Open J of Astrophysics.* 2023; **6**: 39.  
[Publisher Full Text](#)

Attoli A, Poppi S, Buffa F, et al.: **The Sardinia Radio Telescope metrology system.** In: *2023 XXXVth General Assembly and Scientific Symposium of the International Union of Radio Science (URSI GASS).* 2023; 135.  
[Publisher Full Text](#)

Auclair C, Allys E, Boulanger F, et al.: **Separation of dust emission from the cosmic infrared background in *Herschel* observations with wavelet phase harmonics.** *Astron Astrophys.* 2024; **681**: A1.  
[Publisher Full Text](#)

Ayromlou M, Nelson D, Pillepich A, et al.: **An atlas of gas motions in the TNG-Cluster simulation: from cluster cores to the outskirts.** *Astron Astrophys.* 2024; **690**: A20.  
[Publisher Full Text](#)

Bahcall NA, Cen R: **Galaxy clusters and Cold Dark Matter: a low-density unbiased universe?** *Astrophys J Lett.* 1992; **398**: L81.  
[Publisher Full Text](#)

Baldi AS, De Petris M, Sembolini F, et al.: **Kinetic Sunyaev-Zel'dovich effect in rotating galaxy clusters from MUSIC simulations.** *Mon Not R Astron Soc.* 2018; **479**(3): 4028–4040.  
[Publisher Full Text](#)

Bartalesi T, Ettori S, Nipoti C: **Gas rotation and Dark Matter halo shape in cool-core clusters of galaxies.** *Astron Astrophys.* 2024; **682**: A31.  
[Publisher Full Text](#)

Bassini L, Rasia E, Borgani S, et al.: **The DIANOGA simulations of galaxy clusters: characterising star formation in protoclusters.** *Astron Astrophys.* 2020; **642**: A37.  
[Publisher Full Text](#)

Basu K, Sommer M, Erler J, et al.: **ALMA-SZ detection of a galaxy cluster merger shock at half the age of the universe.** *Astrophys J Lett.* 2016; **829**(2): L23.  
[Publisher Full Text](#)

Battaglia N, Bond JR, Pfrommer C, et al.: **On the cluster physics of Sunyaev-Zel'dovich and X-Ray surveys. I. The influence of feedback, non-thermal pressure, and cluster shapes on Y-M scaling relations.** *Astrophys J.* 2012; **758**(2): 74.  
[Publisher Full Text](#)

Battaglia N, Bond JR, Pfrommer C, et al.: **Simulations of the Sunyaev-Zel'dovich Power Spectrum with Active Galactic Nucleus Feedback.** *Astrophys J.* 2010; **725**(1): 91–99.  
[Publisher Full Text](#)

Battaglia N, Natarajan A, Trac H, et al.: **Reionization on Large Scales. III. Predictions for Low- $\ell$  Cosmic Microwave Background Polarization and High- $\ell$  Kinetic Sunyaev-Zel'dovich Observables.** *Astrophys J.* 2013; **776**(2): 83.  
[Publisher Full Text](#)

Battistelli E, Barbarella E, de Bernardis P, et al.: **Observing galaxy clusters and the cosmic web through the Sunyaev-Zel'dovich effect with MISTRAL.** In: *mm Universe 2023 - Observing the Universe at mm Wavelengths.* 2024; **293**: 00005.  
[Publisher Full Text](#)

Baxter EJ, Adhikari S, Vega-Ferrero J, et al.: **Shocks in the stacked Sunyaev-Zel'dovich profiles of clusters - I. Analysis with the Three Hundred simulations.** *Mon Not R Astron Soc.* 2021; **508**(2): 1777–1787.  
[Publisher Full Text](#)

Baxter EJ, Pandey S, Adhikari S, et al.: **The impact of halo concentration on the Sunyaev-Zel'dovich effect signal from massive galaxy clusters.** *Mon Not R Astron Soc.* 2024; **527**(3): 7847–7860.  
[Publisher Full Text](#)

Baxter EJ, Sherwin BD, Raghunathan S: **Constraining the rotational kinematic Sunyaev-Zel'dovich effect in massive galaxy clusters.** *J Cosmology Astropart*

*Phys.* 2019; **2019**: 001.  
[Publisher Full Text](#)

Behar E, Vogel S, Baldi RD, et al.: **The mm-wave compact component of an AGN.** *Mon Not R Astron Soc.* 2018; **478**(1): 399–406.  
[Publisher Full Text](#)

Bennett JS, Sijacki D: **A disturbing FABLE of mergers, feedback, turbulence, and mass biases in simulated galaxy clusters.** *Mon Not R Astron Soc.* 2022; **514**(1): 313–328.  
[Publisher Full Text](#)

Bennett JS, Sijacki D, Costa T, et al.: **The growth of the gargantuan black holes powering high-redshift quasars and their impact on the formation of early galaxies and protoclusters.** *Mon Not R Astron Soc.* 2024; **527**(1): 1033–1054.  
[Publisher Full Text](#)

Béthermin M, Wu HY, Lagache G, et al.: **The impact of clustering and angular resolution on far-infrared and millimeter continuum observations.** *Astron Astrophys.* 2017; **607**: A89.  
[Publisher Full Text](#)

Bhandarkar T, Haridas SK, Iuliano J, et al.: **Simons Observatory: characterization of the Large Aperture Telescope Receiver.** *arxiv e-prints.* arXiv: 2501.09241, 2025.  
[Publisher Full Text](#)

Bhattacharya S, Kosowsky A: **Cosmological constraints from galaxy cluster velocity statistics.** *Astrophys J.* 2007; **659**(2): L83.  
[Publisher Full Text](#)

Bianchini F, Silvestri A: **Kinetic Sunyaev-Zel'dovich effect in modified gravity.** *Phys Rev D.* 2016; **93**(6): 064026.  
[Publisher Full Text](#)

Biffi V, Borgani S, Murante G, et al.: **On the nature of hydrostatic equilibrium in galaxy clusters.** *Astrophys J.* 2016; **827**(2): 112.  
[Publisher Full Text](#)

Biffi V, ZuHone JA, Mroczkowski T, et al.: **The velocity structure of the intracluster medium during a major merger: simulated microcalorimeter observations.** *Astron Astrophys.* 2022; **663**: A76.  
[Publisher Full Text](#)

Birkinshaw M: **The Sunyaev-Zel'dovich effect.** *Phys Rep.* 1999; **310**(2–3): 97–195.  
[Publisher Full Text](#)

Birkinshaw M, Gull SF, Hardebeck H: **The Sunyaev-Zeldovich effect towards three clusters of galaxies.** *Nature.* 1984; **309**: 34–35.  
[Publisher Full Text](#)

Bleem LE, Bocquet S, Stalder B, et al.: **The SPTpol Extended Cluster Survey.** *Astrophys J Suppl Ser.* 2020; **247**(1): 25.  
[Publisher Full Text](#)

Bleem LE, Klein M, Abbott TMC, et al.: **Galaxy clusters discovered via the thermal Sunyaev-Zel'dovich effect in the 500-square-degree SPTpol survey.** *Open J Astrophys.* arXiv: 2311.07512; 2024; 7.  
[Publisher Full Text](#)

Bonafede A, Brunetti G, Rudnick L, et al.: **The Coma cluster at LOFAR frequencies. II. The halo, relic, and a new accretion relic.** *Astrophys J.* 2022; **933**(2): 218.  
[Publisher Full Text](#)

Bonafede A, Vazza F, Brüggen M, et al.: **Unravelling the origin of large-scale magnetic fields in galaxy clusters and beyond through Faraday Rotation Measures with the SKA.** In: *Advancing Astrophysics with the Square Kilometre Array (AASKA14)*. 2015; 95.  
[Publisher Full Text](#)

Bonamente M, Joy MK, LaRoque SJ, et al.: **Determination of the cosmic distance scale from Sunyaev-Zel'dovich Effect and Chandra X-Ray measurements of high-redshift galaxy clusters.** *Astrophys J.* 2006; **647**(1): 25.  
[Publisher Full Text](#)

Booth M, Klaassen P, Cicone C, et al.: **AtLAST science overview report.** *arXiv e-prints.* arXiv: 2407.01413. 2024a.  
[Publisher Full Text](#)

Booth M, Klaassen P, Cicone C, et al.: **The key science drivers for the Atacama Large Aperture Submillimeter Telescope (AtLAST).** In: *Millimeter, Submillimeter, and Far-Infrared Detectors and Instrumentation for Astronomy XII.* 2024b; **13102**: 1310206.  
[Publisher Full Text](#)

Boselli A, Fossati M, Sun M: **Ram pressure stripping in high-density environments.** *Astron Astrophys Rev.* 2022; **30**(1): 3.  
[Publisher Full Text](#)

Botteon A, Brunetti G, Ryu D, et al.: **Shock acceleration efficiency in radio relics.** *Astron Astrophys.* 2020a; **634**: A64.  
[Publisher Full Text](#)

Botteon A, van Weeren RJ, Brunetti G, et al.: **A giant radio bridge connecting two galaxy clusters in Abell 1758.** *Mon Not R Astron Soc Lett.* 2020b; **499**(1): L11–L15.  
[Publisher Full Text](#)

Bouwens RJ, Smit R, Schouws S, et al.: **Reionization Era Bright Emission Line Survey: selection and characterization of luminous Interstellar Medium reservoirs in the  $z > 6.5$  universe.** *Astrophys J.* 2022; **931**(2): 160.  
[Publisher Full Text](#)

Brodin M, McDonald M, Gonzalez AH, et al.: **IDCS J1426.5+3508: the most massive galaxy cluster AT  $z > 1.5$ .** *Astrophys J.* 2016; **817**(2): 122.  
[Publisher Full Text](#)

Brownson S, Maiolino R, Tazzari M, et al.: **Detecting the halo heating from AGN feedback with ALMA.** *Mon Not R Astron Soc.* 2019; **490**(4): 5134–5146.  
[Publisher Full Text](#)

Brunetti G, Jones TW: **Cosmic rays in galaxy clusters and their nonthermal emission.** *Int J Mod Phys D.* 2014; **23**(4): 1430007.  
[Publisher Full Text](#)

Brunetti G, Lazarin A: **Compressible turbulence in galaxy clusters: physics and stochastic particle re-acceleration.** *Mon Not R Astron Soc.* 2007; **378**(1): 245–275.  
[Publisher Full Text](#)

Bryan S, Austermann J, Ferrusca D, et al.: **Optical design of the TolTEC millimeter-wave camera.** In: *Millimeter, Submillimeter, and Far-Infrared Detectors and Instrumentation for Astronomy IX.* 2018; **107080**.  
[Publisher Full Text](#)

Bulbul E, Liu A, Kluge M, et al.: **The SRG/erosITA all-sky survey: the first catalog of galaxy clusters and groups in the western galactic hemisphere.** *arXiv:* 2402.08452, 2024.  
[Publisher Full Text](#)

Butler VL, Feder RM, Daylan T, et al.: **Measurement of the relativistic Sunyaev-Zeldovich correction in RX J1347.5-1145.** *Astrophys J.* 2022; **932**(1): 55.  
[Publisher Full Text](#)

Calafut V, Gallardo PA, Vavagiakis EM, et al.: **The Atacama Cosmolgy Telescope: detection of the pairwise kinematic Sunyaev-Zel'dovich effect with SDSS DR15 galaxies.** *Phys Rev D.* 2021; **104**(4): 043502.  
[Publisher Full Text](#)

Campitelli MG, Ettori S, Lovisari L, et al.: **CHEX-MATE: morphological analysis of the sample.** *Astron Astrophys.* 2022; **665**: A117.  
[Publisher Full Text](#)

Cantalupo S, Pezzulli G, Lilly SJ, et al.: **The large- and small-scale properties of the intergalactic gas in the Slug Ly $\alpha$  nebula revealed by MUSE He II emission observations.** *Mon Not R Astron Soc.* 2019; **483**(4): 5188–5204.  
[Publisher Full Text](#)

Carilli CL, Anderson CS, Tozzi P, et al.: **X-ray emission from the jets and lobes of the spiderweb.** *Astrophys J.* 2022; **928**(1): 59.  
[Publisher Full Text](#)

Carlstrom JE, Ade PAR, Aird KA, et al.: **The 10 meter South Pole Telescope.** *Publ Astron Soc Pac.* 2011; **123**(903): 568.  
[Publisher Full Text](#)

Carlstrom JE, Holder GP, Reese ED: **Cosmology with the Sunyaev-Zel'dovich Effect.** *Annu Rev Astron Astrophys.* 2002; **40**: 643.  
[Publisher Full Text](#)

Carpenter J, Brogan C, Iono D, et al.: **The ALMA Wideband Sensitivity Upgrade.** In: *Physics and Chemistry of Star Formation: The Dynamical ISM Across Time and Spatial Scales.* 2023; 304.  
[Publisher Full Text](#)

CASA Team: **CASA, the Common Astronomy Software Applications for radio astronomy.** *Publ Astron Soc Pac.* 2022; **134**(1041): 114501.  
[Publisher Full Text](#)

Casey CM, Narayanan D, Cooray A: **Dusty star-forming galaxies at high redshift.** *Phys Rep.* 2014; **541**(2): 45–161.  
[Publisher Full Text](#)

Cassano R, Bernardi G, Brunetti G, et al.: **Cluster radio halos at the crossroads between astrophysics and cosmology in the SKA era.** In: *Advancing Astrophysics with the Square Kilometre Array (AASKA14)*. 2015; 73.  
[Publisher Full Text](#)

Cassano R, Cuciti V, Brunetti G, et al.: **The Planck clusters in the LOFAR sky: IV. LoTSS-DR2: statistics of radio haloes and re-acceleration models.** *Astron Astrophys.* 2023; **672**: A43.  
[Publisher Full Text](#)

Castagna F, Andreon S: **JoXSZ: joint X-SZ fitting code for galaxy clusters.** *Astron Astrophys.* 2020; **639**: A73.  
[Publisher Full Text](#)

CCAT-Prime Collaboration: **CCAT-prime collaboration: science goals and forecasts with Prime-Cam on the Fred Young Submillimeter Telescope.** *Astrophys J Suppl Ser.* 2023; **264**(1): 7.  
[Publisher Full Text](#)

Cen R, Ostriker JP: **Where are the baryons?** *Astrophys J.* 1999; **514**(1): 1.  
[Publisher Full Text](#)

Chakraborty A, Chatterjee S, Lacy M, et al.: **Cosmological simulations of galaxy groups and clusters. III. Constraining quasar feedback models with the Atacama Large Millimeter Array.** *Astrophys J.* 2023; **954**(1): 8.  
[Publisher Full Text](#)

Challinor A, Lasenby A: **Relativistic corrections to the Sunyaev-Zeldovich Effect.** *Astrophys J.* 1998; **499**(1): 1–6.  
[Publisher Full Text](#)

CHEX-MATE Collaboration: **The Cluster HERitage project with XMM-Newton: mass assembly and thermodynamics at the endpoint of structure formation: I. Programme overview.** *Astron Astrophys.* 2021; **650**: A104.  
[Publisher Full Text](#)

Chisari NE, Mead AJ, Joudaki S, et al.: **Modelling baryonic feedback for survey**

**cosmology.** *Open J Astrophys.* 2019; **2**(1): 4.  
[Publisher Full Text](#)

Chluba J, Dai L: **Multiple scattering Sunyaev-Zeldovich signal - II. Relativistic effects.** *Mon Not R Astron Soc.* 2014; **438**(2): 1324–1334.  
[Publisher Full Text](#)

Chluba J, Dai L, Kamionkowski M: **Multiple scattering Sunyaev-Zeldovich signal - I. Lowest order effect.** *Mon Not R Astron Soc.* 2014; **437**(1): 67–76.  
[Publisher Full Text](#)

Chluba J, Nagai D, Sazonov S, et al.: **A fast and accurate method for computing the Sunyaev-Zel'dovich signal of hot galaxy clusters.** *Mon Not R Astron Soc.* 2012; **426**(1): 510–530.  
[Publisher Full Text](#)

Chluba J, Switzer E, Nelson K, et al.: **Sunyaev-Zeldovich signal processing and temperature-velocity moment method for individual clusters.** *Mon Not R Astron Soc.* 2013; **430**(4): 3054–3069.  
[Publisher Full Text](#)

Choi SK, Hasselfeld M, Ho SPP, et al.: **The Atacama Cosmology Telescope: a measurement of the Cosmic Microwave Background power spectra at 98 and 150 GHz.** *J Cosmology Phys.* 2020; **2020**(12): 45.  
[Publisher Full Text](#)

Churazov E, Vikhlinin A, Sunyaev R: **(No) dimming of X-ray clusters beyond  $z \sim 1$  at fixed mass: crude redshifts and masses from raw X-ray and SZ data.** *Mon Not R Astron Soc.* 2015; **450**(2): 1984–1989.  
[Publisher Full Text](#)

Clowe D, Bradač M, Gonzalez AH, et al.: **A direct empirical proof of the existence of dark matter.** *Astrophys J.* 2006; **648**(2): L109–L113.  
[Publisher Full Text](#)

Colafrancesco S: **SZ effect from radio-galaxy lobes: astrophysical and cosmological relevance.** *Mon Not R Astron Soc.* 2008; **385**(4): 2041–2048.  
[Publisher Full Text](#)

Colafrancesco S, Marchegiani P, Palladino E: **The non-thermal Sunyaev-Zel'dovich effect in clusters of galaxies.** *Astron Astrophys.* 2003; **397**: 27–52.  
[Publisher Full Text](#)

Condon JJ: **Radio emission from normal galaxies.** *Annu Rev Astron.* 1992; **30**: 575–611.  
[Publisher Full Text](#)

Contini E, De Lucia G, Villalobos Á, et al.: **On the formation and physical properties of the intracluster light in hierarchical galaxy formation models.** *Mon Not R Astron Soc.* 2014; **437**(4): 3787–3802.  
[Publisher Full Text](#)

Cooray A, Chen X: **Kinetic Sunyaev-Zeldovich effect from halo rotation.** *Astrophys J.* 2002; **573**(1): 43.  
[Publisher Full Text](#)

Cooray A, Sheth R: **Halo models of large scale structure.** *Phys Rep.* 2002; **372**(1): 1–129.  
[Publisher Full Text](#)

Coulton WR, Schutt T, Maniyan AS, et al.: **The Atacama Cosmology Telescope: detection of patchy screening of the cosmic microwave background.** *arXiv e-prints.* arXiv: 2401.13033, 2024.  
[Publisher Full Text](#)

Crichton D, Gralla MB, Hall K, et al.: **Evidence for the thermal Sunyaev-Zel'dovich effect associated with quasar feedback.** *Mon Not R Astron Soc.* 2016; **458**(2): 1478–1492.  
[Publisher Full Text](#)

Cruise M, Guainazzi M, Aird J, et al.: **The NewAthena mission concept in the context of the next decade of X-ray astronomy.** *Nat Astron.* 2025; **9**: 36–44.  
[Publisher Full Text](#)

Cuciti V, de Gasperin F, Brüggen M, et al.: **Galaxy clusters enveloped by vast volumes of relativistic electrons.** *Nature.* 2022; **609**(7929): 911–914.  
[PubMed Abstract](#) | [Publisher Full Text](#) | [Free Full Text](#)

Das S, Chiang YK, Mathur S: **Detection of thermal Sunyaev-Zel'dovich effect in the circumgalactic medium of lowmass galaxies—a surprising pattern in self-similarity and baryon sufficiency.** *Astrophys J.* 2023; **951**(2): 125.  
[Publisher Full Text](#)

De Filippis E, Sereno M, Bautz MW, et al.: **Measuring the three-dimensional structure of galaxy clusters. I. Application to a sample of 25 clusters.** *Astrophys J.* 2005; **625**(1): 108.  
[Publisher Full Text](#)

de Graaff A, Cai YC, Heymans C, et al.: **Probing the missing baryons with the Sunyaev-Zel'dovich effect from filaments.** *Astron Astrophys.* 2019; **624**: A48.  
[Publisher Full Text](#)

del Palacio S, Yang C, Aalto S, et al.: **Millimeter emission from supermassive black hole coronae.** *arXiv e-prints.* arXiv:2504.07762, 2025.  
[Publisher Full Text](#)

Delvecchio I, Daddi E, Sargent MT, et al.: **The infrared-radio correlation of Star-Forming Galaxies is strongly  $M_*$ -dependent but nearly redshift-invariant since  $z \sim 4$ .** *Astron Astrophys.* 2021; **647**: A123.  
[Publisher Full Text](#)

Di Mascolo L, Churazov E, Mroczkowski T: **A joint ALMA-Bolocam-Planck SZ study of the pressure distribution in RX J1347.5-1145.** *Mon Not R Astron Soc.* 2019a; **487**(3): 4037–4056.  
[Publisher Full Text](#)

Di Mascolo L, Mroczkowski T, Churazov E, et al.: **An ALMA+ACA measurement of the shock in the bullet cluster.** *Astron Astrophys.* 2019b; **628**: A100.  
[Publisher Full Text](#)

Di Mascolo L, Mroczkowski T, Perrott Y, et al.: **Multiwavelength view of SPT-CL J2106-5844. The radio galaxies and the thermal and relativistic plasmas in a massive galaxy cluster merger at  $z=1.13$ .** *Astron Astrophys.* 2021; **650**: A153.  
[Publisher Full Text](#)

Di Mascolo L, Saro A, Mroczkowski T, et al.: **Forming intracluster gas in a galaxy protocluster at a redshift of 2.16.** *Nature.* 2023; **615**(7954): 809–812.  
[PubMed Abstract](#) | [Publisher Full Text](#) | [Free Full Text](#)

Dicker SR, Ade PAR, Aguirre J, et al.: **MUSTANG 2: a large focal plane array for the 100 m Green Bank telescope.** *J Low Temp Phys.* 2014; **176**: 808–814.  
[Publisher Full Text](#)

Dicker SR, Battistelli ES, Bhandarkar T, et al.: **Observations of compact sources in galaxy clusters using MUSTANG2.** *Mon Not R Astron Soc.* 2021; **508**(2): 2600–2612.  
[Publisher Full Text](#)

Dickinson C, Ali-Haïmoud Y, Barr A, et al.: **The State-of-Play of Anomalous Microwave Emission (AME) research.** *New Astron Rev.* 2018; **80**: 1–28.  
[Publisher Full Text](#)

Dolag K, Komatsu E, Sunyaev R: **SZ effects in the magneticum pathfinder simulation: comparison with the Planck, SPT, and ACT results.** *Mon Not R Astron Soc.* 2016; **463**(2): 1797–1811.  
[Publisher Full Text](#)

Donahue M, Scharf CA, Mack J, et al.: **Distant cluster hunting. II. A comparison of X-Ray and optical cluster detection techniques and catalogs from the ROSAT optical X-Ray survey.** *Astrophys J.* 2002; **569**(2): 689.  
[Publisher Full Text](#)

Doré O, Bock J, Ashby M, et al.: **Cosmology with the SPHEREx all-sky spectral survey.** *arXiv e-prints.* arXiv: 1412.4872, 2014.  
[Publisher Full Text](#)

Duchesne SW, Botteon A, Koribalski BS, et al.: **Evolutionary Map of the Universe (EMU): a pilot search for diffuse, non-thermal radio emission in galaxy clusters with the Australian SKA pathfinder.** *arXiv e-prints.* arXiv: 2402.06192, 2024.  
[Publisher Full Text](#)

Eckert D, Gaspari P, Vazza F, et al.: **On the connection between turbulent motions and particle acceleration in galaxy clusters.** *Astrophys J Lett.* 2017; **843**(2): L29.  
[Publisher Full Text](#)

Eckert D, Molendi S, Paltani S: **The cool-core bias in X-ray galaxy cluster samples I. Method and application to HIFLUGCS.** *Astron Astrophys.* 2011; **526**: A79.  
[Publisher Full Text](#)

Ehlers K, Pfrommer C, Weinberger R, et al.: **The Sunyaev-Zel'dovich effect of simulated jet-inflated bubbles in clusters.** *Astrophys J.* 2019; **872**(1): L8.  
[Publisher Full Text](#)

Emonts BHC, Lehnhert MD, Villar-Martín M, et al.: **Molecular gas in the halo fuels the growth of a massive cluster galaxy at high redshift.** *Science.* 2016; **354**(6316): 1128–1130.  
[PubMed Abstract](#) | [Publisher Full Text](#)

Enßlin TA, Kaiser CR: **Comptonization of the cosmic microwave background by relativistic plasma.** *Astron Astrophys.* 2000; **360**: 417–430.  
[Publisher Full Text](#)

Erler J, Basu K, Chluba J, et al.: **Planck's view on the spectrum of the Sunyaev-Zeldovich effect.** *Mon Not R Astron Soc.* 2018; **476**(3): 3360–3381.  
[Publisher Full Text](#)

Ettori S, Eckert D: **Tracing the non-thermal pressure and hydrostatic bias in galaxy clusters.** *Astron Astrophys.* 2022; **657**: L1.  
[Publisher Full Text](#)

Euclid Collaboration: **Euclid preparation: III. Galaxy cluster detection in the wide photometric survey, performance and algorithm selection.** *Astron Astrophys.* 2019; **627**: A23.  
[Publisher Full Text](#)

Euclid Collaboration, Scaramella R, Amiaux J, et al.: **Euclid preparation: I. The Euclid wide survey.** *Astron Astrophys.* 2022; **662**: A112.  
[Publisher Full Text](#)

Fabian AC: **Observational evidence of active galactic nuclei feedback.** *Annu Rev Astron Astrophys.* 2012; **50**: 455–489.  
[Publisher Full Text](#)

Ferrari C, Dabbech A, Smirnov O, et al.: **Non-thermal emission from galaxy clusters: feasibility study with SKA.** In: *Advancing Astrophysics with the Square Kilometre Array (ASKA14).* 2015; 75.  
[Publisher Full Text](#)

Ferraro S, Smith KM: **Characterizing the epoch of reionization with the small-scale CMB: constraints on the optical depth and duration.** *Phys Rev D.* 2018; **98**(12): 123519.  
[Publisher Full Text](#)

Fujita Y: **Pre-processing of galaxies before entering a cluster.** *Publ Astron Soc*

*Jpn.* 2004; **56**(1): 29–43.  
[Publisher Full Text](#)

Galárraga-Espinosa D, Aghanim N, Langer M, et al.: **Populations of filaments from the distribution of galaxies in numerical simulations.** *Astron Astrophys.* 2020; **641**: A173.  
[Publisher Full Text](#)

Gallardo PA, Benson B, Carlstrom J, et al.: **Optical design concept of the CMB-S4 large-aperture telescopes and cameras.** In: *Millimeter, Submillimeter, and Far-Infrared Detectors and Instrumentation for Astronomy XI.* 2022; 121900C.  
[Publisher Full Text](#)

Gallardo PA, Puddu R, Harrington K, et al.: **Freeform three-mirror anastigmatic large-aperture telescope and receiver optics for CMB-S4.** In: *Appl Opt.* 2024a; **63**(2): 310–321.  
[Publisher Full Text](#)

Gallardo PA, Puddu R, Mroczkowski T, et al.: **The optical design concept for the Atacama Large Aperture Submillimeter Telescope (AtLAST).** In: *Ground-based and Airborne Telescopes X.* 2024b; **13094**: 1309428.  
[Publisher Full Text](#)

Ganguly S, Li Y, Olivares V, et al.: **The nature of the motions of multiphase filaments in the centers of galaxy clusters.** *Front Astron Space Sci.* 2023; **10**: 1138613.  
[Publisher Full Text](#)

Gardner A, Baxter E, Raghunathan S, et al.: **Prospects for studying the mass and gas in protoclusters with future CMB observations.** *The Open Journal of Astrophysics.* 2024; **7**: 2.  
[Publisher Full Text](#)

Gardner JP, Mather JC, Clampin M, et al.: **The James Webb Space Telescope.** *Space Sci Rev.* 2006; **123**(4): 485–606.  
[Publisher Full Text](#)

Gasparrini M, Tombesi F, Cappi M: **Linking macro-, meso- and microscales in multiphase AGN feeding and feedback.** *Nat Astron.* 2020; **4**: 10–13.  
[Publisher Full Text](#)

Gattuzz E, Mohapatra R, Federrath C, et al.: **Measuring the hot ICM velocity structure function using XMM-Newton observations.** *Mon Not R Astron Soc.* 2023; **524**(2): 2945–2953.  
[Publisher Full Text](#)

George EM, Reichardt CL, Aird KA, et al.: **A Measurement of secondary Cosmic Microwave Background anisotropies from the 2500 square-degree SPT-SZ survey.** *Astrophys J.* 2015; **799**(2): 177.  
[Publisher Full Text](#)

Ghirardini V, Bulbul E, Hoang DN, et al.: **Discovery of a supercluster in the eROSITA final equatorial depth survey: X-ray properties, radio halo, and double relics.** *Astron Astrophys.* 2021a; **647**: A4.  
[Publisher Full Text](#)

Ghirardini V, Bulbul E, Kraft R, et al.: **Evolution of the thermodynamic properties of clusters of galaxies out to redshift of 1.8.** *Astrophys J.* 2021b; **910**(1): 14.  
[Publisher Full Text](#)

Ghirardini V, Eckert D, Ettori S, et al.: **Universal thermodynamic properties of the Intracluster Medium over two decades in radius in the X-COP sample.** *Astron Astrophys.* 2019; **621**: A41.  
[Publisher Full Text](#)

Ghirardini V, Ettori S, Amodeo S, et al.: **On the evolution of the entropy and pressure profiles in X-ray luminous galaxy clusters at  $z > 0.4$ .** *Astron Astrophys.* 2017; **604**: A100.  
[Publisher Full Text](#)

Giardiello S, Duivenvoorden AJ, Calabrese E, et al.: **Modeling beam chromaticity for high-resolution CMB analyses.** *Phys Rev D.* 2025; **111**(4): 043502.  
[Publisher Full Text](#)

Giovannini G, Bonafede A, Brown S, et al.: **Mega-parsec scale magnetic fields in low density regions in the SKA era: filaments connecting galaxy clusters and groups.** In: *Advancing Astrophysics with the Square Kilometre Array (AASKA14).* 2015; 104.  
[Publisher Full Text](#)

Gitti M, Tozzi P, Brunetti G, et al.: **The SKA view of cool-core clusters: evolution of radio mini-halos and AGN feedback.** In: *Advancing Astrophysics with the Square Kilometre Array (AASKA14).* 2015; 76.  
[Publisher Full Text](#)

Gobat R, Daddi E, Coogan RT, et al.: **Sunyaev-Zel'dovich detection of the galaxy cluster Cl J1449+0856 at  $z = 1.99$ : the pressure profile in  $uv$  space.** *Astron Astrophys.* 2019; **629**: A104.  
[Publisher Full Text](#)

Gorce A, Douspis M, Salvati L: **Retrieving cosmological information from small-scale CMB foregrounds. II. The kinetic Sunyaev Zel'dovich effect.** *Astron Astrophys.* 2022; **662**: A122.  
[Publisher Full Text](#)

Gorce A, Ilić S, Douspis M, et al.: **Improved constraints on reionisation from CMB observations: a parameterisation of the kSZ effect.** *Astron Astrophys.* 2020; **640**: A90.  
[Publisher Full Text](#)

Govoni F, Murgia M, Xu H, et al.: **Cluster magnetic fields through the study of polarized radio halos in the SKA era.** In: *Advancing Astrophysics with the Square Kilometre Array (AASKA14).* 2015; 105.  
[Publisher Full Text](#)

Grainje K, Borgani S, Colafrancesco S, et al.: **The SKA and galaxy cluster science with the Sunyaev-Zel'dovich effect.** In: *Advancing Astrophysics with the Square Kilometre Array (AASKA14).* 2015; 170.  
[Publisher Full Text](#)

Grayson S, Scannapieco E, Davé R: **Distinguishing Active Galactic Nuclei feedback models with the Thermal Sunyaev-Zel'dovich effect.** *Astrophys J.* 2023; **957**(1): 17.  
[Publisher Full Text](#)

Gupta N, Saro A, Mohr JJ, et al.: **SZE observables, pressure profiles and centre offsets in Magneticum simulation galaxy clusters.** *Mon Not R Astron Soc.* 2017; **469**(3): 3069–3087.  
[Publisher Full Text](#)

Ha JH, Ryu D, Kang H: **Properties of merger shocks in merging galaxy clusters.** *Astrophys J.* 2018; **857**(1): 26.  
[Publisher Full Text](#)

Hadzhiyska B, Ferraro S, Ried Guachalla B, et al.: **Evidence for large baryonic feedback at low and intermediate redshifts from kinematic Sunyaev-Zel'dovich observations with ACT and DESI photometric galaxies.** *arXiv e-prints.* arXiv:2407.07152, 2024.  
[Publisher Full Text](#)

Hall KR, Zakamska NL, Addison GE, et al.: **Quantifying the thermal Sunyaev-Zel'dovich effect and excess millimetre emission in quasar environments.** *Mon Not R Astron Soc.* 2019; **490**(2): 2315–2335.  
[Publisher Full Text](#)

Halverson NW, Lanting T, Ade PAR, et al.: **Sunyaev-Zel'dovich effect observations of the bullet cluster (1E 0657-56) with APEX-SZ.** *Astrophys J.* 2009; **701**(1): 42–51.  
[Publisher Full Text](#)

Hansen SH, Pastor S, Semikoz DV: **First measurement of cluster temperature using the thermal Sunyaev-Zel'dovich effect.** *Astrophys J.* 2002; **573**(2): L69–L71.  
[Publisher Full Text](#)

Hasselfield M, Moodley K, Bond JR, et al.: **The Atacama Cosmology Telescope: beam measurements and the microwave brightness temperatures of Uranus and Saturn.** *Astrophys J Suppl.* 2013; **209**(1): 17.  
[Publisher Full Text](#)

Hensley BS, Clark SE, Fanfani V, et al.: **The Simons Observatory: galactic science goals and forecasts.** *Astrophys J.* 2022; **929**(2): 166.  
[Publisher Full Text](#)

Hill JC, Baxter EJ, Lidz A, et al.: **Two-halo term in stacked thermal Sunyaev-Zel'dovich measurements: implications for self-similarity.** *Phys Rev D.* 2018; **97**(8): 083501.  
[Publisher Full Text](#)

Hill R, Chapman S, Scott D, et al.: **Megaparsec-scale structure around the protocluster core SPT2349-56 at  $z = 4.3$ .** *Mon Not R Astron Soc.* 2020; **495**(3): 3124–3159.  
[Publisher Full Text](#)

Hilton M, Sifón C, Naess S, et al.: **The Atacama Cosmology Telescope: a catalog of >4000 Sunyaev-Zel'dovich galaxy clusters.** *Astrophys J Suppl Ser.* 2021; **253**(1): 3.  
[Publisher Full Text](#)

Hincks AD, Radiconi F, Romero C, et al.: **A high-resolution view of the filament of gas between Abell 399 and Abell 401 from the Atacama Cosmology Telescope and MUSTANG-2.** *Mon Not R Astron Soc.* 2022; **510**(3): 3335–3355.  
[Publisher Full Text](#)

Hlavacek-Larrondo J, Li Y, Churazov E: **AGN Feedback in groups and clusters of galaxies.** In: *Handbook of X-ray and Gamma-ray Astrophysics.* 2022; 5.  
[Publisher Full Text](#)

Hu W, White M: **A CMB polarization primer.** *New Astron.* 1997; **2**(4): 323–344.  
[Publisher Full Text](#)

Huang N, Bleem LE, Stalder B, et al.: **Galaxy clusters selected via the Sunyaev-Zel'dovich effect in the SPTpol 100-square-degree survey.** *Astron J.* 2020; **159**(3): 110.  
[Publisher Full Text](#)

Hughes DH, Jáuregui Correa JC, Schloerb FP, et al.: **The Large Millimeter Telescope.** In: *Ground-based and Airborne Telescopes III.* 2010; **773312**: 773312.  
[Publisher Full Text](#)

Hurier G: **High significance detection of the tSZ effect relativistic corrections.** *Astron Astrophys.* 2016; **596**: A61.  
[Publisher Full Text](#)

Hurier G, Adam R, Keshet U: **First detection of a virial shock with SZ data: implication for the mass accretion rate of Abell 2319.** *Astron Astrophys.* 2019; **622**: A136.  
[Publisher Full Text](#)

Husemann B, Harrison CM: **Reality and myths of AGN feedback.** *Nat Astron.* 2018; **2**: 196–197.  
[Publisher Full Text](#)

Huterer D: **Growth of cosmic structure.** *Astron Astroph Rev.* 2023; **31**(1): 2.  
[Publisher Full Text](#)

Huynh M, Lazio J: **An overview of the Square Kilometre Array.** *arXiv.* 2013;

1311.4288.  
**Publisher Full Text**  
 Iguchi S, Morita KI, Sugimoto M, et al.: **The Atacama Compact Array (ACA).** *Publ Astron Soc Jpn.* 2009; **61**(1): 1–12.  
**Publisher Full Text**

Ijenkarevic J, Reiprich TH, Pacaud F, et al.: **eROSITA spectro-imaging analysis of the Abell 3408 galaxy cluster.** *Astron Astrophys.* 2022; **661**: A26.  
**Publisher Full Text**

Itoh N, Kohyama Y, Nozawa S: **Relativistic corrections to the Sunyaev-Zeldovich effect for clusters of galaxies.** *Astrophys J.* 1998; **502**(1): 7–15.  
**Publisher Full Text**

Ivezic Ž, Kahn SM, Tyson JA, et al.: **LSST: from science drivers to reference design and anticipated data products.** *Astrophys J.* 2019; **873**(2): 111.  
**Publisher Full Text**

Jain D, Choudhury TR, Raghunathan S, et al.: **Probing the physics of reionization using kinematic Sunyaev-Zeldovich power spectrum from current and upcoming cosmic microwave background surveys.** *Mon Not R Astron Soc.* 2024; **530**(1): 35–51.  
**Publisher Full Text**

Javid K, Perrott YC, Rumsey C, et al.: **Physical modelling of galaxy cluster Sunyaev-Zel'dovich data using Einasto dark matter profiles.** *Mon Not R Astron Soc.* 2019; **489**(3): 3135–3148.  
**Publisher Full Text**

Jin S, Dannerbauer H, Emonts B, et al.: **COALAS. I. ATCA CO(1-0) survey and luminosity function in the Spiderweb protocluster at  $z = 2.16$ .** *Astron Astrophys.* 2021; **652**: A11.  
**Publisher Full Text**

Johnston-Hollitt M, Dehghan S, Pratley L: **Using tailed radio galaxies to probe the environment and magnetic field of galaxy clusters in the SKA era.** In: *Advancing Astrophysics with the Square Kilometre Array (ASKA14).* 2015a; 101.  
**Publisher Full Text**

Johnston-Hollitt M, Govoni F, Beck R, et al.: **Using SKA rotation measures to reveal the mysteries of the magnetised Universe.** In: *Advancing Astrophysics with the Square Kilometre Array (ASKA14).* 2015b; 92.  
**Publisher Full Text**

Jones GC, Maiolino R, Carniani S, et al.: **An investigation of the circumgalactic medium around  $z \sim 2.2$  AGN with ACA and ALMA.** *Mon Not R Astron Soc.* 2023; **522**(1): 275–291.  
**Publisher Full Text**

Kamionkowski M, Kosowsky A, Stebbins A: **Statistics of cosmic microwave background polarization.** *Phys Rev D.* 1997; **55**(12): 7368–7388.  
**Publisher Full Text**

Kéruzoré F, Mayet F, Pratt GW, et al.: **Exploiting NIKA2/XMM-Newton imaging synergy for intermediate-mass high- $z$  galaxy clusters within the NIKA2 SZ large program: observations of ACT-CL J0215.4+0030 at  $z \sim 0.9$ .** *Astron Astrophys.* 2020; **644**: A93.  
**Publisher Full Text**

Khabibullin I, Komarov S, Churazov E, et al.: **Polarization of Sunyaev-Zel'dovich signal due to electron pressure anisotropy in galaxy clusters.** *Mon Not R Astron Soc.* 2018; **474**(2): 2389–2400.  
**Publisher Full Text**

Khatri R, Gaspari M: **Thermal SZ fluctuations in the ICM: probing turbulence and thermodynamics in Coma cluster with Planck.** *Mon Not R Astron Soc.* 2016; **463**(1): 655–669.  
**Publisher Full Text**

Kilbinger M: **Cosmology with cosmic shear observations: a review.** *Rep Prof Phys.* 2015; **78**(8): 086901.  
**Publisher Full Text**

Kim J, Sayers J, Sereno M, et al.: **CHEX-MATE: CLUSTER Multi-Probes in three dimensions (CLUMP-3D). I. Gas analysis method using X-ray and Sunyaev-Zel'dovich effect data.** *arXiv e-prints.* arXiv: 2307.04794. 2023.  
**Publisher Full Text**

Kiselev A, Reichert M, Mroczkowski T: **Energy recovery system for large telescopes.** In: *Ground-based and Airborne Telescopes X.* 2024; 130940E.  
**Publisher Full Text**

Kitayama T: **Cosmological and astrophysical implications of the Sunyaev-Zel'dovich effect.** *Prog Theor Exp Phys.* 2014; **2014**(6): 06B111.  
**Publisher Full Text**

Kitayama T, Ueda S, Akahori T, et al.: **Deeply cooled core of the Phoenix galaxy cluster imaged by ALMA with the Sunyaev-Zel'dovich effect.** *Publ Astron Soc Jpn.* 2020; **72**(2): 33.  
**Publisher Full Text**

Kitayama T, Ueda S, Okabe N, et al.: **Galaxy clusters at  $z \sim 1$  imaged by ALMA with the Sunyaev-Zel'dovich effect.** *Publ Astron Soc Jpn.* 2023; **75**(2): 311–337.  
**Publisher Full Text**

Kitayama T, Ueda S, Takakuwa S, et al.: **The Sunyaev-Zel'dovich effect at 5': RX J1347.5–1145 imaged by ALMA.** *Publ Astron Soc Jpn.* 2016; **68**(5): 88.  
**Publisher Full Text**

Klaassen P: **AtLAST sensitivity calculator and telescope simulation notebook.** *figshare.* 2024.  
<http://www.doi.org/10.6084/m9.figshare.23506962.v1>

Klaassen PD, Mroczkowski TK, Ciccone C, et al.: **The Atacama Large Aperture Submillimeter Telescope (AtLAST).** In: *Ground-based and Telescopes.* 2020; 8:  
 114452F.  
**Publisher Full Text**

Klaassen P, Traficante A, Beltrán MT, et al.: **Atacama Large Aperture Submillimeter Telescope (AtLAST) science: our galaxy.** *arXiv e-prints.* arXiv: 2403.00917. 2024.  
**Publisher Full Text**

Knowles K, Cotton WD, Rudnick L, et al.: **The MeerKAT galaxy cluster legacy survey.** *Astron Astrophys.* 2022; **657**: A56.  
**Publisher Full Text**

Knowles K, Pillay DS, Amodeo S, et al.: **MERGHERS pilot: MeerKAT discovery of diffuse emission in nine massive Sunyaev-Zel'dovich-selected galaxy clusters from ACT.** *Mon Not R Astron Soc.* 2021; **504**(2): 1749–1758.  
**Publisher Full Text**

Knox L, Scoccimarro R, Dodelson S: **Impact of inhomogeneous reionization on cosmic microwave background anisotropy.** *Phys Rev Lett.* 1998; **81**(10): 2004–2007.  
**Publisher Full Text**

Kornoelje K, Bleem LE, Rykoff ES, et al.: **The SPT-Deep cluster catalog: sunyaev-Zel'dovich selected clusters from combined SPT-3G and SPTpol measurements over 100 square degrees.** *arXiv e-prints.* arXiv: 2503.17271. 2025.  
**Publisher Full Text**

Kosowsky A, Bhattacharya S: **A future test of gravitation using galaxy cluster velocities.** *Phys Rev D.* 2009; **80**: 062003.  
**Publisher Full Text**

Kozhanyan A, Bourdin H, Mazzotta P, et al.: **Deriving the hubble constant using Planck and XMM-Newton observations of galaxy clusters.** *Astron Astrophys.* 2019; **621**: A34.  
**Publisher Full Text**

Kraft R, Markevitch M, Kilbourne C, et al.: **Line Emission Mapper (LEM): probing the physics of cosmic ecosystems.** *arXiv e-prints.* arXiv: 2211.09827. 2022.  
**Publisher Full Text**

Kraftsvot AV, Borgani S: **Formation of galaxy clusters.** *Annu Rev Astron Astrophys.* 2012; **50**(1): 353–409.  
**Publisher Full Text**

Kusiak A, Bolla B, Ferraro S, et al.: **Constraining the baryon abundance with the kinematic Sunyaev-Zel'dovich effect: Projected-field detection using Planck, WMAP, and unWISE.** *Phys Rev D.* 2021; **104**(4): 043518.  
**Publisher Full Text**

Lacy M, Mason B, Sarazin C, et al.: **Direct detection of quasar feedback via the Sunyaev-Zeldovich effect.** *Mon Not R Astron Soc.* 2019; **483**(1): L22–L27.  
**Publisher Full Text**

Lau ET, Nagai D, Avestruz C, et al.: **Mass accretion and its effects on the self-similarity of gas profiles in the outskirts of galaxy clusters.** *Astrophys J.* 2015; **806**(1): 68.  
**Publisher Full Text**

Laureijs R, Amiaux J, Arduini S, et al.: **Euclid definition study report.** *arXiv e-prints.* arXiv: 1110.3193. 2011.  
**Publisher Full Text**

Le Brun AMC, McCarthy IG, Melin JB: **Testing Sunyaev-Zel'dovich measurements of the hot gas content of dark matter haloes using synthetic skies.** *Mon Not R Astron Soc.* 2015; **451**(4): 3868–3881.  
**Publisher Full Text**

Lee E, Chluba J: **The SZ effect with anisotropic distributions and high energy electrons.** *J Cosmology Astropart Phys.* 2024; **2024**(7): 040.  
**Publisher Full Text**

Lee E, Chluba J, Kay ST, et al.: **Relativistic SZ temperature scaling relations of groups and clusters derived from the BAHAMAS and MACSIS simulations.** *Mon Not R Astron Soc.* 2020; **493**(3): 3274–3292.  
**Publisher Full Text**

Lee MM, Schimek A, Ciccone C, et al.: **Atacama Large Aperture Submillimeter Telescope (AtLAST) science: the hidden circumgalactic medium.** *Open Res Eur.* 2024; **4**: 117.  
**PubMed Abstract** | **Publisher Full Text** | **Free Full Text**

Lepore M, Di Mascolo L, Tozzi P, et al.: **Feeding and feedback processes in the Spiderweb proto-Intracluster Medium.** *Astron Astrophys.* 2024; **682**: A186.  
**Publisher Full Text**

Lewis A, Challinor A, Lasenby A: **Efficient computation of cosmic microwave background anisotropies in closed friedmann-robertson-walker models.** *Astrophys J.* 2000; **538**(2): 473–476.  
**Publisher Full Text**

Li Q, Cui W, Yang X, et al.: **THE THREE HUNDRED Project: the evolution of physical baryon profiles.** *Mon Not R Astron Soc.* 2023; **523**(1): 1228–1246.  
**Publisher Full Text**

Li Y, Gendron-Marsolais ML, Zhuravleva I, et al.: **Direct detection of black hole-driven turbulence in the centers of galaxy clusters.** *Astrophys J Lett.* 2020; **889**(1): L1.  
**Publisher Full Text**

Li Z, Puglisi G, Madhavacheril MS, et al.: **Simulated catalogs and maps of radio galaxies at millimeter wavelengths in Websky.** *J Cosmology Astropart Phys.* 2022; **2022**(08): 029.  
**Publisher Full Text**

Limousin M, Morandi A, Sereno M, et al.: **The three-dimensional shapes of galaxy clusters.** *Space Sci Rev.* 2013; **177**(1–4): 155–194.  
[Publisher Full Text](#)

Liu A, Bulbul E, Ramos-Ceja ME, et al.: **X-ray analysis of JWST's first galaxy cluster lens SMACS J0723.3–7327.** *Astron Astrophys.* 2023; **670**: A96.  
[Publisher Full Text](#)

Liu D, Saintonge A, Bot C, et al.: **Atacama Large Aperture Submillimeter Telescope (AtLAST) science: gas and dust in nearby galaxies.** *arXiv e-prints.* arXiv: 2403.01202. 2024.  
[Publisher Full Text](#)

Lokken M, Cui W, Bond JR, et al.: **Boundless baryons: how diffuse gas contributes to anisotropic tSZ signal around simulated Three Hundred clusters.** *Mon Not R Astron Soc.* 2023; **523**(1): 1346–1363.  
[Publisher Full Text](#)

Louis T, Alonso D: **Calibrating cluster number counts with CMB lensing.** *Phys Rev D.* 2017; **95**(4): 043517.  
[Publisher Full Text](#)

Lungu M, Storer ER, Hasselfield M, et al.: **The Atacama Cosmology Telescope: measurement and analysis of 1D beams for DR4.** *J Cosmology Astropart Phys.* 2022; **2022**: 044.  
[Publisher Full Text](#)

Madhavacheril MS, Battaglia N, Miyatake H: **Fundamental physics from future weak-lensing calibrated Sunyaev-Zel'dovich galaxy cluster counts.** *Phys Rev D.* 2017; **96**(10): 103525.  
[Publisher Full Text](#)

Madhavacheril MS, Hill JC, Næss S, et al.: **Atacama Cosmology Telescope: component-separated maps of cmb temperature and the thermal Sunyaev-Zel'dovich effect.** *Phys Rev D.* 2020; **102**(2): 023534.  
[Publisher Full Text](#)

Mandelbaum R: **Weak lensing for precision cosmology.** *Annu Rev Astron Astrophys.* 2018; **56**: 393–433.  
[Publisher Full Text](#)

Mantz AB, Abdulla Z, Allen SW, et al.: **The XXL Survey. XVII. X-ray and Sunyaev-Zel'dovich properties of the redshift 2.0 galaxy cluster XLSSC 122.** *Astron Astrophys.* 2018; **620**: A2.  
[Publisher Full Text](#)

Mantz A, Allen SW, Ebeling H, et al.: **The observed growth of massive galaxy clusters - II. X-ray scaling relations.** *Mon Not R Astron Soc.* 2010; **406**(3): 1773–1795.  
[Publisher Full Text](#)

Marchegiani P: **Sunyaev Zel'dovich effect in galaxy clusters cavities: thermal or non-thermal origin?** In: *mm Universe @ NIKA2 - Observing the mm Universe with the NIKA2 Camera.* 2022; **257**(2): 00030.  
[Publisher Full Text](#)

Markevitch M, Vikhlinin A: **Shocks and cold fronts in galaxy clusters.** *Phys Rep.* 2007; **443**(1): 1–53.  
[Publisher Full Text](#)

Mason BS, Dicker SR, Korngut PM, et al.: **Implications of a high angular resolution image of the Sunyaev-Zel'dovich effect in RXJ1347-1145.** *Astrophys J.* 2010; **716**(1): 739–745.  
[Publisher Full Text](#)

Matsuda Y, Yamada T, Hayashino T, et al.: **Large-scale filamentary structure around the protocluster at redshift  $z = 3.1$ .** *Astrophys J.* 2005; **634**(2): L125–L128.  
[Publisher Full Text](#)

Maughan BJ, Giles PA, Randall SW, et al.: **Self-similar scaling and evolution in the galaxy cluster X-ray luminosity–temperature relation.** *Mon Not R Astron Soc.* 2012; **421**(2): 1583–1602.  
[Publisher Full Text](#)

Mazzotta P, Rasia E, Moscardini L, et al.: **Comparing the temperatures of galaxy clusters from hydrodynamical  $N$ -body simulations to Chandra and XMM-Newton observations.** *Mon Not R Astron Soc.* 2004; **354**(1): 10–24.  
[Publisher Full Text](#)

McCarthy F, Battaglia N, Bean R, et al.: **The Atacama Cosmology Telescope: large-scale velocity reconstruction with the kinematic Sunyaev-Zel'dovich effect and DESI LRGs.** *arXiv e-prints.* arXiv: 2410.06229. 2024.  
[Publisher Full Text](#)

McDonald M, Benson BA, Vikhlinin A, et al.: **The redshift evolution of the mean temperature, pressure, and entropy profiles in 80 spt-selected galaxy clusters.** *Astrophys J.* 2014; **794**(1): 67.  
[Publisher Full Text](#)

McQuinn M, Furlanetto SR, Hernquist L, et al.: **The kinetic Sunyaev-Zel'dovich effect from reionization.** *Astrophys J.* 2005; **630**(2): 643–656.  
[Publisher Full Text](#)

Melin JB, Pratt GW: **Joint measurement of the galaxy cluster pressure profile with Planck and SPT-SZ.** *Astron Astrophys.* 2023; **678**: A197.  
[Publisher Full Text](#)

Merloni A, Lamer G, Liu T, et al.: **The SRG/eROSITA all-sky survey. First X-ray catalogues and data release of the western Galactic hemisphere.** *Astron Astrophys.* 2024; **682**: A34.  
[Publisher Full Text](#)

Migkas K, Kox D, Schellenberger G, et al.: **The SRG/eROSITA all-sky survey: SRG/eROSITA cross-calibration with chandra and XMM-Newton using galaxy cluster gas temperatures.** *arXiv e-prints.* arXiv: 2401.17297. 2024.  
[Publisher Full Text](#)

Molnar SM, Hearn N, Haiman Z, et al.: **Accretion shocks in clusters of galaxies and their SZ signature from cosmological simulations.** *Astrophys J.* 2009; **696**(2): 1640–1656.  
[Publisher Full Text](#)

Monllor-Berbegal Ò, Vallés-Pérez D, Planelles S, et al.: **Imprints of the internal dynamics of galaxy clusters on the Sunyaev-Zeldovich effect.** *Astron Astrophys.* 2024; **686**: A243.  
[Publisher Full Text](#)

Moser E, Amodeo S, Battaglia N, et al.: **The impacts of modeling choices on the inference of circumgalactic medium properties from Sunyaev-Zeldovich observations.** *Astrophys J.* 2021; **919**(1): 2.  
[Publisher Full Text](#)

Moser E, Battaglia N, Amodeo S: **Searching for systematics in forward modeling Sunyaev-Zeldovich profiles.** *arXiv e-prints.* arXiv: 2307.10919. 2023.  
[Publisher Full Text](#)

Moser E, Battaglia N, Nagai D, et al.: **The Circumgalactic Medium from the CAMELS simulations: forecasting constraints on feedback processes from future Sunyaev-Zeldovich observations.** *Astrophys J.* 2022; **933**(2): 133.  
[Publisher Full Text](#)

Mroczkowski T, Cicone C, Reichert M, et al.: **Progress in the design of the Atacama Large Aperture Submillimeter Telescope.** In: *2023 XXXVth General Assembly and Scientific Symposium of the International Union of Radio Science (URSI GASS).* 2023; 174.  
[Publisher Full Text](#)

Mroczkowski T, Dicker S, Sayers J, et al.: **A multi-wavelength study of the Sunyaev-Zel'dovich Effect in the triple-merger cluster macs J0717.5+3745 with MUSTANG and Bolocam.** *Astrophys J.* 2012; **761**(1): 47.  
[Publisher Full Text](#)

Mroczkowski T, Gallardo PA, Timpe M, et al.: **The conceptual design of the 50-meter Atacama Large Aperture Submillimeter Telescope (AtLAST).** *Astron Astrophys.* 2025; **694**: A142.  
[Publisher Full Text](#)

Mueller EM, de Bernardis F, Bean R, et al.: **Constraints on gravity and dark energy from the pairwise kinematic Sunyaev-Zel'dovich effect.** *Astrophys J.* 2015; **808**(1): 47.  
[Publisher Full Text](#)

Muñoz-Echeverría M, Macías-Pérez JF, Pratt GW, et al.: **Multi-probe analysis of the galaxy cluster CL J1226.9+3332. Hydrostatic mass and hydrostatic-to-lensing bias.** *Astron Astrophys.* 2023; **671**: A28.  
[Publisher Full Text](#)

Muralidhara V, Basu K: **Constraining the average magnetic field in galaxy clusters with current and upcoming CMB surveys.** *J Cosmology Astropart Phys.* 2024; **2024**(11): 010.  
[Publisher Full Text](#)

Murphy EJ, Bremseth J, Mason BS, et al.: **The star formation in radio survey: GBT 33 GHz observations of nearby galaxy nuclei and extranuclear star-forming regions.** *Astrophys J.* 2012; **761**(2): 97.  
[Publisher Full Text](#)

Murphy EJ, Condon JJ, Schinnerer E, et al.: **Calibrating extinction-free star formation rate diagnostics with 33 GHz free-free emission in NGC 6946.** *Astrophys J.* 2011; **737**(2): 67.  
[Publisher Full Text](#)

Naess S, Aiola S, Austermann JE, et al.: **The Atacama Cosmology Telescope: arcminute-resolution maps of 18 000 square degrees of the microwave sky from ACT 2008–2018 data combined with Planck.** *J Cosmology Astropart Phys.* 2020; **2020**(12): 046.  
[Publisher Full Text](#)

Naess S, Guan Y, Duivenvoorden AJ, et al.: **The Atacama Cosmology Telescope: DR6 Maps.** *arXiv e-prints.* arXiv: 2503.14451. 2025.  
[Publisher Full Text](#)

Nagai D, Kravtsov AV, Kosowsky A: **Effect of internal flows on Sunyaev-Zeldovich measurements of cluster peculiar velocities.** *Astrophys J.* 2003; **587**(2): 524–532.  
[Publisher Full Text](#)

Nakano S, Tamura Y, Taniguchi A, et al.: **Characterization of sensitivity and responses of a 2-element prototype wavefront sensor for millimeter-wave adaptive optics attached to the Nobeyama 45m Telescope.** In: *Adaptive Optics Systems VIII.* 2022; **12185**.  
[Publisher Full Text](#)

Nelson D, Pilipich A, Ayromlou M, et al.: **Introducing the TNG-Cluster simulation: overview and the physical properties of the gaseous intracluster medium.** *Astron Astrophys.* 2024; **686**: A157.  
[Publisher Full Text](#)

Nicastro F, Kaastra J, Krongold Y, et al.: **Observations of the missing baryons**

in the warm-hot intergalactic medium. *Nature*. 2018; **558**(7710): 406–409.  
[PubMed Abstract](#) | [Publisher Full Text](#)

Nozawa S, Itoh N, Kohyama Y: Relativistic corrections to the Sunyaev-Zeldovich effect for clusters of galaxies. *Astrophys J*. 1998; **508**(1): 7–15.  
[Publisher Full Text](#)

Okabe N, Dicker D, Eckert D, et al.: Active gas features in three HSC-SSP CAMIRA clusters revealed by high angular resolution analysis of MUSTANG-2 SZE and XXL X-ray observations. *Mon Not R Astron Soc*. 2021; **501**(2): 1701–1732.  
[Publisher Full Text](#)

Olamai M, Hobson MP, Grainge KJB: A simple parametric model for spherical galaxy clusters. *Mon Not R Astron Soc*. 2012; **423**: 1534–1543.  
[Publisher Full Text](#)

Orłowski-Scherer J, Haridas SK, Di Mascolo L, et al.: GBT/MUSTANG-2 9" resolution imaging of the SZ effect in MS0735.6+7421. Confirmation of the SZ cavities through direct imaging. *Astron Astrophys*. 2022; **667**: L6.  
[Publisher Full Text](#)

Overzier RA: The realm of the galaxy protoclusters. A review. *Astron Astrophys Rev*. 2016; **24**(1): 14.  
[Publisher Full Text](#)

Pacaud F, Pierre M, Adami C, et al.: The XMM-LSS survey: the class 1 cluster sample over the initial 5 deg<sup>2</sup> and its cosmological modelling. *Mon Not R Astron Soc*. 2007; **382**(3): 1289–1308.  
[Publisher Full Text](#)

Padoani P, Alexander DM, Assef RJ, et al.: Active Galactic Nuclei: what's in a name? *Astron Astrophys Rev*. 2017; **25**(1): 2.  
[Publisher Full Text](#)

Paiella A, Cacciotti F, Isopi G, et al.: The MISTRAL instrument and the characterization of its detector array. *J Low Temp Phys*. 2024; **217**(3–4): 436–445.  
[Publisher Full Text](#)

Paine S: The am atmospheric model. *Zenodo*. 2019.  
[Publisher Full Text](#)

Palwal A, De Petris M, Ferragamo A, et al.: Exploiting the high-resolution NIKA2 data to study the intracluster medium and dynamical state of ACT-CL J0240.0+0116. *arXiv e-prints*. arXiv: 2410.11668. 2024.  
[Publisher Full Text](#)

Panessa F, Baldi RD, Laor A, et al.: The origin of radio emission from radio-quiet active galactic nuclei. *Nat Astron*. 2019; **3**: 387–396.  
[Publisher Full Text](#)

Patki R, Battaglia N, Hill JC: A novel bispectrum estimator of the kinematic Sunyaev-Zel'dovich effect using projected fields. *arXiv e-prints*. arXiv: 2411.11974. 2024.  
[Publisher Full Text](#)

Patnaude DJ, Kraft RP, Kilbourne C, et al.: Line Emission Mapper: an X-ray probe mission concept to study the cosmic ecosystems and the physics of galaxy formation. *J Astron Telesc Instrum Syst*. 2023; **9**: 041008.  
[Publisher Full Text](#)

Perratt Y: Bayesian recalibration of *Planck* galaxy cluster scaling relations including relativistic Sunyaev-Zel'dovich corrections. *Publ Astron Soc Pac*. 2024; **41**: e087.  
[Publisher Full Text](#)

Pfrommer C, Enßlin TA, Sarazin CL: Unveiling the composition of radio plasma bubbles in galaxy clusters with the Sunyaev-Zel'dovich effect. *Astron Astrophys*. 2005; **430**: 799–810.  
[Publisher Full Text](#)

Plagge TJ, Marrone DP, Abdalla Z, et al.: CARMA measurements of the Sunyaev-Zel'dovich effect in RX J1347.5-1145. *Astrophys J*. 2013; **770**(2): 112.  
[Publisher Full Text](#)

Planck Collaboration: *Planck* 2015 results. XXIV. Cosmology from Sunyaev-Zeldovich cluster counts. *Astron Astrophys*. 2016a; **594**: A24.  
[Publisher Full Text](#)

Planck Collaboration: *Planck* early results. IX. *XMM-Newton* follow-up for validation of *Planck* cluster candidates. *Astron Astrophys*. 2011; **536**: A9.  
[Publisher Full Text](#)

Planck Collaboration: *Planck* intermediate results. I. Further validation of new *Planck* clusters with *XMM-Newton*. *Astron Astrophys*. 2012; **543**: A102.  
[Publisher Full Text](#)

Planck Collaboration: *Planck* intermediate results. VIII. Filaments between interacting clusters. *Astron Astrophys*. 2013; **550**: A134.  
[Publisher Full Text](#)

Planck Collaboration: *Planck* 2015 results. XXVII. The second *Planck* catalogue of Sunyaev-Zeldovich sources. *Astron Astrophys*. 2016b; **594**: A27.  
[Publisher Full Text](#)

Popik C, Battaglia N, Kusiak A, et al.: On the impacts of Halo model implementations in Sunyaev-Zeldovich cross-correlation analyses. *arXiv e-prints*. arXiv: 2502.13291. 2025.  
[Publisher Full Text](#)

Prandoni I, Murgia M, Tarchi A, et al.: The Sardinia Radio Telescope. From a technological project to a radio observatory. *Astron Astrophys*. 2017; **608**: A40.  
[Publisher Full Text](#)

Prandoni I, Seymour N: Revealing the physics and evolution of galaxies and galaxy clusters with SKA continuum surveys. In: *Advancing Astrophysics with the Square Kilometre Array (AASKA14)*. 2015; 67.  
[Publisher Full Text](#)

Pratt GW, Arnaud M, Biviano A, et al.: The galaxy cluster mass scale and its impact on cosmological constraints from the cluster population. *Space Sci Rev*. 2019; **215**(2): 25.  
[Publisher Full Text](#)

Pratt GW, Arnaud M, Piffaretti R, et al.: Gas entropy in a representative sample of nearby X-ray galaxy clusters (REXCESS): relationship to gas mass fraction. *Astron Astrophys*. 2010; **511**: A85.  
[Publisher Full Text](#)

Prokhorov DA, Antonuccio-Delogu V, Silik J: Comptonization of the cosmic microwave background by high energy particles residing in AGN cocoons. *Astron Astrophys*. 2010; **520**: A106.  
[Publisher Full Text](#)

Prokhorov DA, Colafrancesco S: The first measurement of temperature standard deviation along the line of sight in galaxy clusters. *Mon Not R Astron Soc*. 2012; **424**(1): L49–L53.  
[Publisher Full Text](#)

Puddu R, Gallardo PA, Mroczkowski T, et al.: A physical optics characterization of the beam shape and sidelobe levels for the Atacama Large Aperture Submillimeter Telescope (AtLAST). In: *Ground-based and Airborne Telescopes X*. 2024; **13094**: 130945.  
[Publisher Full Text](#)

Radiconi F, Vacca V, Battistelli E, et al.: The thermal and non-thermal components within and between galaxy clusters Abell 399 and Abell 401. *Mon Not R Astron Soc*. 2022; **517**(4): 5232–5246.  
[Publisher Full Text](#)

Raghunathan S, Ade PAR, Anderson AJ, et al.: First constraints on the epoch of reionization using the non-gaussianity of the kinematic Sunyaev-Zel'dovich effect from the South Pole Telescope and Herschel-SPIRE observations. *Phys Rev Lett*. 2024; **133**(12): 121004.  
[PubMed Abstract](#) | [Publisher Full Text](#)

Raghunathan S: Assessing the importance of noise from thermal Sunyaev-Zel'dovich signals for CMB cluster surveys and cluster cosmology. *Astrophys J*. 2022; **928**(1): 16.  
[Publisher Full Text](#)

Raghunathan S, Omori Y: A cross-internal linear combination approach to probe the secondary CMB anisotropies: kinematic Sunyaev-Zel'dovich effect and CMB lensing. *Astrophys J*. 2023; **954**(1): 83.  
[Publisher Full Text](#)

Raghunathan S, Whitehorn N, Alvarez MA, et al.: Constraining cluster virialization mechanism and cosmology using Thermal-SZ-selected clusters from future CMB surveys. *Astrophys J*. 2022; **926**(2): 172.  
[Publisher Full Text](#)

Ramasawmy J, Klaassen PD, Ciccone C, et al.: The Atacama Large Aperture Submillimetre Telescope: key science drivers. In: *Millimeter, Submillimeter, and Far-Infrared Detectors and Instrumentation for Astronomy XI*. 2022; **12190**: 1219007.  
[Publisher Full Text](#)

Rasia E, Borgani S, Murante G, et al.: Cool core clusters from cosmological simulations. *Astrophys J*. 2015; **813**(1): L17.  
[Publisher Full Text](#)

Régalado-Saint Blanchard B, Eickenberg M: Statistical component separation for targeted signal recovery in noisy mixtures. *Transact Mach Learn Res*. arXiv: 2306.15012. 2024.  
[Publisher Full Text](#)

Reichardt CL, Patil S, Ade PAR, et al.: An improved measurement of the secondary cosmic microwave background anisotropies from the SPT-SZ + SPTpol surveys. *Astrophys J*. 2021; **908**(2): 199.  
[Publisher Full Text](#)

Reichardt CL: Observing the Epoch of Reionization with the cosmic microwave background. In: *Understanding the epoch of cosmic reionization. Challenges and Progress*. 2016; **423**: 227.  
[Publisher Full Text](#)

Reichert M, Timpe M, Kærcher H, et al.: Technical requirements flow-down for the concept design of the novel 50-meter Atacama Large Aperture Submm Telescope (AtLAST). In: *Ground-based and airborne telescopes X*. 2024; **13094**: 130941.  
[Publisher Full Text](#)

Remazeilles M, Chluba J: Mapping the relativistic electron gas temperature across the sky. *Mon Not R Astron Soc*. 2020; **494**(4): 5734–5750.  
[Publisher Full Text](#)

Remazeilles M, Chluba J: Evidence for relativistic Sunyaev-Zeldovich effect in *Planck* CMB maps with an average electron-gas temperature of  $T_e \approx 5$  keV. *Mon Not R Astron Soc*. 2025; **538**(3): 1576–1586.  
[Publisher Full Text](#)

Ricci M, Adam R, Eckert D, et al.: The XXL survey. XLIV. Sunyaev-Zel'dovich

**mapping of a low-mass cluster at  $z \sim 1$ : a multi-wavelength approach.** *Astron Astrophys.* 2020; **642**: A126.  
**Publisher Full Text**

**Romero CE: Forecasting constraints from surface brightness fluctuations in galaxy clusters.** *Astrophys J.* 2024; **975**(2): 197.  
**Publisher Full Text**

Rossetti M, Gastaldello F, Eckert D, et al.: **The cool-core state of *Planck* SZ-selected clusters versus X-ray-selected samples: evidence for cool-core bias.** *Mon Not R Astron Soc.* 2017; **468**(2): 1917–1930.  
**Publisher Full Text**

Romero CE, Gaspari M, Schellenberger G, et al.: **Inferences from surface brightness fluctuations of Zwicky 3146 via the Sunyaev-Zel'dovich effect and X-ray observations.** *Astrophys J.* 2023; **951**(1): 41.  
**Publisher Full Text**

Romero C, Gaspari M, Schellenberger G, et al.: **SZ-X-ray surface brightness fluctuations in the SPT-XMM clusters.** *arXiv e-prints.* arXiv: 2412.05478, 2024.  
**Publisher Full Text**

Romero CE, Sievers J, Ghirardini V, et al.: **Pressure profiles and mass estimates using high-resolution Sunyaev-Zel'dovich effect observations of Zwicky 3146 with MUSTANG-2.** *Astrophys J.* 2020; **891**(1): 90.  
**Publisher Full Text**

Ruan JJ, Quinn TR, Babul A, et al.: **The observable thermal and kinetic Sunyaev-Zel'dovich effect in merging galaxy clusters.** *Mon Not R Astron Soc.* 2013; **432**(4): 3508–3519.  
**Publisher Full Text**

Ruppin F, Adam R, Comis B, et al.: **Non-parametric deprojection of NIKA SZ observations: pressure distribution in the *Planck*-discovered cluster PSZ1 G045.85+57.71.** *Astron Astrophys.* 2017; **597**: A110.  
**Publisher Full Text**

Ruppin F, Mayet F, Pratt GW, et al.: **First Sunyaev-Zel'dovich mapping with the NIKA2 camera: implication of cluster substructures for the pressure profile and mass estimate.** *Astron Astrophys.* 2018; **615**: A112.  
**Publisher Full Text**

Ruppin F, McDonald M, Bleem LE, et al.: **Stability of cool cores during galaxy cluster growth: a joint Chandra/SPT analysis of 67 galaxy clusters along a common evolutionary track spanning 9 Gyr.** *Astrophys J.* 2021; **918**(2): 43.  
**Publisher Full Text**

Ryu D, Kang H, Hallman E, et al.: **Cosmological shock waves and their role in the large-scale structure of the universe.** *Astrophys J.* 2003; **593**(2): 599–610.  
**Publisher Full Text**

Sanders JS: **Contour binning: a new technique for spatially resolved X-ray spectroscopy applied to cassiopeia A.** *Mon Not R Astron Soc.* 2006; **371**(2): 829–842.  
**Publisher Full Text**

Sanders JS, Biffi V, Brüggen M, et al.: **Studying the merging cluster Abell 3266 with eROSITA.** *Astron Astrophys.* 2022; **661**: A36.  
**Publisher Full Text**

Sayers J, Mantz AB, Rasia E, et al.: **The evolution and mass dependence of galaxy cluster pressure profiles at  $0.05 \leq z \leq 0.60$  and  $4 \times 10^{14} M_{\odot} \leq M_{500} \leq 30 \times 10^{14} M_{\odot}$ .** *Astrophys J.* 2023; **944**(2): 221.  
**Publisher Full Text**

Sayers J, Montaño A, Mroczkowski T, et al.: **Imaging the thermal and kinematic Sunyaev-Zel'dovich effect signals in a sample of 10 massive galaxy clusters: constraints on internal velocity structures and bulk velocities.** *Astrophys J.* 2019; **880**(1): 45.  
**Publisher Full Text**

Sayers J, Mroczkowski T, Zemcov M, et al.: **A measurement of the kinetic Sunyaev-Zel'dovich signal toward macs J0717.5+3745.** *Astrophys J.* 2013; **778**(1): 52.  
**Publisher Full Text**

Sayers J, Sereno M, Ettori S, et al.: **CLUMP-3D: the lack of non-thermal motions in galaxy cluster cores.** *Mon Not R Astron Soc.* 2021; **505**(3): 4338–4344.  
**Publisher Full Text**

Sazonov SY, Sunyaev RA: **Cosmic microwave background radiation in the direction of a moving cluster of galaxies with hot gas: relativistic corrections.** *Astrophys J.* 1998; **508**(1): 1–5.  
**Publisher Full Text**

Sazonov SY, Sunyaev RA: **Microwave polarization in the direction of galaxy clusters induced by the CMB quadrupole anisotropy.** *Mon Not R Astron Soc.* 1999; **310**(3): 765–772.  
**Publisher Full Text**

Schaan E, Ferraro S, Amodeo S, et al.: **Atacama Cosmology Telescope: combined kinematic and thermal Sunyaev-Zel'dovich measurements from BOSS CMASS and LOWZ halos.** *Phys Rev D.* 2021; **103**(6): 063513.  
**Publisher Full Text**

Schechter P: **An analytic expression for the luminosity function for galaxies.** *Astrophys J.* 1976; **203**: 297–306.  
**Publisher Full Text**

Schellenberger G, Reiprich TH, Lovisari L, et al.: **XMM-Newton and Chandra cross-calibration using HIFLUGCS galaxy clusters. Systematic temperature differences and cosmological impact.** *Astron Astrophys.* 2015; **575**: A30.  
**Publisher Full Text**

Schimek A, Decataldo D, Shen S, et al.: **High resolution modelling of [CII], [CI], [OIII], and CO line emission from the interstellar medium and circumgalactic medium of a star-forming galaxy at  $z \sim 6.5$ .** *Astron Astrophys.* 2024; **682**: A98.  
**Publisher Full Text**

Schneider R, Maiolino R: **The formation and cosmic evolution of dust in the early Universe: I. Dust sources.** *Astron Astrophys Rev.* 2024; **32**(2): 2.  
**Publisher Full Text**

Schuecker P, Finoguenov A, Miniati F, et al.: **Probing turbulence in the Coma galaxy cluster.** *Astron Astrophys.* 2004; **426**(2): 387–397.  
**Publisher Full Text**

Sehgal N, Aiola S, Akrami Y, et al.: **CMB-HD: an Ultra-Deep, high-resolution millimeter-wave survey over half the sky.** *Bulletin of the American Astronomical Society.* 2019; **51**(7): 6.  
**Publisher Full Text**

Selina RJ, Murphy EJ, McKinnon M, et al.: **The next-generation Very Large Array: a technical overview.** *Ground-based and Airborne Telescopes VII.* 2018; **10700**: 107001.  
**Publisher Full Text**

Sereno M, Lovisari L, Cui W, et al.: **The thermalization of massive galaxy clusters.** *Mon Not R Astron Soc.* 2021; **507**(4): 5214–5223.  
**Publisher Full Text**

Sereno M, Umetsu K, Ettori S, et al.: **CLUMP-3D: testing  $\Lambda$ CDM with galaxy cluster shapes.** *Astrophys J.* 2018; **860**(1): L4.  
**Publisher Full Text**

Shaw LD, Rudd DH, Nagai D: **Deconstructing the kinetic SZ power spectrum.** *Astrophys J.* 2012; **756**(1): 15.  
**Publisher Full Text**

Shi X, Komatsu E, Nagai D, et al.: **Analytical model for non-thermal pressure in galaxy clusters - III. Removing the hydrostatic mass bias.** *Mon Not R Astron Soc.* 2016; **455**(3): 2936–2944.  
**Publisher Full Text**

Shull JM, Smith BD, Danforth CW: **The baryon census in a multiphase intergalactic medium: 30% of the baryons may still be missing.** *Astrophys J.* 2012; **759**(1): 23.  
**Publisher Full Text**

Silich EM, Bellomi E, Sayers J, et al.: **ICM-SHOX. Paper I: methodology overview and discovery of a gas–dark matter velocity decoupling in the MACS J0018.5+1626 merger.** *Astrophys J.* 2024a; **968**(2): 74.  
**Publisher Full Text**

Silich EM, Bellomi E, Sayers J, et al.: **Improved Constraints on Mergers with SZ, Hydrodynamical simulations, Optical, and X-ray (ICM-SHOX). Paper II: Galaxy cluster sample overview".** In: *mm Universe 2023 - Observing the Universe at mm Wavelengths.* 2024b; **293**: 00050.  
**Publisher Full Text**

Simoneescu A, Allen SW, Mantz A, et al.: **Baryons at the edge of the X-ray-brightest galaxy cluster.** *Science.* 2011; **331**(6024): 1576.  
**PubMed Abstract** | **Publisher Full Text**

Simoneescu A, Zuhone J, Zhuravleva I, et al.: **Constraining gas motions in the Intra-Cluster Medium.** *Space Sci Rev.* 2019; **215**(2): 24.  
**Publisher Full Text**

Simons Observatory Collaboration: **The Simons Observatory: science goals and forecasts.** *J Cosmology Astropart Phys.* 2019; **2019**: 056.  
**Publisher Full Text**

Singari B, Ghosh T, Khatri R: **Detection of WHIM in the *Planck* data using Stack First approach.** *J Cosmology Astropart Phys.* 2020; **2020**(8): 028.  
**Publisher Full Text**

Smith KM, Ferraro S: **Detecting patchy reionization in the Cosmic Microwave Background.** *Phys Rev Lett.* 2017; **119**(2): 021301.  
**Publisher Full Text**

Sobrin JA, Ade PAR, Ahmed Z, et al.: **Design and characterization of the SPT-3G receiver.** In: *Millimeter, Submillimeter, and Far-Infrared Detectors and Instrumentation for Astronomy IX.* 2018; **10708**: 107081H.  
**Publisher Full Text**

Sobrin JA, Anderson AJ, Bender N, et al.: **The design and integrated performance of SPT-3G.** *Astrophys J Suppl.* 2022; **258**(2): 42.  
**Publisher Full Text**

Soergel B, Saro A, Giannantonio T, et al.: **Cosmology with the pairwise kinematic SZ effect: calibration and validation using hydrodynamical simulations.** *Mon Not R Astron Soc.* 2018; **478**(4): 5320–5335.  
**Publisher Full Text**

Sommovigo L, Ferrara A, Pallottini A, et al.: **The ALMA REBELS survey: cosmic dust temperature evolution out to  $z \sim 7$ .** *Mon Not R Astron Soc.* 2022; **513**(3): 3122–3135.  
**Publisher Full Text**

Spergel D, Gehrels N, Baltay C, et al.: **Wide-Field Infrared Survey Telescope-Astrophysics Focused Telescope Assets WFIRST-AFTA 2015 report.** *arXiv eprints.* arXiv: 1503.03757, 2015.  
**Publisher Full Text**

Stanek R, Evrard AE, Böhringer H, et al.: **The X-ray luminosity-mass relation for local clusters of galaxies.** *Astrophys J.* 2006; **648**(2): 956–968.  
**Publisher Full Text**

Sullivan A, Shabala S, Power C, et al.: **Predicting the non-thermal pressure in**

galaxy clusters. *Publ Astron Soc Aust.* 2024; **41**: e064. [Publisher Full Text](#)

Sunyaev RA, Norman ML, Bryan GL: **On the detectability of turbulence and bulk flows in X-ray clusters.** *Astron Lett.* 2003; **29**: 783–790. [Publisher Full Text](#)

Sunyaev RA, Zeldovich YB: **Small-scale fluctuations of relic radiation.** *Astrophys Space Sci.* 1970; **7**(1): 3–19. [Publisher Full Text](#)

Sunyaev RA, Zeldovich YB: **The observations of relic radiation as a test of the nature of X-Ray radiation from the clusters of galaxies.** *Comments on Astrophysics and Space Physics.* 1972; **4**: 173. [Reference Source](#)

Sunyaev RA, Zeldovich IB: **The velocity of clusters of galaxies relative to the microwave background. The possibility of its measurement.** *Mon Not R Astron Soc.* 1980; **190**(3): 413–420. [Publisher Full Text](#)

Sweat DS, Ade PAR, Amiri M, et al.: **Overview of the Atacama Cosmology Telescope: receiver, instrumentation, and telescope systems.** *Astrophys J Suppl Ser.* 2011; **194**(2): 41. [Publisher Full Text](#)

Tamura Y, Kawabe R, Fukasaku Y, et al.: **Wavefront sensor for millimeter/submillimeter-wave adaptive optics based on aperture-plane interferometry.** In: *Ground-based and Airborne Telescopes VIII.* 2020; **11445**: 11445N. [Publisher Full Text](#)

Tanimura H, Aghanim N, Douspis M, et al.: **X-ray emission from cosmic web filaments in SRG/eROSITA data.** *Astron Astrophys.* 2022; **667**: A161. [Publisher Full Text](#)

Tanimura H, Aghanim N, Kolodzig A, et al.: **First detection of stacked X-ray emission from cosmic web filaments.** *Astron Astrophys.* 2020; **643**: L2. [Publisher Full Text](#)

Tanimura H, Hinshaw G, McCarthy IG, et al.: **A search for warm/hot gas filaments between Pairs of SDSS Luminous Red Galaxies.** *Mon Not R Astron Soc.* 2019; **483**(1): 223–234. [Publisher Full Text](#)

The CMB-HD Collaboration: **Snowmass2021 CMB-HD white paper.** *arXiv e-prints.* arXiv: 2203.05728, 2022. [Publisher Full Text](#)

Thorne B, Dunkley J, Alonso D, et al.: **The python sky model: software for simulating the Galactic microwave sky.** *Mon Not R Astron Soc.* 2017; **469**(3): 2821–2833. [Publisher Full Text](#)

Thornton RJ, Ade PAR, Aiola S, et al.: **The Atacama Cosmology Telescope: the polarization-sensitive ACTPol instrument.** *Astrophys J Suppl.* 2016; **227**(2): 21. [Publisher Full Text](#)

Tinker J, Kravtsov AV, Klypin A, et al.: **Toward a halo mass function for precision cosmology: the limits of universality.** *Astrophys J.* 2008; **688**(2): 709–728. [Publisher Full Text](#)

Towler I, Kay ST, Schaye J, et al.: **Inferring the dark matter splashback radius from cluster gas and observable profiles in the FLAMINGO simulations.** *Mon Not R Astron Soc.* 2024; **529**(3): 2017–2031. [Publisher Full Text](#)

Tozzi P, Norman C: **The evolution of X-Ray clusters and the entropy of the Intracluster Medium.** *Astrophys J.* 2001; **546**(1): 63–84. [Publisher Full Text](#)

Tozzi P, Santos JS, Jee MJ, et al.: **Chandra deep observation of xdcp j0044.0-2033, a massive galaxy cluster AT z > 1.5.** *Astrophys J.* 2015; **799**(1): 93. [Publisher Full Text](#)

Umetsu K, Sereno M, Medezinski E, et al.: **Three-dimensional multi-probe analysis of the galaxy cluster A1689.** *Astrophys J.* 2015; **806**(2): 207. [Publisher Full Text](#)

Valenzuela-Venegas G, Lode ML, Viole I, et al.: **A renewable and socially accepted energy system for astronomical telescopes.** *Nat Sustain.* 2024; **7**(12): 1642–1650. [Publisher Full Text](#)

van Daalen MP, McCarthy IG, Schaye J: **Exploring the effects of galaxy formation on matter clustering through a library of simulation power spectra.** *Mon Not R Astron Soc.* 2020; **491**(2): 2424–2446. [Publisher Full Text](#)

van Kampen E, Bakx T, De Breuck C, et al.: **Atacama Large Aperture Submillimeter Telescope (AtLAST) science: surveying the distant Universe [version 1; peer review: 2 approved, 3 approved with reservations].** *Open Res Eur.* 2024; **4**: 122. [PubMed Abstract](#) | [Publisher Full Text](#) | [Free Full Text](#)

van Marrewijk J, Di Mascolo L, Gill AS, et al.: **XLSSC 122 caught in the act of growing up: spatially resolved SZ observations of a  $z = 1.98$  galaxy cluster.** *Astron Astrophys.* 2024b; **689**: A41. [Publisher Full Text](#)

van Marrewijk J, Morris TW, Mroczkowski T, et al.: **Maria: a novel simulator for forecasting (sub-)mm observations.** *Open J Astrophys.* 2024a; **7**: 118. [Publisher Full Text](#)

van Weeren RJ, Andrade-Santos F, Dawson WA, et al.: **The case for electron re-acceleration at galaxy cluster shocks.** *Nat Astron.* 2017; **1**: 0005. [Publisher Full Text](#)

van Weeren RJ, de Gasperin F, Akamatsu H, et al.: **Diffuse radio emission from galaxy clusters.** *Space Sci Rev.* 2019; **215**(1): 16. [Publisher Full Text](#)

Vavagiakis EM, Ahmed Z, Ali A, et al.: **Prime-Cam: a first-light instrument for the CCAT-prime telescope.** In: *Millimeter, Submillimeter, and Far-Infrared Detectors and Instrumentation for Astronomy IX.* 2018; **10708**: 107081U. [Publisher Full Text](#)

Vavagiakis EM, Duell CJ, Austermann J, et al.: **CCAT-prime: design of the Mod-Cam receiver and 280 GHz MKID instrument module.** In: *Millimeter, Submillimeter, and Far-Infrared Detectors and Instrumentation for Astronomy XI.* 2022; **12190**: 121904. [Publisher Full Text](#)

Vavagiakis EM, Gallardo PA, Calafut V, et al.: **The Atacama Cosmology Telescope: probing the baryon content of SDSS DR15 galaxies with the thermal and kinematic Sunyaev-Zel'dovich effects.** *Phys Rev D.* 2021; **104**(4): 043503. [Publisher Full Text](#)

Vikhlinin A, Burenin RA, Ebeling H, et al.: **Chandra cluster cosmology project. II. Samples and X-ray data reduction.** *Astrophys J.* 2009; **692**(2): 1033–1059. [Publisher Full Text](#)

Viole I, Shen L, Camargo LR, et al.: **Sustainable astronomy: a comparative life cycle assessment of off-grid hybrid energy systems to supply large telescopes.** *Int J Life Cycle Assess.* 2024; **29**(9): 1706–1726. [Publisher Full Text](#)

Viole I, Valenzuela-Venegas G, Zeyringer M, et al.: **A renewable power system for an off-grid sustainable telescope fueled by solar power, batteries and green hydrogen.** *Energy.* 2023; **282**: 128570. [Publisher Full Text](#)

Voit GM: **Tracing cosmic evolution with clusters of galaxies.** *Rev Mod Phys.* 2005; **77**(1): 207–258. [Publisher Full Text](#)

Voit GM, Kay ST, Bryan GL: **The baseline intracluster entropy profile from gravitational structure formation.** *Mon Not R Astron Soc.* 2005; **364**(3): 909–916. [Publisher Full Text](#)

Walker SA, Fabian AC, Sanders JS, et al.: **Galaxy cluster outskirts: a universal entropy profile for relaxed clusters?** *Mon Not R Astron Soc.* 2012; **427**(1): L45–L49. [Publisher Full Text](#)

Wan JT, Mantz AB, Sayers J, et al.: **Measuring  $H_0$  using X-ray and SZ effect observations of dynamically relaxed galaxy clusters.** *Mon Not R Astron Soc.* 2021; **504**(1): 1062–1076. [Publisher Full Text](#)

Wedemeyer S, Barta M, Brajša R, et al.: **Science development study for the Atacama Large Aperture Submillimeter Telescope (AtLAST): solar and stellar observations [version 1; peer review: 1 approved, 2 approved with reservations].** *Open Res Eur.* 2024; **4**: 140. [PubMed Abstract](#) | [Publisher Full Text](#) | [Free Full Text](#)

Werner N, McNamara BR, Churazov E, et al.: **Hot Atmospheres, Cold Gas, AGN feedback and the evolution of early type galaxies: a topical perspective.** *Space Sci Rev.* 2019; **215**(1): 5. [Publisher Full Text](#)

Whelan B, Veronica A, Pacaud F, et al.: **X-ray studies of the Abell 3158 galaxy cluster with eROSITA.** *Astron Astrophys.* 2022; **663**: A171. [Publisher Full Text](#)

White SDM, Efstathiou G, Frenk CS: **The amplitude of mass fluctuations in the universe.** *Mon Not R Astron Soc.* 1993; **262**(4): 1023–1028. [Publisher Full Text](#)

White E, Ghigo FD, Prestage RM, et al.: **Green Bank Telescope: overview and analysis of metrology systems and pointing performance.** *Astron Astrophys.* 2022; **659**: A113. [Publisher Full Text](#)

Willis JP, Oguri M, Ramos-Ceja ME, et al.: **Understanding X-ray and optical selection of galaxy clusters: a comparison of the XXL and CAMIRA cluster catalogues obtained in the common XXL-HSC SSP area.** *Mon Not R Astron Soc.* 2021; **503**(4): 5624–5637. [Publisher Full Text](#)

Woody DP, Beasley AJ, Bolatto AD, et al.: **CARMA: a new heterogeneous millimeter-wave interferometer.** In: *Z-Spec: A Broadband Millimeter-Wave Grating Spectrometer: Design, Construction, and First Cryogenic Measurements.* 2004; **5498**: 30–41. [Publisher Full Text](#)

Wootton A, Thompson AR: **The Atacama Large Millimeter/Submillimeter Array.** *IEEE Proceedings.* 2009; **97**(8): 1463–1471. [Publisher Full Text](#)

XRISM Collaboration: **The bulk motion of gas in the core of the Centaurus galaxy cluster.** *Nature.* 2025a; **638**(8050): 365–369. [PubMed Abstract](#) | [Publisher Full Text](#)

XRISM Collaboration: **XRISM reveals low nonthermal pressure in the core of**

the hot, relaxed galaxy cluster A2029. *Astrophys J.* 2025b; **982**(1): L5.  
[Publisher Full Text](#)

XRISM Collaboration: **XRISM forecast for the Coma cluster: stormy, with a steep power spectrum.** arXiv e-prints. arXiv: 2504.2092, 2025c.  
[Publisher Full Text](#)

Yang T, Cai YC, Cui W, et al.: **Understanding the relation between thermal Sunyaev-Zeldovich decrement and halo mass using the SIMBA and TNG simulations.** *Mon Not R Astron Soc.* 2022; **516**(3): 4084–4096.  
[Publisher Full Text](#)

Yu L, Nelson K, Nagai D: **The influence of mergers on scatter and evolution in Sunyaev-Zel'dovich effect scaling relations.** *Astrophys J.* 2015; **807**(1): 12.  
[Publisher Full Text](#)

Zemcov M, Aguirre J, Bock J, et al.: **High spectral resolution measurement of the Sunyaev-Zel'dovich effect null with Z-Spec.** *Astrophys J.* 2012; **749**(2): 114.  
[Publisher Full Text](#)

Zhang C, Zhuravleva I, Kravtsov A, et al.: **Evolution of splashback boundaries**

and gaseous outskirts: insights from mergers of self-similar galaxy clusters. *Mon Not R Astron Soc.* 2021; **506**(1): 839–863.  
[Publisher Full Text](#)

Zhao Y, Xu H, Liu A, et al.: **The warm-hot intergalactic medium in inter-cluster filaments: a forecast for HUBS observations based on eRASS1 superclusters.** *Astron Astrophys.* 2025; **695**: A15.  
[Publisher Full Text](#)

Zhu N, Bhandarkar T, Coppi G, et al.: **The simons observatory large aperture telescope receiver.** *Astrophys J Suppl.* 2021; **256**(1): 23.  
[Publisher Full Text](#)

Zhuravleva I, Churazov E, Schekochihin AA, et al.: **Suppressed effective viscosity in the bulk intergalactic plasma.** *Nat Astron.* 2019; **3**: 832–837.  
[Publisher Full Text](#)

Zwicky F: **Die rotverschiebung von extragalaktischen Nebeln.** *Helv Phys Acta.* 1933; **6**: 110–127.  
[Reference Source](#)

## Open Peer Review

Current Peer Review Status:    

---

### Version 2

Reviewer Report 25 June 2025

<https://doi.org/10.21956/openreseurope.22160.r55133>

© 2025 Salvati L. This is an open access peer review report distributed under the terms of the [Creative Commons Attribution License](#), which permits unrestricted use, distribution, and reproduction in any medium, provided the original work is properly cited.

 **Laura Salvati**

IAS, Université Paris-Saclay, CNRS, Orsay, France

The authors have answered to and implemented all the suggested modifications, and also have substantially improved the introductory sections, helping the readability of the paper. I believe the paper is ready for indexing.

**Competing Interests:** No competing interests were disclosed.

**Reviewer Expertise:** Cosmology and Astrophysics

**I confirm that I have read this submission and believe that I have an appropriate level of expertise to confirm that it is of an acceptable scientific standard.**

Reviewer Report 14 June 2025

<https://doi.org/10.21956/openreseurope.22160.r55131>

© 2025 Battistelli E. This is an open access peer review report distributed under the terms of the [Creative Commons Attribution License](#), which permits unrestricted use, distribution, and reproduction in any medium, provided the original work is properly cited.

 **Elia Stefano Battistelli**

Sapienza University of Rome, Rome, Italy

I recommend this manuscript be approved.

**Competing Interests:** No competing interests were disclosed.

**Reviewer Expertise:** CMB, Sunyaev Zeldovich effect, millimetric instrumentation

**I confirm that I have read this submission and believe that I have an appropriate level of expertise to confirm that it is of an acceptable scientific standard.**

Reviewer Report 14 June 2025

<https://doi.org/10.21956/openreseurope.22160.r55132>

© 2025 Désert F. This is an open access peer review report distributed under the terms of the [Creative Commons Attribution License](#), which permits unrestricted use, distribution, and reproduction in any medium, provided the original work is properly cited.

✓ **François-Xavier Désert** 

Institut de Planétologie et d'Astrophysique de Grenoble, Univ. Grenoble Alpes, CNRS, IPAG, Grenoble, France

I would like to thank the authors for taking my comments into account. The sensitivity in both instantaneous and survey modes seem very optimistic.

The prospect of a large single-dish (sub)millimetre telescope at a high altitude within the next decade justifies the indexing of this comprehensive paper on the potential of SZ science for astrophysics and cosmology.

**Competing Interests:** No competing interests were disclosed.

**Reviewer Expertise:** Clusters of galaxies, CMB, ISM

**I confirm that I have read this submission and believe that I have an appropriate level of expertise to confirm that it is of an acceptable scientific standard.**

Reviewer Report 14 June 2025

<https://doi.org/10.21956/openreseurope.22160.r55130>

© 2025 Remazeilles M. This is an open access peer review report distributed under the terms of the [Creative Commons Attribution License](#), which permits unrestricted use, distribution, and reproduction in any medium, provided the original work is properly cited.

✓ **Mathieu Remazeilles** 

Instituto de Física de Cantabria (CSIC - UC), Santander, Spain

The authors have satisfactorily addressed all the concerns I raised in my previous review. As a result, I have updated my approval status accordingly.

**Competing Interests:** No competing interests were disclosed.

**Reviewer Expertise:** Cosmology, CMB, foregrounds, component separation

**I confirm that I have read this submission and believe that I have an appropriate level of expertise to confirm that it is of an acceptable scientific standard.**

---

## Version 1

Reviewer Report 03 April 2025

<https://doi.org/10.21956/openreseurope.18856.r51896>

© 2025 Remazeilles M. This is an open access peer review report distributed under the terms of the [Creative Commons Attribution License](#), which permits unrestricted use, distribution, and reproduction in any medium, provided the original work is properly cited.



Mathieu Remazeilles

<sup>1</sup> Instituto de Física de Cantabria (CSIC - UC), Santander, Spain

<sup>2</sup> Instituto de Física de Cantabria (CSIC - UC), Santander, Spain

The paper presents a compelling case for the Atacama Large Aperture Submillimeter Telescope (AtLAST) as a next-generation facility for Sunyaev-Zeldovich (SZ) effect studies. It effectively outlines the scientific motivations, observational requirements, and technical advancements necessary to explore the complex thermal evolution of cosmic structures, from galaxies to clusters and filaments. The authors provide theoretical forecasts to justify AtLAST's remarkable capabilities and its expected contributions to astrophysics.

The paper is well-structured, comprehensive, and presents a strong scientific rationale for AtLAST. The writing is generally clear and well-supported by references to prior work. However, there are several areas where the manuscript could be improved, particularly in terms of clarity and technical rigour.

This paper deserves indexing after the authors address the comments below.

### Main comments:

1. While the manuscript discusses the limitations of current and future submillimeter facilities, a more quantitative comparison with upcoming telescopes such as FYST, CMB-S4, and CMB-HD would strengthen the argument. A graphical representation comparing AtLAST's expected frequency coverage, sensitivity, resolution, and field of view with these facilities would help clarify its unique capabilities and how it complements or surpasses other projects.
2. Section 3.3 emphasizes the potential of AtLAST for kinetic SZ (kSZ) studies. However, given the inherent spectral degeneracy between the kSZ effect and CMB temperature anisotropies, how does AtLAST intend to disentangle these signals within the ICM? I would expect AtLAST's high spatial resolution to play a crucial role in overcoming this degeneracy, but this advantage is not emphasized in the discussion of the kSZ science case.
3. In Figure 3, the Compton-y profiles evolve with redshift. The reason for this evolution should be

explicitly discussed, as the thermal SZ effect is generally considered redshift-independent. How much of this evolution is driven by intrinsic astrophysical effects (e.g., AGN feedback, accretion, non-thermal pressure) versus observational biases (e.g., resolution limits, selection effects)?

4. Despite AtLAST's high instrumental sensitivity, it remains unclear whether the residual foreground contamination can be reduced below the thermal SZ confusion noise or if a 'foreground floor' will persist, preventing accurate separation of faint SZ signals( $y = 10^{-7}$ ) in the WHIM or CGM.

In particular, Figure 10 shows very low residual foreground contamination from the ILC method compared to the tSZ power spectrum across multipoles. However, how do these residuals compare to the tSZ confusion noise and other SZ-related signals, such as kSZ, relativistic SZ corrections, or non-thermal SZ, which AtLAST also aims to extract? If possible, over plotting these additional spectra in Figure 10 would provide a clearer understanding of their relative importance.

5. The low residual foreground levels in Figure 10 suggest that the ILC method is highly effective. However, it is unclear whether this is primarily due to the availability of nine sensitive frequency channels by AtLAST or if it results from simplified assumptions in the foreground simulations. Providing more details on the sky simulations used in Section 4.2 and Figure 10 would help clarify this. Specifically:

Are extragalactic foregrounds (e.g., CIB and radio sources) spatially correlated with the thermal SZ signal in these simulations?

Are the SEDs of extragalactic foregrounds redshift-dependent?

6. The terminology "kinetic SZ spectral distortion" in Section 3.3 is misleading, as the kSZ effect does not introduce a spectral distortion but instead follows the same spectral shape as the CMB. Similarly, the middle panel of Figure 4 labels the "Kinetic SZ Compton y parameter", which is confusing because the kSZ effect is not characterized by a y-distortion. Could the authors clarify whether there is a unit conversion applied to represent kSZ in this way?

7. While beam chromaticity across different frequency bands can be mitigated through deconvolution and convolution, intra-band beam variations could introduce spectral distortions and biases in SZ reconstruction, particularly for relativistic SZ and diffuse WHIM studies. Has the impact of intra-band beam variations been quantified for AtLAST? What strategies are planned to mitigate this effect?

8. Figures 14-15 suggest using an SED-fitting approach, similar to Erler et al. (2018), to separate the relativistic SZ effect from correlated dust contamination. However, this method does not appear to take full advantage of AtLAST's high angular resolution. In contrast, multi-scale, map-based component separation techniques would likely be more effective at distinguishing relativistic SZ corrections from the dust emission of star-forming galaxies in clusters, which occupy much smaller angular scales than the cluster itself. The authors should emphasize how AtLAST's high resolution could enhance this separation, if applicable.

#### **Minor comments:**

1. The paper includes a large number of references, but adding explicit definitions and equations

for key quantities (e.g., tSZ, rtSZ, kSZ, non-thermal SZ) would improve clarity and self-containment.

2. In Section 3.2, when discussing current constraints on the relativistic SZ effect, the authors could reference the recent stacking analysis of Planck data by Remazeilles & Chluba (MNRAS, 2025), which used a blind map-based component separation approach.

3. The right panel's label in Figure 7 is unclear. Is this ACT data alone, or ACT+Planck combined? The caption and body text seem inconsistent and should be clarified.

4. In Section 4.1, the statement "At the same time, we would like to consider a minimum setup in order not to result in an oversampling of the target spectral range" is unclear. Could the authors clarify? Intuitively, increasing the number of frequency channels should improve foreground cleaning and component separation. Is there a trade-off between the number of channels and instrument sensitivity that limits the spectral sampling to nine channels?

5. What is "active, closed loop metrology"? A short description/definition could be helpful.

6. Figure 4 (page 8) is referenced much later in the text (page 15), whereas other figures (e.g., Figure 5) appear earlier. The figures could be reordered to improve the logical flow.

#### Typos:

- Figure 1 caption: "(ICM) of the" -> "(ICM), and of the"?
- Section 4.1: "we decide do not include" -> "we decide to not include" or "we decide to exclude"
- Section 5.2.4: "meta-Irich" -> "metal-rich"
- Section 6: "mapping the SZ signal from at low or intermediate redshift astrophysical sources" -> Needs rewording (e.g., "mapping the SZ signal from astrophysical sources at low or intermediate redshift")

#### References

1. Remazeilles M, Chluba J: Evidence for relativistic Sunyaev-Zeldovich effect in Planck CMB maps with an average electron-gas temperature of  $T_e \simeq 5$  keV. *Monthly Notices of the Royal Astronomical Society*. 2025; **538** (3): 1576-1586 [Publisher Full Text](#)

#### Is the background of the case's history and progression described in sufficient detail?

Yes

#### Is the work clearly and accurately presented and does it cite the current literature?

Yes

#### If applicable, is the statistical analysis and its interpretation appropriate?

Yes

#### Are all the source data underlying the results available to ensure full reproducibility?

Not applicable

#### Are the conclusions drawn adequately supported by the results?

Partly

**Is the case presented with sufficient detail to be useful for teaching or other practitioners?**

Yes

**Competing Interests:** No competing interests were disclosed.

**Reviewer Expertise:** Cosmology, CMB, foregrounds, component separation

**I confirm that I have read this submission and believe that I have an appropriate level of expertise to confirm that it is of an acceptable scientific standard, however I have significant reservations, as outlined above.**

Author Response 17 May 2025

**Luca Di Mascolo**

We thank the reviewer for the valuable and detailed report. We include the detailed responses to the individual comments below.

**referee:**

1. While the manuscript discusses the limitations of current and future submillimeter facilities, a more quantitative comparison with upcoming telescopes such as FYST, CMB-S4, and CMB-HD would strengthen the argument. A graphical representation comparing AtLAST's expected frequency coverage, sensitivity, resolution, and field of view with these facilities would help clarify its unique capabilities and how it complements or surpasses other projects.

**authors:** Following the referee's comment, we included a new figure (Fig. 10) for comparing the proposed spectral coverage of AtLAST with past, current, and future (sub)mm facilities. Plots showing AtLAST's performances in terms of angular resolution and field of view in comparison to other facilities are already provided in past AtLAST works (see, for instance, Klaassen+2020). Booth+2024 also report a comparison of the number counts of detectors for AtLAST and other facilities. As such, we prefer not to include these plots in our manuscript and refer to the aforementioned papers.

**referee:** 2. Section 3.3 emphasizes the potential of AtLAST for kinetic SZ (kSZ) studies.

However, given the inherent spectral degeneracy between the kSZ effect and CMB temperature anisotropies, how does AtLAST intend to disentangle these signals within the ICM? I would expect AtLAST's high spatial resolution to play a crucial role in overcoming this degeneracy, but this advantage is not emphasized in the discussion of the kSZ science case.

**authors:** This is indeed the case, as we plan to integrate recent advances in statistical data processing in our analysis pipelines. One example is the application of wavelet phase harmonics for performing a data-driven statistical component separation (as tested, for instance, on Herschel measurements for disentangling the CIB from large-scale Galactic dust emission; <https://ui.adsabs.harvard.edu/abs/2024A%26A...681A...1A/abstract>). We included a brief statement in Sec. 3.3.2 (after splitting Sec. 3.3 in two subsections for the sake of readability).

**referee:** 3. In Figure 3, the Compton-y profiles evolve with redshift. The reason for this evolution should be explicitly discussed, as the thermal SZ effect is generally considered

redshift-independent. How much of this evolution is driven by intrinsic astrophysical effects (e.g., AGN feedback, accretion, non-thermal pressure) versus observational biases (e.g., resolution limits, selection effects)?

**authors:** The referee is right in underlining the redshift independence of the SZ surface brightness. This is true when considering a system with a given Compton  $y$ . However, Fig. 3 shows the evolution of the pressure profiles at fixed mass, considering for this the definition with respect to the critical density at a given redshift (i.e., M500). Since the critical density evolves with cosmic time (redshift), systems with the same M500 but different redshift will exhibit SZ signals with different amplitudes. At the same time, the overall radial extent of the SZ profiles depends on the specific angular diameter distance at the corresponding redshift.

Since this could cause some confusion, we included a short statement for explaining the redshift-dependence of the SZ profiles in the figure.

**referee:** 4. Despite AtLAST's high instrumental sensitivity, it remains unclear whether the residual foreground contamination can be reduced below the thermal SZ confusion noise or if a 'foreground floor' will persist, preventing accurate separation of faint SZ signals ( $y = 10^{-7}$ ) in the WHIM or CGM.

In particular, Figure 10 shows very low residual foreground contamination from the ILC method compared to the tSZ power spectrum across multipoles. However, how do these residuals compare to the tSZ confusion noise and other SZ-related signals, such as kSZ, relativistic SZ corrections, or non-thermal SZ, which AtLAST also aims to extract? If possible, over plotting these additional spectra in Figure 10 would provide a clearer understanding of their relative importance.

**authors:** The residuals in the Compton  $y$  panel of Fig. 11 (previously Fig. 10) results from the application of ILC method on a mock sky realization comprising CMB, infrared and radio backgrounds, as well as kSZ components (we refer to the updated Sect. 4.3.1 for details). As such, the residuals themselves include any residual power associated with CMB and kSZ signals. We however note that, for simplicity, we did not include any relativistic SZ correction. We included a note about this assumption in Sect. 4.3.1.

To further support the discussion and following the suggestion by another referee, we included a second panel showing the kSZ residuals, along with their comparison with the primary CMB spectrum.

Finally, we note that the tSZ signal in the left panel of Fig. 11 denotes the power spectrum of the tSZ confusion noise itself. A detailed analysis of the impact of tSZ confusion noise on (sub)mm survey experiments and the impact of the removal of the most massive haloes on the detection capabilities of low-mass clusters was already discussed in Raghunathan+2022, to which we refer for further details. Given the relevance, we included a more explicit reference to the paper.

**referee:** 5. The low residual foreground levels in Figure 10 suggest that the ILC method is highly effective. However, it is unclear whether this is primarily due to the availability of nine sensitive frequency channels by AtLAST or if it results from simplified assumptions in the foreground simulations. Providing more details on the sky simulations used in Section 4.2 and Figure 10 would help clarify this.

**authors:** Compared to the previous version of the paper, we significantly expanded the description of the simulation setup used for inferring the ILC residuals. More details can be

found in the dedicated Sect. 4.3.1.

**referee:** Are extragalactic foregrounds (e.g., CIB and radio sources) spatially correlated with the thermal SZ signal in these simulations?

**authors:** The model currently adopted in our analysis does not encode any correlation between the tSZ effect and the signal from dusty and radio sources. As tested by Raghunathan+2024 in the case of CMB-S4, though, such a term is expected to introduce only a minor bias on the measured SZ effect (<0.2sigma), with the most extreme (and unrealistic) case reaching an upper limit of a 1sigma bias with respect to the true SZ signal. Modelling such an effect in the case of AtLAST-like observations will require a major effort for extending current sky models down to arcsecond scales, along for developing dedicated tools that could allow for a proper spatio-spectral component separation. As such, we decided to clarify that we are not including a correlation term (Sect. 4.3.1), but to extend the discussion only by adding the reference to the paper by Raghunathan+2024 and by briefly mentioning the results reported in that work.

**referee:** Are the SEDs of extragalactic foregrounds redshift-dependent?

**authors:** The extragalactic foreground/background components are based on past measurements by the South Pole Telescope (George+2015). As such, any redshift evolution of the source SED is included in the adopted model, as it encodes the inherent properties of the observed population of extragalactic sources.

**referee:** 6. The terminology "kinetic SZ spectral distortion" in Section 3.3 is misleading, as the kSZ effect does not introduce a spectral distortion but instead follows the same spectral shape as the CMB. Similarly, the middle panel of Figure 4 labels the "Kinetic SZ Compton y parameter", which is confusing because the kSZ effect is not characterized by a y-distortion. Could the authors clarify whether there is a unit conversion applied to represent kSZ in this way?

**authors:** We changed "spectral distortion" with "spectral signature". We further updated the central panel of Fig.4 to refer to  $y_{\text{ksz}}$  as "pseudo-Compton y", consistently with the new definition introduced in Sect. 2.2. This is a common definition in various observational studies of the kSZ found in the literature.

**referee:** 7. While beam chromaticity across different frequency bands can be mitigated through deconvolution and reconvolution, intra-band beam variations could introduce spectral distortions and biases in SZ reconstruction, particularly for relativistic SZ and diffuse WHIM studies. Has the impact of intra-band beam variations been quantified for AtLAST? What strategies are planned to mitigate this effect?

**authors:** We agree with the referee that the impact of beam chromaticity on the effective resolutions might be severe in the case of high-sensitivity broad-band measurements of the SZ effects. However, as demonstrated by Giardiello+2025 (<https://ui.adsabs.harvard.edu/abs/2025PhRvD.111d3502G/abstract>) in the context of CMB power spectrum reconstruction, the effect of in-band beam variations can be mitigated by means of the integration of a corresponding model component in the data analysis stage. For AtLAST, we aim at exploring similar solutions (along with applications of component separation techniques to the extreme spatial dynamic range of AtLAST) in more detailed and focused follow-up works. Still, given the relevance of beam chromaticity, we decided to

include a reference to the aforementioned work in Sect. 4.2 of our manuscript.

**referee:** 8. Figures 14-15 suggest using an SED-fitting approach, similar to Erler et al. (2018), to separate the relativistic SZ effect from correlated dust contamination. However, this method does not appear to take full advantage of AtLAST's high angular resolution. In contrast, multi-scale, map-based component separation techniques would likely be more effective at distinguishing relativistic SZ corrections from the dust emission of star-forming galaxies in clusters, which occupy much smaller angular scales than the cluster itself. The authors should emphasize how AtLAST's high resolution could enhance this separation, if applicable.

**authors:** The referee is correct in highlighting the role of AtLAST's high angular resolution in enhancing the separation of compact sources. In fact, this was already noted in Sect. 4.4.2 and the simulation is specifically aimed at testing the case for diffuse contamination for which it is not possible to take advantage of scale separation. We however noted that it would have been worth including a short mention to such a possibility also earlier in the text, and we added a short closing statement in Sect. 4.2.

**referee:** 1. The paper includes a large number of references, but adding explicit definitions and equations for key quantities (e.g., tSZ, rtSZ, kSZ, non-thermal SZ) would improve clarity and self-containment.

**authors:** Following the referee's suggestion, we included a more extensive definition of the thermal, kinetic and relativistic SZ equations in the introduction to the paper. For the sake of readability, we decided to restructure Sect. 2 in subsections, each focusing on one of the SZ flavors discussed in the paper.

**referee:** 2. In Section 3.2, when discussing current constraints on the relativistic SZ effect, the authors could reference the recent stacking analysis of Planck data by Remazeilles & Chluba (MNRAS, 2025), which used a blind map-based component separation approach.

**authors:** This was indeed an oversight on our part. We included the reference when mentioning stacking analyses.

**referee:** 3. The right panel's label in Figure 7 is unclear. Is this ACT data alone, or ACT+Planck combined? The caption and body text seem inconsistent and should be clarified. **authors:** It is indeed a combined Planck+ACT Compton y map. We updated the description in the caption and added a reference to Madhavacheril et al. 2020 for details on the generation of the combined ACT+Planck Compton y map.

**referee:** 4. In Section 4.1, the statement "At the same time, we would like to consider a minimum setup in order not to result in an oversampling of the target spectral range" is unclear. Could the authors clarify? Intuitively, increasing the number of frequency channels should improve foreground cleaning and component separation. Is there a trade-off between the number of channels and instrument sensitivity that limits the spectral sampling to nine channels?

**authors:** The constraint of finding a minimal spectral configuration is driven mostly by considerations on the future costs. It is indeed true that considering a finer spectral sampling would allow for an improved component separation, but the addition of extra bands would necessarily increase the instrument's complexity and overall resource

requirements. We included a brief mention of this issue in the corresponding paragraph.

**referee:** 5. What is "active, closed loop metrology"? A short description/definition could be helpful.

**authors:** Following a similar suggestion by another reviewer, Sect. 4.3.3 now includes a short description of the "closed-loop" metrology concept (but refer to the dedicated paper by Mroczkowski+2025 for more details).

**referee:** 6. Figure 4 (page 8) is referenced much later in the text (page 15), whereas other figures (e.g., Figure 5) appear earlier. The figures could be reordered to improve the logical flow.

**authors:** We improved the overall description of the figures in the main text, and Fig. 4 is now mentioned already in Sect. 3.1.

**referee:** Typos:

- Figure 1 caption: "(ICM) of the" -> "(ICM), and of the"?
- Section 4.1: "we decide do not include" -> "we decide to not include" or "we decide to exclude"
- Section 5.2.4: "meta-lrich" -> "metal-rich"
- Section 6: "mapping the SZ signal from at low or intermediate redshift astrophysical sources" -> Needs rewording (e.g., "mapping the SZ signal from astrophysical sources at low or intermediate redshift")

**authors:** We addressed all the aforementioned typos either directly or as a result of major rewriting of parts of the text and captions.

**Competing Interests:** No competing interests were disclosed.

Reviewer Report 27 March 2025

<https://doi.org/10.21956/openreseurope.18856.r51895>

© 2025 Battistelli E. This is an open access peer review report distributed under the terms of the [Creative Commons Attribution License](#), which permits unrestricted use, distribution, and reproduction in any medium, provided the original work is properly cited.



**Elia Stefano Battistelli**

<sup>1</sup> Sapienza University of Rome, Rome, Italy

<sup>2</sup> Sapienza University of Rome, Rome, Italy

**Report for Manuscript: "Atacama Large Aperture Submillimeter Telescope (AtLAST) science: Resolving the hot and ionized Universe through the Sunyaev-Zeldovich effect"**

**General Assessment:**

This paper presents a compelling case for advancing our understanding of the warm/hot ionized gas in the cosmic web through high-resolution, multi-wavelength Sunyaev-Zeldovich (SZ) effect

observations. The authors highlight the critical role of this gas phase in the cosmic matter budget and its implications for galaxy evolution and large-scale structure formation. The proposal for a dedicated instrument on the Atacama Large Aperture Submillimeter Telescope (AtLAST) is timely, given the limitations of current facilities. The paper is well-structured and scientifically rigorous. A few clarifications and additions would however strengthen the manuscript. Below, I provide detailed comments and suggestions.

**Strengths:****1. Motivation & Scientific Importance:**

- The paper effectively underscores the significance of the warm/hot gas in the cosmic web as a key component of the baryon budget, connecting galactic to cosmological scales.
- The emphasis on the SZ effect as a redshift-independent probe is well-justified, as well as the SZ dependence on the electron density particularly important for low-density environments where X-ray emission becomes inefficient. This point should be stressed more clearly in the text.

**2. Technical Feasibility & Innovation:**

- The proposal for a wide-field, broad-band, multi-chroic instrument on AtLAST addresses critical limitations of existing facilities.
- The inclusion of theoretical forecasts to define instrumental requirements strengthens the case for technical development.

**3. Clarity & Structure:**

- The abstract succinctly outlines the scientific goals, methodological approach, and broader implications.
- The logical flow from the cosmic web's multi-phase nature to the need for improved SZ observations is compelling.

**Specific Comments and Suggestions for Improvement:****General Comments:****1. Polarization Capabilities:**

- It is not clear whether the proposed instrument will include polarization capabilities. Given the importance of polarized signals for probing gas kinematics and magnetic fields, this should be explicitly addressed.

**2. SZ vs. X-ray for Low-Density Environments:**

- The authors should stress more clearly that the SZ effect is uniquely suited for probing low-density environments (e.g., filaments and voids) where X-ray emission is too faint to detect. This is a key advantage of SZ observations.

**3. Low-Frequency Channel and AME Science:**

- The low-frequency channel of the proposed instrument could significantly advance the possibility to disentangle different emissions including understanding of Anomalous Microwave Emission (AME). The authors should highlight this opportunity especially considering the angular resolution and the spectral coverage, as it would broaden the scientific impact of the project.

**4. Instrumental Comparisons:**

- The authors should mention that AtLAST will fill the gap between instruments like the Simons Observatory (SO) and ALMA in terms of angular scale coverage and *uv*-coverage, providing a unique window into the multi-scale nature of the cosmic web.

**Section-Specific Comments:**

**Section 3.2:**

- The authors should cite the seminal work by **Itoh et al. 1998** (ApJ, 502, 1, 1998) on the SZ effect and explicitly mention the decomposition of the SZ signal in terms of powers of electron temperature ( $T_e$ ).

**Section 3.3 (Kinetic SZ):**

- The kinetic SZ effect is noted for measuring line-of-sight gas motions. Could SZ polarization be used to probe motions *perpendicular* to the line of sight? Despite being very faint, this would be an interesting point to discuss, as it could open new avenues for studying gas dynamics.

**Section 3.5 (Angular Resolution):**

- The authors should stress more strongly that **high angular resolution** is critical for resolving small-scale structures (e.g., clumps in filaments, CGM around galaxies) and for minimizing confusion with other signals (e.g., dusty galaxies).

**Section 3.6 (Single-Dish Facilities):**

- The statement that other single-dish facilities (e.g., Nobeyama, GBT, SRT) are limited to lower frequencies is inaccurate for the GBT and SRT, as high-frequency instruments like MISTRAL are now being commissioned.

**Section 3.7 (AtLAST Resolution):**

- The claim that AtLAST has **8.3× better resolution** than ACT should specify the frequency (e.g., at 150 GHz, it is closer to **10× better**).
- The observation of A401-A399 in 10 hours may hold for sensitivity, but the sky coverage should be verified, as this is crucial for mapping large-scale structures.

**Section 4 (Instrumentation):**

- Among the cited instruments, the authors may want to include other instruments now being commissioned for instance at the SRT.
- The phrase "current state-of-the-art continuum cameras (e.g., transition edge sensor bolometers or kinetic inductance detectors)" is misleading, as these are **detectors**, not cameras. The authors should cite specific instruments (e.g., MUSTANG-2, NIKA2, MISTRAL) for clarity.

**Section 5.2.2 (Angular Resolution):**

- The statement that medium-resolution experiments are "limited to resolutions approximately 8.33× lower than AtLAST" is overly precise. A more rounded figure (e.g., " $\sim$ 8× lower") would be more appropriate.

**Other Comments:**

- The suggestion of a **1200 GHz band** to resolve dust/SZ degeneracies should be reconsidered, as the SZ signal is negligible at this frequency. The authors should clarify or justify this claim.
- **Figure 10 caption:** The parenthesis after "Sehgal et al., 2019" should be closed.

**Overall Recommendation:**

This paper makes a persuasive argument for advancing SZ observations to probe the thermal history of cosmic structures. The proposed instrument would fill a critical niche in multi-scale astrophysics and has the potential to transform our understanding of the cosmic web. With the suggested revisions, the manuscript will be suitable for publication.

I would like to congratulate the authors for their significant effort in producing this comprehensive study. The manuscript demonstrates substantial dedication to advancing our understanding of the cosmic web through innovative SZ observations, and the proposed instrument concept for AtLAST represents a thoughtful contribution to the field. The thorough

theoretical analysis and clear presentation of scientific motivations are particularly noteworthy.

**Is the background of the case's history and progression described in sufficient detail?**

Yes

**Is the work clearly and accurately presented and does it cite the current literature?**

Yes

**If applicable, is the statistical analysis and its interpretation appropriate?**

Yes

**Are all the source data underlying the results available to ensure full reproducibility?**

Yes

**Are the conclusions drawn adequately supported by the results?**

Yes

**Is the case presented with sufficient detail to be useful for teaching or other practitioners?**

Yes

**Competing Interests:** No competing interests were disclosed.

**Reviewer Expertise:** CMB, Sunyaev Zeldovich effect, millimetric instrumentation

**I confirm that I have read this submission and believe that I have an appropriate level of expertise to confirm that it is of an acceptable scientific standard.**

Reviewer Report 08 November 2024

<https://doi.org/10.21956/openreseurope.18856.r44539>

© 2024 Salvati L. This is an open access peer review report distributed under the terms of the Creative Commons Attribution License, which permits unrestricted use, distribution, and reproduction in any medium, provided the original work is properly cited.



**Laura Salvati**

<sup>1</sup> IAS, Université Paris-Saclay, CNRS, Orsay, France

<sup>2</sup> IAS, Université Paris-Saclay, CNRS, Orsay, France

The paper presents the upcoming AtLAST telescope and the science that can be done through the observation of hot gas in mm wavelength. The authors present the scientific case in details, discussing the different goals and how they can be achieved with AtLAST.

I believe the paper is worth getting indexed after minor improvements that I am suggesting below.

### General comments:

- the Figures should be described and discussed a bit more in the main text. What are we seeing and what should be the take-home-message from the plots?
- example: Fig. 1 showing the different components/processes happening in galaxy clusters and how they can be observed. A short discussion is done only on the caption of the figure, but it would help the reader to present the main points also in the main text.
- and same general considerations for the other figures.
- In the initial part of paper there should be a short introduction to the AtLAST experiment: it is true that this paper is part of a series of papers presenting the mission and science in general, most of them referred to in this paper, but I still believe that each paper should be able to "stand alone", presenting a very short description of the experiment. Most of the information are spread over the full text, but a general introduction could be useful.

### Section 2

- I believe few standard equations to introduce the thermal, kinetic SZ would be useful in this introductory section, instead of just proportionality proposed in the text.
- I would also suggest to introduce more in details (and with the equation definition) the relativistic contribution, to help better understanding the discussion in section 3.2 (also related to  $T_e$  estimation) and in section 4.3.
- When listing references for SZ observations, I believe more recent papers need to be cited, eg. all the newest catalogs from SPT, ACT, Planck, and ALMA works, etc..

### Section 3

- when introducing Fig. 2 for the first time, it is worth introducing also Table 1, at least to stress even more the frequency coverage.

#### Section 3.1

- Introducing "hydrostatic mass bias": worth adding a short definition, apart from citing Biffi's paper.

#### 3.3 at the end

- For patchy kSZ and reionisation contribution in general, please look also at works of Adelie Gorce, such as Gorce et al 2020 (Ref - 1), A&A 640 (2020), A90

### Link between section 3 and 4:

Section 3 lists all different scientific goals of the experiment, stressing the importance of given resolution, depth, field of view etc.. to achieve these goals.

To help highlighting what are the requirements needed from an instrumental point of view to reach the scientific goals, a short summary (eg. bullet-point style or table) could be useful, maybe at the beginning of section 4, before going into details in section 4.1. I believe all the information is there but there's a risk they get lost in the long text before 4.1.

### Section 4

- Fig. 9 is not mentioned in the text.
- AtLAST-like simulations: the authors mention that the analysis is based on Raghunathan et al. 2022: it would be worth putting more details and in particular explain if the steps discussed after (the flat sky realisations, the foreground modelling, etc..) are part of the Raghunathan et al. 2022 (Ref - 2) analysis or they are in addition to that.
- some concepts are introduced in the section but not explained, for example in section 4.2 the SZ confusion limit and the closed-loop metrology. It is necessary to add a short definition.

- Figure 12: there is a line for  $T_e = 0$  KeV. What does it mean?

### References

1. Gorce A, Ilić S, Douspis M, Aubert D, et al.: Improved constraints on reionisation from CMB observations: A parameterisation of the kSZ effect. *Astronomy & Astrophysics*. 2020; **640**. [Publisher Full Text](#)
2. Raghunathan S, Darshan Singh A, Sharma B: Study of Resilience in Learning Environments During the Covid-19 Pandemic. *Frontiers in Education*. 2022; **6**. [Publisher Full Text](#)

### Is the background of the case's history and progression described in sufficient detail?

Yes

### Is the work clearly and accurately presented and does it cite the current literature?

Partly

### If applicable, is the statistical analysis and its interpretation appropriate?

Yes

### Are all the source data underlying the results available to ensure full reproducibility?

Not applicable

### Are the conclusions drawn adequately supported by the results?

Yes

### Is the case presented with sufficient detail to be useful for teaching or other practitioners?

Partly

**Competing Interests:** No competing interests were disclosed.

**Reviewer Expertise:** Cosmology and Astrophysics

**I confirm that I have read this submission and believe that I have an appropriate level of expertise to confirm that it is of an acceptable scientific standard, however I have significant reservations, as outlined above.**

Author Response 17 May 2025

**Luca Di Mascolo**

We are grateful to the referee for the useful and insightful comments, which helped us address key aspects of our paper. Our responses to the individual comments in the report are provided below.

**referee:** *the Figures should be described and discussed a bit more in the main text. What are we seeing and what should be the take-home-message from the plots?*

**example:** *Fig. 1 showing the different components/processes happening in galaxy clusters and how they can be observed. A short discussion is done only on the caption of the figure, but it*

would help the reader to present the main points also in the main text.

**authors:** For what concerns Fig. 1 specifically, we decided to move its first mention at the beginning of the new SZ section (Sect. 2). This seems a more appropriate paragraph, as it specifically introduces the SZ effect with respect to the possibility of probing different astrophysical processes.

Still, we prefer to keep the figure (and the caption) self-contained and not to extensively introduce the figure in the main text, as we intended it as a schematic summary of the different topics discussed in the paper. Given this, we extended the caption and provided forward references to the various subsections of Sect. 3 (“Proposed science goals”) to facilitate the connection between the cartoon and the text itself.

**referee:** and same general considerations for the other figures.

**authors:** Following the referee’s suggestions, we decided to review all the figure captions and corresponding discussion in the main text to improve the overall description of the key points of each plot. For the figures, we decided to adopt a “self-contained” approach, so that the main message of the figure is reported in the caption (improving the stand-alone readability of each figure). Accordingly, we edited the caption where such a message was missing.

Regarding the discussions in the main text, we introduced minor edits to most of the paragraphs including a mention to a figure. The more extensive edits are instead listed below:

- Sect. 3.1 now includes a more detailed and explicit reference to Fig. 3
- We noticed that Fig. 4 was cited only in Sect. 4.1, while it was initially intended as a visual reference for the discussions in Sect. 3.1 and Sect. 3. As such, we included a short description of the thermal SZ panel of the figure at the end of Sect. 3.1, and a corresponding discussion of the kinetic SZ panel in Sect. 3.3.
- We introduced a more extended discussion of Fig. 5 in the second to last paragraph of Sect. 3.5.
- Despite already mentioning Fig. 9, we decided to expand upon the previous reference to better highlight the importance of the high-frequency bands for the reduction of the contamination from dusty galaxies to the SZ effect.
- We improved the description of Figure 11 (previously Fig. 10) in Sect. 4.3.1.
- We corrected a typo in the description of Fig. 17 (previously Fig. 16) in the main body, and introduced a minor edit to the corresponding discussion.

**referee:** *In the initial part of paper there should be a short introduction to the AtLAST experiment: it is true that this paper is part of a series of papers presenting the mission and science in general, most of them referred to in this paper, but I still believe that each paper should be able to “stand alone”, presenting a very short description of the experiment. Most of the information are spread over the full text, but a general introduction could be useful.*

**Authors:** The introduction now includes a short summary paragraph for introducing AtLAST. For consistency with the other works in the ORE series, we however decided to limit the discussion to the very key aspects of the AtLAST design, and refer to the readers to the relevant works.

**referee:** I believe few standard equations to introduce the thermal, kinetic SZ would be useful in this introductory section, instead of just proportionalities proposed in the text.

**authors:** Following the referee's suggestion, we included a more extensive definition of the thermal, kinetic and relativistic SZ equations in the introduction to the paper. For the sake of readability, we decided to restructure Sect. 2 in subsections, each focusing on one of the SZ flavors discussed in the paper.

**referee:** I would also suggest to introduce more in details (and with the equation definition) the relativistic contribution, to help better understanding the discussion in section 3.2 (also related to  $T_e$  estimation) and in section 4.3.

**authors:** Consistently with the refactoring of the tSZ and kSZ sections, we extended the relativistic SZ discussion and provided a more thorough description of the impact of relativistic temperatures and non-thermal electrons on the measured SZ signal.

**referee:** When listing references for SZ observations, I believe more recent papers need to be cited, eg. all the newest catalogs from SPT, ACT, Planck, and ALMA works, etc.

**authors:** More up to date references were already included in the relevant section, but we agree that it is worth expanding upon the previous references. Section 2 now includes a longer introduction to past observational SZ studies, along with more up to date references. For the survey works, we included citations to the most recent cluster samples by Planck, SPT, and ACT. For what concerns the resolved SZ observations, including a complete list would be impractical. As such, we limit this to a subset of relevant works specific to the mentioned topics or to the first analysis with data from a given high-resolution facility.

**referee:** when introducing Fig. 2 for the first time, it is worth introducing also Table 1, at least to stress even more the frequency coverage.

**authors:** We included a direct mention to Table 1 in the introductory paragraph of Section 3.

**referee:** Introducing "hydrostatic mass bias": worth adding a short definition, apart from citing Biffi's paper.

**authors:** Following the suggestion by the referee, we included a definition of the hydrostatic mass bias right after its first mention in Sect. 3.1

**referee:** For patchy kSZ and reionisation contribution in general, please look also at works of Adelie Gorce, such as Gorce et al 2020 (Ref - 1), A&A 640 (2020), A90

**authors:** After the referee's comment, we realised that the reionization-kSZ paragraph was lacking a proper set of references to past works. We updated this.

**referee:** Section 3 lists all different scientific goals of the experiment, stressing the importance of given resolution, depth, field of view etc..to achieve these goals.

**authors:** To help highlighting what are the requirements needed from an instrumental point of view to reach the scientific goals, a short summary (eg. bullet-point style or table) could be useful, maybe at the beginning of section 4, before going into details in section 4.1. I believe all the information is there but there's a risk they get lost in the long text before 4.1.

We agree that a list of required characteristics will help guiding the overall discussion in Sect. 4. We now moved the previous introductory text to Sect. 4 in a new subsection (now Sect. 4.1) and added a short bullet list description of the key requirements at the beginning of Sect. 4.

**referee:** Fig. 9 is not mentioned in the text.

**authors:** We mention Fig. 9 in the second paragraph of Sect. 4.1 “Optimizing the spectral setup”, as well as in Sect. 5.1 “AtLAST scientific cross-synergies”. As mentioned above, we expanded the associated discussion about dust contamination in Sect. 4.1.

**referee:** AtLAST-like simulations: the authors mention that the analysis is based on Raghunathan et al. 2022: it would be worth putting more details and in particular explain if the steps discussed after (the flat sky realisations, the foreground modelling, etc..) are part of the Raghunathan et al. 2022 (Ref - 2) analysis or they are in addition to that.

**authors:** The description of the simulated maps included in the previous section refers to a specific test aimed at simulating targeted observations rather than survey-mode runs. As such, despite sharing some similarities with the approach adopted by Raghunathan 2022, it has been adapted to allow a more general treatment of arcsecond-level components and for obtaining an independent estimate of the estimated sensitivity. We note that the former implies that the existing models for the foreground and background models have had to be extended down to such angular scales, with potential issues associated with unphysical modes introduced by the model extrapolation. In order to clarify this, we thus included a brief description of the method used to extend the results by Raghunathan 2022 to the AtLAST case, as well as separating the two discussions in separate subsections.

**referee:** some concepts are introduce in the section but not explained, for example in section 4.2 the SZ confusion limit and the closed-loop metrology. It is necessary to add a short definition.

**authors:** We reworded the paragraph mentioning the SZ confusion limit to make its definition more explicit. As mentioned now in the text, we define as “SZ confusion limit” the confusion floor in any SZ measurements induced by low-mass haloes that fall below the detection threshold of a given experiment, or are associated (either physically or due to projection effects) with more massive structures.

Regarding the closed-loop metrology system that will be integrated in AtLAST, we believe that including a thorough description of the proposed designs would fall outside the scope of the present paper. All the technical details are reported in Mroczkowski+2025. We thus decided to include only a minimal description of the concept of “closed-loop” control system, and refer to the aforementioned paper for a more extensive description.

**referee:** Figure 12: there is a line for  $Te = 0$  KeV. What does it mean?

**authors:** The  $Te=0$ keV denotes the classical spectrum of the thermal SZ effect, i.e., without introducing relativistic corrections for the non-null electron temperature. We included a brief explanatory note in the caption of Fig. 13 (previously Fig. 12).

**Competing Interests:** No competing interests were disclosed.

© 2024 Désert F. This is an open access peer review report distributed under the terms of the [Creative Commons Attribution License](#), which permits unrestricted use, distribution, and reproduction in any medium, provided the original work is properly cited.



François-Xavier Désert

<sup>1</sup> Institut de Planétologie et d'Astrophysique de Grenoble, Univ. Grenoble Alpes, CNRS, IPAG, Grenoble, France

<sup>2</sup> Institut de Planétologie et d'Astrophysique de Grenoble, Univ. Grenoble Alpes, CNRS, IPAG, Grenoble, France

The paper discusses the fantastic scientific capabilities of Atlast (50m, 2deg FOV) with the SZ toolbox. It describes in detail all aspects of the physics of clusters, where Atlast would give a huge gain. This is not like CMB cosmology, where the gain is measured with a few parameters. Here, the vast astrophysics of the large-scale structure of the Universe would see a giant leap in many ways thanks to Atlast.

The paper is well written and detailed enough to give us a good idea of the effort involved. Many citations are given in order to grasp all the ideas, which are numerous and very rich. This paper is also a step forward in designing the best survey strategy (wide or deep surveys).

Nevertheless, I think that there are some unsubstantiated claims about this telescope that must at least be acknowledged: the ability to recover large scales thanks to the large field of view, and the ability to recover very small scales at high frequencies. For large scales, we would need some sky noise simulations to show that 1-2 degree scales can be recovered (but I admit this is beyond the scope of this paper). For small scales, this is a technical issue: how to build a telescope with sufficient surface accuracy on a 50m surface and with sufficient pointing accuracy (also beyond this paper).

The paper can be accepted if the following comments are addressed.

**Major comment:** Sensitivity problem: For point sources, a 50m telescope is fantastic, as we gain something like the square of the diameter. For extended sources, the sensitivity brightness does not depend on the size of the telescope, but if we look at a given angular size, the gain is like the diameter of the telescope. Atlast can compete with Alma for point sources although it loses by a factor of about 3 in collecting area. Atlast can outperform other telescopes because of its superior diameter, but the gain in surface brightness sensitivity goes only like the diameter (so not a huge factor). I would rather emphasise mapping speed and angular resolution as the definitive winning parameters.

You need a reference for the Atlast sensitivity calculator. Finally, I don't understand the last two columns of table 1. It seems that this is a telescope that is 10-100 times better for point sources than existing telescopes. For example, an rms of 0.600 mJy in one second at 1mm is unheard of! If I convert page 17, the one hour sensitivity in  $\mu$ Jy per beam of  $2\text{E-}6$ , I get less than 1 mJy in one second, which is also a very optimistic sensitivity. To get  $\mu$ Jy to  $5\text{E-}7$  you need 16 hours per FOV, so 64000 hours for 4000 deg<sup>2</sup>. At 9000 hours per year that is seven years without any overhead!

**Minor comments:** Fig. 2 describe ntSZ( $p=4$ )

Tab. 1 : Can you give the  $\mu$ Jy sensitivity per  $\sqrt{\text{hour}}$ , and the mapping speed (I see some indications in page 17 only). The caption is cryptic to me "*but consider the broad-band re-implementation of the AtLAST sensitivity calculator. The specific frequencies of the band edges correspond to the ones that minimizes the output noise RMS level in the corresponding band per given*

*integration time.*?" What is survey noise?

There is a claim that large scales can be recovered, say up to the scales of the field-of-view of Atlast. Is that claim based on simulations of the sky noise? Does it depend on the frequencies (I would expect higher frequencies are more difficult to deal with)?

Fig. 3 : use of theta B10 and B2 is not the best illustration for SZ effect as the sensitivity will mostly be at 2-1mm. Also, for a radius in abscissae, shouldn't we use theta/2 ? Finally, SZ effect is independent of redshift, if the cluster is resolved (which it is with Atlast). There are clearly some inconsistencies in that figure.

Fig. 4 : kSZ y parameter is a misnomer. It is not a tSZ distortion. We should rather use something like b=beta. tau where b is the adimensional distortion parameter (like DeltaT/T), beta=v/c and tau is the cluster line-of-sight opacity.

Fig. 8: what is shown in the left panel? What is the colour scale on the right panel?

Fig 10. What is the kSZ power spectrum? Isn't that a goal to measure it? To be fair, you address the issue qualitatively at the end of 3.3. Can you extend the figure to 20000 in  $\ell$  (claimed on page 10)?

rtSZ, by measuring the cluster temperature (without X-rays) will give a brand-new avenue in cluster physics. But it will provide results only for the hottest clusters (how many are there) which are the most massive ones.

**Is the background of the case's history and progression described in sufficient detail?**

Yes

**Is the work clearly and accurately presented and does it cite the current literature?**

Yes

**If applicable, is the statistical analysis and its interpretation appropriate?**

Yes

**Are all the source data underlying the results available to ensure full reproducibility?**

Yes

**Are the conclusions drawn adequately supported by the results?**

Partly

**Is the case presented with sufficient detail to be useful for teaching or other practitioners?**

Yes

**Competing Interests:** No competing interests were disclosed.

**Reviewer Expertise:** Clusters of galaxies, CMB, ISM

**I confirm that I have read this submission and believe that I have an appropriate level of expertise to confirm that it is of an acceptable scientific standard, however I have**

significant reservations, as outlined above.

Author Response 17 May 2025

**Luca Di Mascolo**

We thank the referee for the detailed report and the insightful comments. We think they helped in significantly improving the quality and completeness of our manuscript. Below we provide our responses to the individual comments in the report. ----- **referee**

*The paper discusses the fantastic scientific capabilities of Atlast (50m, 2deg FOV) with the SZ toolbox. It describes in detail all aspects of the physics of clusters, where Atlast would give a huge gain. This is not like CMB cosmology, where the gain is measured with a few parameters. Here, the vast astrophysics of the large-scale structure of the Universe would see a giant leap in many ways thanks to Atlast.*

*The paper is well written and detailed enough to give us a good idea of the effort involved. Many citations are given in order to grasp all the ideas, which are numerous and very rich. This paper is also a step forward in designing the best survey strategy (wide or deep surveys).*

*Nevertheless, I think that there are some unsubstantiated claims about this telescope that must at least be acknowledged: the ability to recover large scales thanks to the large field of view, and the ability to recover very small scales at high frequencies. For large scales, we would need some sky noise simulations to show that 1-2 degree scales can be recovered (but I admit this is beyond the scope of this paper). For small scales, this is a technical issue: how to build a telescope with sufficient surface accuracy on a 50m surface and with sufficient pointing accuracy (also beyond this paper). **authors***

We agree with the reviewer that the statement about the large-scale recovery capability of AtLAST would have required a more extensive discussion. As correctly noted, the accurate determination of the large-scale transfer function goes beyond the scope of this paper.

However, we note that first attempts have been reported in van Marrewijk+2024, to which we mainly refer for an extensive discussion. In general, the expected large-scale behaviour of AtLAST is based on the extrapolation from the characterization of the transfer function of survey telescopes like ACT and SPT, and high-resolution millimeter instruments like NIKA/NIKA2 and MUSTANG/MUSTANG2. Although the actual extension to the AtLAST case is deferred to future studies, we however believe that better supporting our claim with real-case results from the literature would strengthen the case study. We thus expanded the discussion in Section 4.1 to include direct references to past works, and acknowledge that the AtLAST case (large-scale recovery capabilities and their frequency dependence) will be considered in future dedicated investigations.

For what concerns the surface and pointing accuracy, we refer to the extensive description of the first conceptual design by Mroczkowski+2025. There, Section 5.3 is specifically aimed at exploring solutions for achieving the required 2.5" pointing accuracy, demonstrating the mechanical feasibility of such a goal. The control of the surface accuracy will instead rely on the proposed integrated closed-loop metrology system (Reichert+2024, Mroczkowski+2025), stemming from undergoing developments for the Sardinia Radio Telescope and the Nobeyama Radio Observatory 45m telescope. To better detail such key advances, we integrated a more extended discussion in Sect. 4.3.3. We finally note that the development of the metrology system will represent a major part of the AtLAST Phase 2 study.

Mroczkowski+2025: <https://ui.adsabs.harvard.edu/abs/2025A%26A...694A.142M/abstract>  
Reichert+2024: <https://ui.adsabs.harvard.edu/abs/2024SPIE13094E..1UR>

van Marrewijk+2024: <https://ui.adsabs.harvard.edu/abs/2024OJAp....7E.118V>

----- **referee**

*Sensitivity problem: For point sources, a 50m telescope is fantastic, as we gain something like the square of the diameter. For extended sources, the sensitivity brightness does not depend on the size of the telescope, but if we look at a given angular size, the gain is like the diameter of the telescope. Atlast can compete with Alma for point sources although it loses by a factor of about 3 in collecting area. Atlast can outperform other telescopes because of its superior diameter, but the gain in surface brightness sensitivity goes only like the diameter (so not a huge factor). I would rather emphasise mapping speed and angular resolution as the definitive winning parameters.* **authors**

We agree with the reviewer and we implement numerous edits of the manuscript (following also other referees' suggestions) throughout the paper to better emphasize how the combination of mapping speed and angular resolution is what is making AtLAST unique. Still, we decided to mention the enhanced beam-level sensitivity as AtLAST's collecting area will make it much more sensitive than more standard wide-field (sub)millimeter facilities (generally limited to 6-meter diameters) for the same number of detectors and integration time.

----- **referee**

*You need a reference for the Atlast sensitivity calculator.* **authors**

Consistently with the ORE guidelines, links and references to any software employed in the publication are reported in the "Software availability" section. Any citations relevant to the Sensitivity Calculator are reported there. Following the referee's suggestions, we however repeat the citations through the paper, when referring to the calculator and to any associated sensitivity estimates. ----- **referee**

*Finally, I don't understand the last two columns of table 1. It seems that this is a telescope that is 10-100 times better for point sources than existing telescopes. For example, an rms of 0.600 mJy in one second at 1mm is unheard of!*

*If I convert page 17, the one hour sensitivity in y per beam of 2E-6, I get less than 1 mJy in one second, which is also a very optimistic sensitivity. To get y to 5E-7 you need 16 hours per FOV, so 64000 hours for 4000 deg^2. At 9000 hours per year that is seven years without any overhead!*

**authors**

Among the key aspects of the whole AtLAST project is enabling a major leap in our observing capabilities over the (sub)millimeter wavelength range. The ambitious sensitivity targets are thus inherent to the same idea motivating the SZ case study.

To assess whether the provided sensitivity estimates fall within a realistic regime, we however tested them against independent measurements:

- we first rescaled the mean sensitivity levels reported in the latest ACT paper about the ACT Data Release 6 (Naess+2025) to the same units reported in our summary Table 1, and obtained consistent estimates; in particular, the average sensitivity across all the f150 arrays – the closest in terms of spectral coverage to one of the AtLAST bands – is equal to 7.23 uJy sqrt(h), broadly consistent with the corresponding AtLAST Band 4 sensitivity of 7.14 uJy sqrt(h);
- we the considered the sensitivity calculator developed for TolTEC (Bryan+2018); after adapting this to allow for the proposed AtLAST spectral bands, we obtain sensitivity estimates that are a factor 2-3x better than what we are reporting in the paper, owing to different assumptions about the overall system efficiency; in turn, the reported band-specific sensitivities can be considered as conservative limits compared to the

case of background-limited detectors.

- Finally, we would like to note that the Compton y depth of 5e-7 reported by the referee is specifically computed in the case of targeted observations. As such, it can not be extrapolated directly to wide-field/survey-type observations. For the latter case, we refer to the results of dedicated simulations reported in Fig. 11

Bryan+2018: <https://ui.adsabs.harvard.edu/abs/2018SPIE10708E..0JB/abstract>

Naess+2025: <https://ui.adsabs.harvard.edu/abs/2025arXiv250314451N/abstract>

----- **referee**

*Fig. 2 describe ntSZ( $p=4$ )*

**authors**

We thank the referee for the note, as we overlooked the definition of the non-thermal SZ term in the caption of Fig. 2. We integrated this with a corresponding note. -----

**referee**

*Tab. 1 : Can you give the y sensitivity per sqrt(hour), and the mapping speed (I see some indications in page 17 only). authors*

As suggested by the referee, we included the sensitivity levels in units of compton y  $\text{sqrt}(\text{hour})$  in Table 1. As also noted in the extended caption, we emphasize that these estimates are not fully representative of AtLAST's performances in measuring the SZ effect, as multi-band component separation techniques could mitigate the impact of astrophysical and atmospheric contamination in each bands.

Regarding the mapping speed, we prefer not to include individual values in Table 1. The present work is a case study specifically intended at motivating and driving the definition of the technical requirements for AtLAST, comprising its target mapping speed. Further, many undefined parameters would need to enter the mapping speed calculation – among others, the detector count and extent of the mapped area – and any estimates would thus be too tentative.

We however point to the information provided in Fig. 12 regarding the detector count required to achieve the proposed survey depth as a function of time and observed area. Although not explicitly, this figure encodes the same information one could obtain from a tabulated set of mapping speeds as a function of the number of detectors and observed sky fraction. We finally note that the accurate definition of AtLAST's performances will be the main focus of future forecast analyses. ----- **referee**

The caption is cryptic to me “but consider the broad-band re-implementation of the AtLAST sensitivity calculator. The specific frequencies of the band edges correspond to the ones that minimizes the output noise RMS level in the corresponding band per given integration time.”? What is survey noise? **authors**

We improved the description of the broad-band sensitivity estimate and added details regarding the “survey noise” levels. The latter is equivalent to the sensitivity definition commonly adopted in the case of arcminute-resolution survey facilities, and is provided for facilitating the comparison with such experiments.

With “broad-band re-implementation of the AtLAST sensitivity calculator” we refer to an extension of the official sensitivity calculator specifically intended for accounting for the variability of the atmospheric transmittance and system temperature within a given band. In practice, the effective sensitivity is estimated by computing the inverse root mean square average of the system equivalent flux densities provided by the sensitivity calculator within the frequency range of the considered band. More details are provided in the official online documentation for the AtLAST sensitivity calculator: <https://atlast-sensitivity->

[calculator.readthedocs.io/en/latest/calculator\\_info/sensitivity.html](calculator.readthedocs.io/en/latest/calculator_info/sensitivity.html)

Finally, full details on the optimization procedure for defining the optical bandwidths are provided in Sect. 4.1, that is now directly referred to in the table caption. ----- **referee**

There is a claim that large scales can be recovered, say up to the scales of the field-of-view of Atlast. Is that claim based on simulations of the sky noise? Does it depend on the frequencies (I would expect higher frequencies are more difficult to deal with)? **authors** We refer the reviewer to the comment at the beginning of this report. -----

**referee**

Fig. 3 : use of theta B10 and B2 is not the best illustration for SZ effect as the sensitivity will mostly be at 2-1mm. Also, for a radius in abscissae, shouldn't we use theta/2? **authors** We initially considered the radius as tracing the individual resolution element along the radial direction and not as radial distance itself. We however agree that the theta/2 representation is more appropriate, and we thus adapted the plot accordingly.

On the other hand, we decided to keep the B2 and B10 references instead of the 1-2mm (Band 4 to 6) resolutions, as we think that the former best represents the full range of angular resolutions that will be provided by AtLAST. ----- **referee**

Finally, SZ effect is independent of redshift, if the cluster is resolved (which it is with Atlast). There are clearly some inconsistencies in that figure. **authors**

Although the surface brightness of the SZ effect is in fact independent of redshift, the simulated profiles shown in Fig. 3 take fully into account the evolution of the critical density and angular diameter distance with redshift. As such, for a fixed mass value M500, we can expect a redshift-dependent evolution in the amplitude and radial extent of the SZ profile. ----- **referee**

Fig. 4 : kSZ y parameter is a misnomer. It is not a tSZ distortion. We should rather use something like  $b=\beta\tau$  where  $b$  is the adimensional distortion parameter (like  $\Delta T/T$ ),  $\beta=v/c$  and  $\tau$  is the cluster line-of-sight opacity. **authors**

We agree with the referee that the use of the term "kinetic Compton y parameter" could cause confusion in the reader. We however believe that such an issue could lie in the lack of a proper introduction of the term. We thus adapted the introduction to the paper to specifically introduce the "pseudo-Compton y" parameter for the kinetic SZ effect ( $y_{\text{kSZ}}$ ) and adapted the colorbar labels accordingly. We prefer to keep the notation  $y_{\text{kSZ}}$  instead of introducing a different parameter for matching the notation employed in several works from the literature specifically focused on the study of the kSZ effect. For consistency, we now refer to the thermal Compton y as  $y_{\text{tSZ}}$ . ----- **referee**

Fig. 8: what is shown in the left panel? What is the colour scale on the right panel? **authors** The left map is the input thermal Compton y map obtained by projecting the reference DIANOVA galaxy cluster, while the right panel is in brightness temperature units ( $uK_J$ ). We adapted the figure to include colorbars for the input model and for the ALMA, MUSTANG2 and AtLAST outputs. ----- **referee**

Fig 10. What is the kSZ power spectrum? Isn't that a goal to measure it? To be fair, you address the issue qualitatively at the end of 3.3. Can you extend the figure to 20000 in l (claimed on page 10)? **authors**

In the previous version of the paper, we did not provide enough details regarding the kSZ reconstruction, but we agree with the reviewer that it would be worth introducing a more extensive discussion on the topic. For such a reason, we extended Fig. 11 (Fig. 10 in the previous version) with a second panel including a comparison of the kSZ power spectrum

with the corresponding residuals as a function of sky coverage.

We however decided not to extend the multipole range to 20,000, as, to date, we don't have enough information on the tSZ and kSZ spectra on the corresponding scales that would allow us to build an accurate model. ----- **referee**

rtSZ, by measuring the cluster temperature (without X-rays) will give a brand-new avenue in cluster physics. But it will provide results only for the hottest clusters (how many are there) which are the most massive ones. **authors**

Fig. 18 is specifically intended at highlighting the specific issue mentioned by the referee, i.e., the mass-limited capabilities in obtaining SZ-based estimates of cluster temperatures. To further emphasize this, we included a consistent statement in the caption of Fig. 18. Regarding the abundance of clusters for which it would be possible to draw a comparison between the curves in Fig. 18 and the mass-redshift distributions of the SZ-detected clusters in Fig. 5. To facilitate the comparison, we converted the mass values in Fig. 18 to M500. We also include here

([https://drive.google.com/file/d/1fgJgh\\_4ISp7GHbwYHkcoW3r6fOgtcv4S/view?usp=sharing](https://drive.google.com/file/d/1fgJgh_4ISp7GHbwYHkcoW3r6fOgtcv4S/view?usp=sharing)) a link to a plot with a direct comparison of the data points from Fig. 5 with the contours from Fig. 18, but we decide not to include it in the paper due to its limited readability.

**Competing Interests:** No competing interests were disclosed.